NASA Contractor Report 4014

Preliminary Control Law and Hardware Designs for a Ride Quality Augmentation System for Commuter Aircraft

Donald J. Davis, Dennis J. Linse,
Reiner Suikat, and David P. Entz

NASA

NASA Contractor Report 4014

Preliminary Control Law and Hardware Designs for a Ride Quality Augmentation System for Commuter Aircraft

Donald J. Davis, Dennis J. Linse,
Reiner Suikat, and David P. Entz

The University of Kansas Center for Research, Inc.
Lawrence, Kansas

NASA

National Aeronautics
and Space Administration

**Scientific and Technical
Information Branch**

1986

ABSTRACT

This report documents the continued investigation of the design of Ride Quality Augmentation Systems (RQAS) for commuter aircraft. The purpose of these RQAS is the reduction of the vertical and lateral acceleration response of the aircraft due to atmospheric turbulence by the application of active control. The current investigations include the refinement of the sample data feedback control laws based on the control-rate-weighting and output-weighting optimal control design techniques. These control designs were evaluated using aircraft time simulations driven by Dryden spectra turbulence. Fixed gain controllers were tested throughout the aircraft operating envelope. The preliminary design of the hardware modifications necessary to implement and test the RQAS on a commuter aircraft is included. These include a separate surface elevator and the flap modifications to provide both direct lift and roll control.

The results indicate that vertical acceleration reductions of 45% and lateral reductions of more than 50% are possible. A fixed gain controller appears to be feasible with only minor response degradation.

TABLE OF CONTENTS

iv

LIST OF FIGURES

LIST OF FIGURES (Concluded)

LIST OF TABLES

LIST OF TABLES (Continued)

xi

NOTATION

For this report, bold-face upper-case letters are used to denote matrices while bold-face lower-case letters are used to denote vectors. The prime symbol (') is used with matrices to denote matrix transpose and the superscript (-1) is used to denote matrix inverse. A dot over a variable is used to denote differentiation with respect to time.

LIST OF SYMBOLS

Symbol	Definition	Units
a_y	Perturbed lateral acceleration	ft/s^2
a_z	Perturbed vertical acceleration	ft/s^2
f	Force	lbs
g	Acceleration due to gravity	ft/s^2
I	Moment of inertia	$slugs\text{-}ft^2$
J	Performance index	-
l	Rolling moment	ft-lbs
m	Mass	slugs
m	Pitching moment	ft-lbs
m	Number of controls	-
n	Yawing moment	ft-lbs
n	Number of states	-
p	Perturbed roll rate	rad/s (deg/s)
q	Perturbed pitch rate	rad/s (deg/s)
r	Number of output variables	-

Symbol	Definition	Units
r	Perturbed yaw rate	rad/s (deg/s)
T	Sample time	sec
T_s	Sample time	sec
T_d	Computational delay time	sec
t	Time	sec
u	Perturbed forward velocity	ft/s
v	Perturbed lateral velocity	ft/s
w	Perturbed vertical velocity	ft/s

Greek Symbols

Symbol	Definition	Units
α	Perturbed angle of attack	rad (deg)
β	Perturbed side-slip angle	rad (deg)
θ	Perturbed attitude angle	rad (deg)
γ	Perturbed glide-path angle	rad (deg)
ϕ	Perturbed bank angle	rad (deg)
ψ	Perturbed heading angle	rad (deg)
δ_{se}	Separate surface elevator deflection	rad (deg)

Symbol	Definition	Units
δ_{sr}	Separate surface rudder deflection	rad (deg)
δ_f	Flap deflection	rad (deg)
δ_{df}	Differential flap deflection	rad (deg)

Matrices and Vectors

Symbol	Definition	Size
A	State matrix	n x n
B	Control effectiveness matrix	n x m
C	Output equation state coefficient matrix	r x n
D	Output equation control coefficient matrix	r x m
K	Feedback gain matrix	m x n
M	Cross weighting matrix	n x n
P	Riccati matrix	n x n
Q	State or output weighting matrix	n x n or r x r
R	Control weighting matrix	m x m
S	Control rate weighting matrix	m x m
u	Control vector	m x 1
x	State vector	n x 1
y	Output vector	m x 1

Symbol	Definition	Size
Φ	State transition matrix	n x n
Γ	Control power matrix	n x m

Abbreviations

Symbol	Definition
A/D	Analog to Digital Converter
C.G.	Center of Gravity
C.R.W.	Control-Rate-Weighting
D/A	Digital to Analog Converter
ICAD	Interactive Control Augmentation Design Program
KU-FRL	University of Kansas Flight Research Laboratory
NASA LaRC	National Aeronautics and Space Administration Langley Research Center
ORACLS	Optimal Regulator Algorithms for the Control of Linear Systems
O.W.	Output-Weighting
P.O.E.	Probability of Exceedance
RQAS	Ride Quality Augmentation System

Subscripts

Symbol	Definition
A	Aerodynamic
c	Control-rate-weighting
df	Differential flaps
f	Flaps
n	Index
o	Output-weighting
se	Separate surface elevator
sr	Separate surface rudder
T	Thrust
x	x axis
y	y axis
z	z axis
1	Steady state

CHAPTER 1.

INTRODUCTION

Since the 1978 federal deregulation of the major air carriers, there has been an expansion in the smaller, commuter class air carriers into the routes that are not profitable for the larger carriers. With the renewed market for small (15-50 passengers) aircraft, comes renewed interest in technological advances for small aircraft. While many new advances are being incorporated into existing aircraft and new designs, one area has received little attention, that of ride smoothness or ride quality. Due to the inherent characteristics of smaller aircraft, they are more susceptible to atmospheric gusts. This report gives an update on the work on a Ride Quality Augmentation System (RQAS) by the University of Kansas Flight Research Laboratory (KU-FRL). RQAS is the implementation of an active digital flight control system for the expressed purpose of reducing aircraft vertical and lateral accelerations due to atmospheric turbulence. All of the research on the RQAS conducted at KU-FRL was done under the support and guidance of NASA Langley Research Center.

The initial investigations which led to the current work involved a study of previous ride quality research

and a feasibility study to determine the best approach to implementing a active digital control system. (Reference 1) The first phase of the current work (Reference 2) began the theoretical design phase of a digital controller to be implemented on a Cessna 402B aircraft. This phase included the development of the Interactive Control Augmentation Design (ICAD) program which incorporates classical and optimal control design techniques along with several different analysis techniques into one package. Using the ICAD program, longitudinal RQAS controllers were designed and evaluated in batch simulations, on the KU-FRL hybrid simulator and on the NASA Langley Research Center nonlinear moving-base simulator.

The current work, described in this report, involves the continuation of the work of phase 1. The lateral and longitudinal RQAS controllers are designed using both the control-rate-weighting and output-weighting sampled-data optimal control techniques. A basic experimental system is defined. Preliminary design of the necessary aircraft modifications for installing direct lift flaps and a separate surface elevator are described. These surfaces will provide the necessary active control power while preventing annoying feedback to the pilot. It was originally intended to include a separate surface rudder to provide control in the later-

al direction. All theoretical designs are based upon a separate surface rudder which is 33% as effective as the full rudder. This is the separate surface rudder refered to throughout the current work. Since the theoretical work was completed, the decision was made to use the entire rudder for lateral control. Since all models used are linear, all results for the separate surface rudder can be converted directly to full rudder results by a simple scale factor.

The basic RQAS design problem is presented in Chapter 2. This includes models and chosen design parameters. The sampled data optimal control designs are given in Chapter 3. The fixed gain controllers are included in Chapter 3. Chapter 4 outlines the work completed on the system modifications including the preliminary separate surface designs.

CHAPTER 2.

PROBLEM DEFINITION

A ride quality augmentation system (RQAS) is an active control system which improves passenger and flight crew comfort. This type of system is generally designed to suppress an aircraft's rigid body response to moderate to heavy continuous atmospheric turbulence. Although no standard criteria now exist for predicting comfort, several mathematical models of passenger response to aircraft motion have been developed and all agree that the dominant factors are the vertical and lateral accelerations (Reference 2).

In this chapter, the RQAS problem is defined. The small-perturbation equations of motion for the Cessna 402B aircraft are presented and the system design criteria are established. The atmospheric turbulence model to be used in the control law analysis is also discussed.

2.1 CESSNA 402B AIRCRAFT EQUATIONS OF MOTION

The RQAS control law designs presented in this report were designed using variations of the optimal linear quadratic regulator. The fundamental assumption

4

in applying these techniques to RQAS design is that the aircraft dynamics can be described by a set of linear, small-perturbation equations of motion in a state-matrix form;

$$\dot{x} = Ax + Bu \quad , \tag{2.1}$$

$$y = Cx + Du \quad , \tag{2.2}$$

where x is the aircraft state vector, u is the aircraft control vector and y is the aircraft output vector. The matrices A, B, C and D are constant coefficient matrices.

The linear, small-perturbation mathematical models used in this study were furnished for the Cessna 402B aircraft (Figure 2.1) by NASA Langley Research Center (LaRC). These models were obtained from a nonlinear simulation model using standard NASA LaRC techniques (Reference 3). The primary assumptions which restrict the validity of these models are:

1. The airframe is a rigid body:

2. The earth is an inertial reference frame:

3. The aircraft mass and mass distribution are constant:

4. The XZ-plane is a plane of symmetry:

5. The flow is quasi-steady:

6. The effect of engine gyroscopics is negligible:

THREE-VIEW DRAWING

* MAXIMUM HEIGHT OF AIRPLANE WITH
  NOSE GEAR DEPRESSED IS 11'10".

11'8" *

10'5.7"

36'1"

39'10.3"

6'4.5"
PROPELLER
DIAMETER

7'4"

14'8"

17'0"

1. NORMAL PROPELLER
   TIP TO GROUND
   CLEARANCE IS 8.15
   INCHES.
2. TOTAL WING AREA,
   INCLUDING NACELLES
   AND FUSELAGE WITHIN
   THE WING PLANFORM,
   IS 195.72 SQUARE FEET.
3. MINIMUM TURNING
   RADIUS IS 54'6".

10'0"
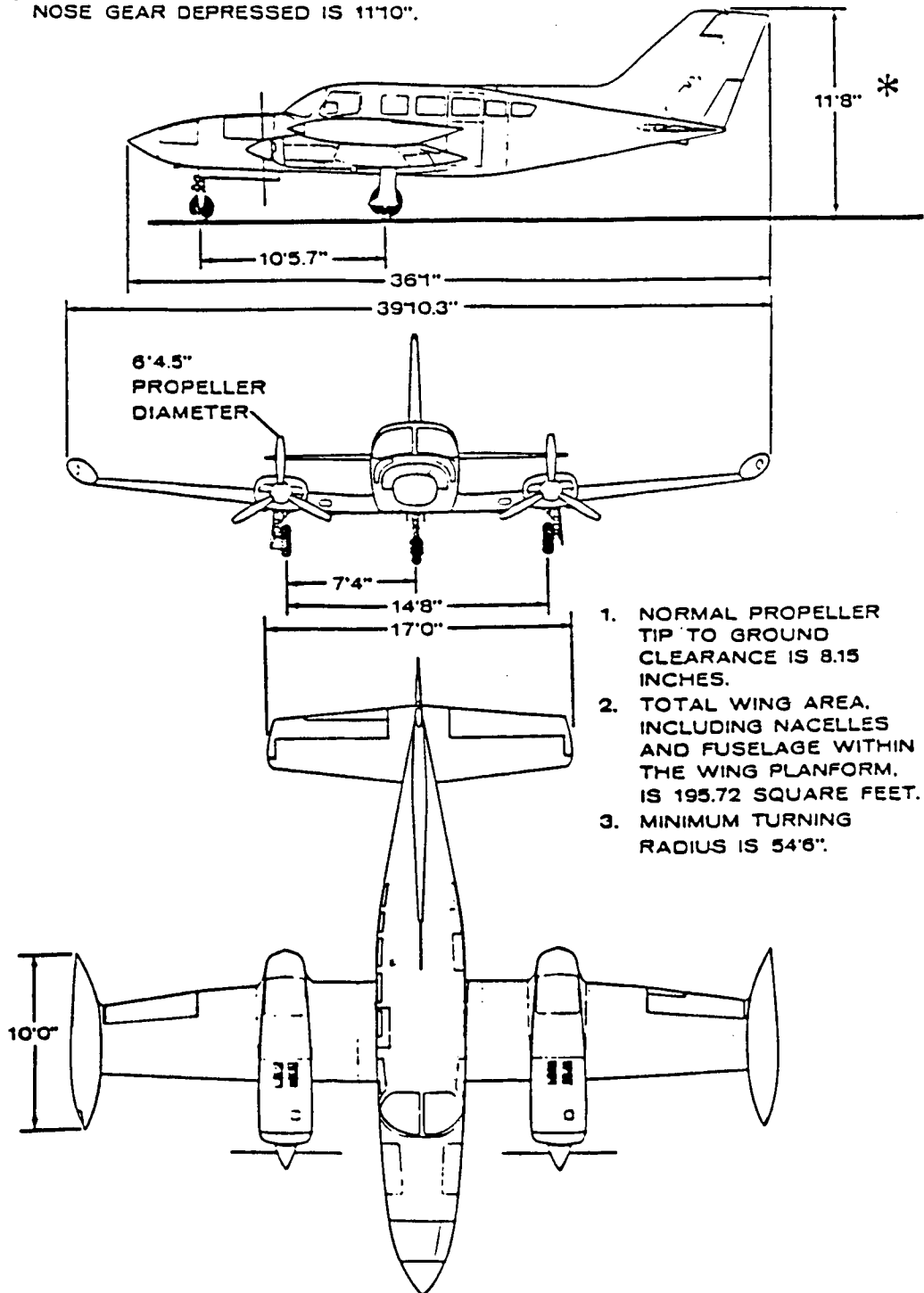
Figure 2.1   Cessna 402B – Three view

6

7. The steady-state conditions are for straight line trimmed flight:

8. The perturbations from steady-state are small:

9. The equations are written with respect to the stability axis system.

The state-matrix models were furnished for a coupled six-degree-of-freedom linear model. These equations were decoupled into the standard longitudinal and lateral-directional modes by assuming that the longitudinal forces and moments due to lateral perturbations are negligible and vice versa. This assumption is valid since the coupling terms in the provided models were indeed small and the eigenvalues of the decoupled matrices matched those of the fully coupled matrices.

The derivation of the equations of motion can be found in any standard text on airplane flight mechanics (Reference 4). The conversion of these equations to state matrix form is discussed in Appendix A.

The standard controls for the 402B are the elevator for pitch control, the rudder for yaw control and the ailerons for roll control. The longitudinal controls used by the RQAS are direct lift flaps and a separate surface elevator. The lateral-directional controls used by the system are a separate surface rudder and differential flaps. The outboard flaps are used as both longitudinal and lateral controls. Direct lift is achieved

when both the right and left flaps operate in the same direction and roll moments are developed by operating them differentially. The separate surface controls are provided so that the augmentation system is completly separate from the aircraft primary control system. A detailed description of how these controls are to be implemented on a Cessna 402B is contained in Chapter 4.

The longitudinal equations of motion can therefore be written in the form of Equation (2.1) as follows:

$$
\begin{bmatrix} \dot{\alpha} \\ \dot{u} \\ \dot{q} \\ \dot{\theta} \end{bmatrix} = \begin{bmatrix} Z'_\alpha & Z'_u & Z'_q & Z_\theta \\ X'_\alpha & X'_u & 0 & X_\theta \\ M'_\alpha & M'_u & M'_q & M_\theta \\ 0 & 0 & 1 & 0 \end{bmatrix} \begin{bmatrix} \alpha \\ u \\ q \\ \theta \end{bmatrix} + \begin{bmatrix} Z_{\delta_{se}} & Z_{\delta_f} \\ X_{\delta_{se}} & X_{\delta_f} \\ M_{\delta_{se}} & M_{\delta_f} \\ 0 & 0 \end{bmatrix} \begin{bmatrix} \delta_{se} \\ \delta_f \end{bmatrix}
$$

(2.3)

where the elements of the longitudinal **A** and **B** matrices are related to the standard aircraft longitudinal dimensional derivatives (Appendix A).

The lateral-directional equations of motion can also be written in the form of Equation (2.1) as follows:

8

$$
\begin{bmatrix} \dot{\beta} \\ \dot{p} \\ \dot{r} \\ \dot{\phi} \end{bmatrix} =
\begin{bmatrix} Y'_\beta & Y'_p & Y'_r & Y'_\phi \\ L'_\beta & L'_p & L'_r & 0 \\ N'_\beta & N'_p & N'_r & 0 \\ 0 & 1 & \tan\theta_1 & 0 \end{bmatrix}
\begin{bmatrix} \beta \\ p \\ r \\ \phi \end{bmatrix} +
\begin{bmatrix} Y'_{\delta_{df}} & Y'_{\delta_{sr}} \\ L'_{\delta_{df}} & L'_{\delta_{sr}} \\ N'_{\delta_{df}} & N'_{\delta_{sr}} \\ 0 & 0 \end{bmatrix}
\begin{bmatrix} \delta_{df} \\ \delta_{sr} \end{bmatrix}
\tag{2.4}
$$

where the elements of the lateral-directional **A** and **B** matrices are related to the standard aircraft lateral-directional dimensional stability derivatives (Appendix A).

2.2 OUTPUT EQUATION FORMULATION

As stated earlier, the dominant factors which influence aircraft passenger comfort are the vertical and lateral accelerations. The three angular rates, pitch rate q, roll rate p, and yaw rate r, are also factors to a smaller extent. The yaw rate and roll rate can be especially uncomfortable in combination. Therefore, while the primary objective of a ride quality augmentation system is to reduce the gust induced vertical and lateral accelerations, the systems designed should also try to maintain at least the open loop state response. With this in mind, the output vector is simply the state

9

vector with the addition of the two accelerations. The designer therefore has direct control over all of the pertinent (from a ride quality point of view) motion variables.

The aircraft longitudinal state, control, and output vectors are:

$$x' = (\alpha, u, q, \theta)$$

$$u' = (\delta_{se}, \delta_f)$$

$$y' = (a_z, \alpha, u, q, \theta)$$

and the aircraft lateral-directional state, control, and output vectors are:

$$x' = (\beta, p, r, \phi)$$

$$u' = (\delta_{df}, \delta_{sr})$$

$$y' = (a_y, \beta, p, r, \phi).$$

The aircraft output equations must be written in the form of Equation (2.2). To do this, the accelerations a_z and a_y must be written as linear combinations of the states and controls. This is done by manipulating the following equations of motion from Appendix A:

$$m(\dot{w} - U_1 q) = -mg\gamma\sin\gamma_1 + f_{A_z} + f_{T_z} \qquad (2.5)$$

$$m(\dot{v} + U_1 r) = mg\phi\cos\theta_1 + f_{A_y} + f_{T_y} . \qquad (2.6)$$

10

The perturbed vertical acceleration a_z can be obtained from Equation (2.5) by introducing the expressions;

$$\dot{w} = U_1\dot{\alpha} \qquad \text{and} \qquad \gamma = \alpha - \theta \quad :$$

$$m(U_1\dot{\alpha} - U_1q - g\alpha\sin\gamma_1 + g\theta\sin\gamma_1) = f_{A_z} + f_{T_z} \quad .$$

Solving for a_z results in:

$$a_z = (f_{A_z} + f_{T_z})/m = U_1\dot{\alpha} - g\alpha\sin\gamma_1 - U_1q + g\theta\sin\gamma_1 \quad . \quad (2.7)$$

Introducing the expression for $\dot{\alpha}$ from Equation (2.3) into Equation (2.7) leads to the following equation for a_z:

$$a_z = Z_\alpha''\alpha + Z_u''u + Z_q''q + Z_\theta''\theta + Z_{\delta_{se}}''\delta_{se} + Z_{\delta_f}''\delta_f \quad . \quad (2.8)$$

A similar derivation can be used to find the expression for a_y. Substituting the equation $\dot{v} = U_1\dot{\beta}$ into Equation (2.6) and rearranging results in the equation

$$a_y = (f_{A_y} + f_{T_y})/m = U_1\dot{\beta} + U_1r - g\phi\cos\theta_1 \qquad (2.9)$$

Eliminating $\dot{\beta}$ from this expression using Equation (2.4) leads to the following equation for a_y:

11

$$a_y = Y_\beta'\beta + Y_p'p + Y_r'r + Y_\phi'\phi + Y_{\delta_{df}}'\delta df + Y_{\delta_{sr}}'\delta sr. \quad (2.10)$$

The definitions of the modified dimensional stability derivatives contained in Equations (2.8) and (2.10) are summarized in Table 2.1.

Table 2.1 Modified Dimensional Stability Derivatives
For Use In The Aircraft Output Equations

Longitudinal

$$Z_\alpha' = U_1 Z_\alpha' - g\sin\gamma_1$$

$$Z_u' = U_1 Z_u'$$

$$Z_q' = (Z_q' - 1)U_1$$

$$Z_\theta' = U_1 Z_\theta + g\sin\gamma_1$$

$$Z_{\delta_{se}}' = U_1 Z_{\delta_{se}}$$

$$Z_{\delta_f}' = U_1 Z_{\delta_f}$$

Lateral-Directional

$$Y_\beta' = U_1 Y_\beta$$

$$Y_p' = U_1 Y_p$$

$$Y_r' = (Y_r' + 1)U_1$$

$$Y_\theta' = U_1 Y_\theta - g\cos\theta_1$$

$$Y_{\delta_{se}}' = U_1 Y_{\delta_{se}}$$

$$Y_{\delta_f}' = U_1 Y_{\delta_f}$$

Note: The primed values (') are defined in Appendix A.

The longitudinal output equations can now be writ-
ten in the form of Equation (2.2) as follows:

$$
\begin{bmatrix} a_z \\ \alpha \\ u \\ q \\ \theta \end{bmatrix} =
\begin{bmatrix} Z_\alpha{}'{}' & Z_u{}'{}' & Z_q{}'{}' & Z_\theta{}'{}' \\ 1 & 0 & 0 & 0 \\ 0 & 1 & 0 & 0 \\ 0 & 0 & 1 & 0 \\ 0 & 0 & 0 & 1 \end{bmatrix}
\begin{bmatrix} \alpha \\ u \\ q \\ \theta \end{bmatrix} +
\begin{bmatrix} Z_{\delta_{se}}{}' & Z_{\delta_f}{}' \\ 0 & 0 \\ 0 & 0 \\ 0 & 0 \\ 0 & 0 \end{bmatrix}
\begin{bmatrix} \delta_{se} \\ \delta_f \end{bmatrix}
\qquad (2.11)
$$

Similarly, the lateral-directional output equations
can be written as:

$$
\begin{bmatrix} a_y \\ \beta \\ p \\ r \\ \phi \end{bmatrix} =
\begin{bmatrix} Y_\beta{}' & Y_p{}'{}' & Y_r{}'{}' & Y_\phi{}'{}' \\ 1 & 0 & 0 & 0 \\ 0 & 1 & 0 & 0 \\ 0 & 0 & 1 & 0 \\ 0 & 0 & 0 & 1 \end{bmatrix}
\begin{bmatrix} \beta \\ p \\ r \\ \phi \end{bmatrix} +
\begin{bmatrix} Y_{\delta_{df}}{}' & Y_{\delta_{sr}}{}' \\ 0 & 0 \\ 0 & 0 \\ 0 & 0 \\ 0 & 0 \end{bmatrix}
\begin{bmatrix} \delta_{df} \\ \delta_{sr} \end{bmatrix}
\qquad (2.12)
$$

13

As an example of the models used in the RQAS designs, the longitudinal and lateral-directional equations of motion for the 402B during a sea level climb are presented in Tables 2.2 and 2.3. Models for all of the flight conditions investigated are included in Appendix B.

2.3 DYNAMIC MODEL OF ATMOSPHERIC TURBULENCE

Atmospheric turbulence may be described as individual patches in which the flow-field as seen by an airplane is a continuous random vector process composed of a steady mean value with turbulent fluctuations superposed. Each patch is assumed random, homogeneous (statistical properties are the same at each point in the field) and isotropic (statistical properties are independent of the axis orientation). The turbulence intensity $,\sigma,$ is used to distinguish one patch of turbulence from another. The frequency spectrum of the turbulence in each patch is related to this intensity. A more detailed explanation of the important concepts of turbulence as applied to the aircraft problem can be found in Reference 5.

The spectral form for the random continuous turbulence model chosen for this project is the Dryden

Table 2.2 Cessna 402B Longitudinal Mathematical Model
For Sea Level Climb

$\dot{x} = Ax + Bu$

$$\begin{bmatrix} \dot{\alpha} \\ \dot{u} \\ \dot{q} \\ \dot{\theta} \end{bmatrix} = \begin{bmatrix} -1.3325 & -0.0014 & 0.9189 & -0.0120 \\ 12.7885 & -0.0228 & 0.0000 & -32.0688 \\ -6.4781 & 0.0023 & -8.1525 & 0.0406 \\ 0.0000 & 0.0000 & 1.0000 & 0.0000 \end{bmatrix} \begin{bmatrix} \alpha \\ u \\ q \\ \theta \end{bmatrix}$$

$$+ \begin{bmatrix} -0.0389 & -0.2595 \\ 0.0000 & -5.9354 \\ -4.6678 & 1.4135 \\ 0.0000 & 0.0000 \end{bmatrix} \begin{bmatrix} \delta_{se} \\ \delta_f \end{bmatrix}$$

$y = Cx + Du$

$$\begin{bmatrix} a_z \\ \alpha \\ u \\ q \\ \theta \end{bmatrix} = \begin{bmatrix} -283.5580 & -0.2857 & -17.1010 & 0.0780 \\ 1.0000 & 0.0000 & 0.0000 & 0.0000 \\ 0.0000 & 1.0000 & 0.0000 & 0.0000 \\ 0.0000 & 0.0000 & 1.0000 & 0.0000 \\ 0.0000 & 0.0000 & 0.0000 & 1.0000 \end{bmatrix} \begin{bmatrix} \alpha \\ u \\ q \\ \theta \end{bmatrix}$$

$$+ \begin{bmatrix} -8.2010 & -54.7130 \\ 0.0000 & 0.0000 \\ 0.0000 & 0.0000 \\ 0.0000 & 0.0000 \\ 0.0000 & 0.0000 \end{bmatrix} \begin{bmatrix} \delta_{se} \\ \delta_f \end{bmatrix}$$

15

Table 2.3 Cessna 402B Lateral-Directional
Mathematical Model For Sea Level Climb

$\dot{x} = Ax + Bu$

$$
\begin{bmatrix} \dot{\beta} \\ \dot{p} \\ \dot{r} \\ \dot{\phi} \end{bmatrix} =
\begin{bmatrix}
-0.1879 & 0.0874 & -0.9971 & 0.1505 \\
-3.7107 & -2.6275 & 0.3918 & -0.0070 \\
3.7138 & -0.2901 & -0.3503 & -0.0065 \\
0.0000 & 1.0000 & 0.1700 & 0.0000
\end{bmatrix}
\begin{bmatrix} \beta \\ p \\ r \\ \phi \end{bmatrix}
$$

$$
+
\begin{bmatrix}
0.0000 & 0.0162 \\
-2.6247 & 0.3362 \\
-0.0611 & -0.7013 \\
0.0000 & 0.0000
\end{bmatrix}
\begin{bmatrix} \delta_{df} \\ \delta_{sr} \end{bmatrix}
$$

$y = Cx + Du$

$$
\begin{bmatrix} a_y \\ \beta \\ p \\ r \\ \phi \end{bmatrix} =
\begin{bmatrix}
-39.6290 & 18.4390 & 0.6125 & 0.0193 \\
1.0000 & 0.0000 & 0.0000 & 0.0000 \\
0.0000 & 1.0000 & 0.0000 & 0.0000 \\
0.0000 & 0.0000 & 1.0000 & 0.0000 \\
0.0000 & 0.0000 & 0.0000 & 1.0000
\end{bmatrix}
\begin{bmatrix} \beta \\ p \\ r \\ \phi \end{bmatrix}
$$

$$
+
\begin{bmatrix}
0.0000 & 3.4133 \\
0.0000 & 0.0000 \\
0.0000 & 0.0000 \\
0.0000 & 0.0000 \\
0.0000 & 0.0000
\end{bmatrix}
\begin{bmatrix} \delta_{df} \\ \delta_{sr} \end{bmatrix}
$$

spectral form. The Dryden spectral form has the advantage over the Von Karman form in that it is easy to implement in the time domain. The basic approach is to set up a random gust disturbance file whose points have a root mean square value of one and a frequency spectrum whose behavior approximates that of the Dryden spectrum. The reader is referred to Reference 2 for a detailed discussion on how atmospheric turbulence is implemented in the simulation portion of the ICAD program.

2.4 RQAS DESIGN CRITERIA

As stated earlier in this chapter, the main objective of a ride quality augmentation system is to reduce the vertical and lateral accelerations without significantly degrading the other state variable responses from the aircraft's open loop response. Also, the three angular rates, q, p, and r contribute to passenger comfort to some degree. Therefore, any reduction in these rates is also desirable.

The two factors which limit the performance of an RQAS are the rate and deflection limits for the control surfaces. For the 402B aircraft, the flaps are limited to deflections of 15 degrees up and 45 degrees down. These limits allow the RQAS to deflect ±15 degrees about

any trimmed flap setting. The flap rate limit is set at 120 degrees/second. The separate surface elevator deflection and rate limits are set at ± 5 degrees and 50 degrees/second respectively and the rudder deflection and rate limits are set at ± 5 degrees and 50 degrees/second respectively. These limits are representative of available actuators (Reference 6) and will be shown to be adequate to provide good RQAS performance (Reference 1).

The RQAS design criteria outlined above are listed in Table 2.4.

Table 2.4   RQAS Design Criteria

Longitudinal Mode

Variable	Criterion
a_z(rms)	< 3.54 (ft/sec^2)
$\dot{\delta}_f$	< 120 (deg/sec)
$\dot{\delta}_{se}$	< 50 (deg/sec)
$|\delta_f|$	< 15 (deg)
$|\delta_{se}|$	< 5 (deg)
α, u, q, θ	As close to the open loop values as possible.

Lateral-Directional Mode

Variable	Criterion
a_y(rms)	< 50% of open loop
$\dot{\delta}_{df}$	< 120 (deg/sec)
$\dot{\delta}_{sr}$	< 50 (deg/sec)
$|\delta_{df}|$	< 15 (deg)
$|\delta_r|$	< 5 (deg)
p, r	Any reduction is desirable.
β, ϕ	As close to the open loop values as possible.

19

2.5 DESIGN PARAMETERS AND FLIGHT CONDITIONS

Based upon the preliminary results from phase 1 (Reference 2), it was decided to use a digital, linear quadratic regulator formulation for the control system designs. The designs wil be evaluated using a digital simulation in both the time and frequency domains. The sample time for the control law designs is 0.02 seconds, with a computational delay time assumed to be 0.002 seconds. Also servos with bandwidths of 10 radians/second are assumed for each control. The gust intensity is selected by assuming a probability of exceedence of 0.001. These design parameters are summarized in Table 2.5.

Five flight conditions were chosen to represent a complete mission of the 402B. Table 2.6 summarizes these flight conditions.

Table 2.5   RQAS Design Parameters

Digital, Optimal Regulator Controller

Sample Time: $\qquad$ T_s = 0.02 seconds

Computational Delay Time: $\qquad$ T_d = 0.002 seconds

Control Servos: $\qquad$ $\dfrac{10}{s + 10}$

Table 2.6   Flight Conditions

Aircraft: Cessna 402B (2 crew / 6 passenger commuter)

Condition	Speed (ft/sec)	0.001 P.O.E. $\sigma_z = \sigma_y$ (ft/sec^2)
Takeoff at Sea Level	184	9.5
Climb at Sea Level	211	9.5
Climb at 5,000 Feet	227	10.2
Cruise at 20,000 Feet	358	7.4
Approach at Sea Level	160	9.5

CHAPTER 3.

OPTIMAL CONTROL DESIGNS

In phase 1 (Reference 2), the RQAS control laws
were designed using the sampled-data control-rate-
weighting design technique. This method allowed the
vertical acceleration to be written as a state variable.
In the current phase of this work, a second control
structure, output-weighting, was used to investigate
alternative designs. (Reference 7) Both the control-
rate weighting and the output-weighting design tech-
niques are implemented in the ICAD program. This chap-
ter will summarize the equations upon which both output-
weighting and control-rate-weighting are based. These
techniques will then be applied to the Cessna 402B model
for all flight conditions. Since the optimal gains vary
with flight conditions, the topic of gain scheduling
will be investigated.

3.1 DESIGN TECHNIQUES

While both control-rate-weighting and output-
weighting allow the control designer to weight outputs
which are linear combinations of states and controls,
each technique has distinct advantages and disadvan-
tages. Control-rate-weighting allows the designer to

weight the control surface deflection rates directly, while output-weighting only allows weights on the control deflection and gives no direct access to the control rates. Control-rate-weighting, however, has the disadvantage in that the surface positions must be measured and fed back. By contrast, only the states must be fed back in output-weighting.

Using the linear, small-perturbation equations of motion in state-matrix form as given in Equations (2.1) and (2.2), the continuous and sampled-data standard optimal regulator problem can be defined. The equations necessary to solve the continuous and the sampled-data problem are summarized in Tables 3.1 and 3.2, respectively. Included in these tables are the state and output equations which defined the equations of motion for the aircraft, and the quadratic cost functional, which is the basis of the optimal control problem. This functional is minimized by defining the feedback gains, K, based upon the solution of the matrix Riccati equation.

To solve the control-rate-weighting optimal control problem, an extension of the standard optimal regulator problem is made. In addition to the matrices that weight the outputs and controls in the cost functional, Q and R, a third matrix is included in the functional.

The S matrix weights the control deflection rates. To use the ORACLS design routines (Reference 8) on this newly defined cost functional, some matrix manipulation is done. This manipulation creates several new matrices which are combinations of the previous matrices. This converts the problem into the standard optimal regulator problem for which a solution is known. The basic equations and new matrix definitions are presented in Tables 3.1 and 3.2 for the continuous and the sampled-data cases. For a complete derivation of the equations the reader is referred to Reference 2 or 7.

The output-weighting problem is solved by similar techniques. First, the matrices are manipulated to form the problem into one analogous to the standard regulator problem, and then the problem is solved by existing techniques. The matrices that result from this process are presented in Tables 3.1 and 3.2 also. Once again the reader is referred to Reference 7 for a complete discussion and derivation of the output-weighting problem.

Tables 3.1 and 3.2 obviously contain a vast amount of information, much more than has been discussed here. They are presented in such a condensed form for the purpose of completeness of the problem definition and solution.

24

In both formulations, the optimal controller designs require the solution of a nonlinear algebraic matrix equation. ICAD is structured to perform the matrix manipulations to construct the required matrices and then solve the nonlinear algebraic equation.

	State Equation / Output Equation	Quadratic Cost Functional	Optimal Control Riccati Equation
Standard Regulator	$\dot{x} = Ax + Bu$	$J = \frac{1}{2}\int_0^\infty (x'Qx + u'Ru)dt$	$u = -Kx$ $K = R^{-1}B'P$ $A'P + PA - PBR^{-1}B'P + Q = 0$
	$\dot{x} = Ax + Bu$ $y = Cx$	$J = \frac{1}{2}\int_0^\infty (y'Qy + u'Ru)dt$	$u = -Kx$ $K = R^{-1}B'P$ $A'P + PA - PBR^{-1}B'P + Q_S = 0$
Control-Rate-Weighted Regulator	$\dot{x} = Ax + Bu$ $y = Cx + Du$	$J = \frac{1}{2}\int_0^\infty (y'Qy + u'Ru + u'S\dot{u})dt$	$\dot{u} = -K_1 x - K_2 u$ $[K_1\ \ K_2] = R_C^{-1}B_C'P$ $A_C'P + PA_C - PB_C R_C^{-1}B_C'P + Q_C = 0$
Output-Weighted Regulator	$\dot{x} = Ax + Bu$ $y = Cx + Du$	$J = \frac{1}{2}\int_0^\infty (y'Qy + u'Ru)dt$	$u = -Kx$ $K = R_O^{-1}(D'QC + B'P)$ $A_O'P + PA_O - PBR_O^{-1}B_O'P + Q_O = 0$

where

$$A_C = \begin{bmatrix} A & B \\ 0 & 0 \end{bmatrix} \qquad Q_C = \begin{bmatrix} C'QC & C'QD \\ D'QC & D'QD+R \end{bmatrix} \qquad A_O = A - BR_O^{-1}D'QC$$

$$Q_O = -C'(QDR_O^{-1}D'Q - Q)C$$

$$B_C = \begin{bmatrix} 0 \\ I \end{bmatrix} \qquad R_C = S \qquad R_O = (D'QD + R)$$

Table 3.1   Summary of Continuous Optimal Regulator Problems and Solutions (Reference 7)

Sampled State Equation Output Equation	Sampled Quadratic Cost Functional	Optimal Control Riccati Equation
$x = \Phi x_n + \Gamma u_n$	$J = \frac{1}{2}\sum_{n=0}^{\infty}(x_n'\bar{Q}x_n + 2x_n'\bar{M}u_n + u_n'\bar{R}u_n)$	$u_n = -Kx_n$ $K = (\bar{R}+\Gamma'P\Gamma)^{-1}(\Gamma'P\Phi+\bar{M}')$ $P = \Phi'P\Phi - (\Gamma'P\Phi+\bar{M}')'(\bar{R}+\Gamma'P\Gamma)^{-1}(\Gamma'P\Phi+\bar{M}')+\bar{Q}$
Standard Regulator $x = \Phi x_n + \Gamma u_n$ $y = Cx$	$J = \frac{1}{2}\sum_{n=0}^{\infty}(x_n'\bar{Q}_s x_n + 2x_n'\bar{M}u_n + u_n'\bar{R}u_n)$	$u_n = -Kx_n$ $K = (\bar{R}+\Gamma'P\Gamma)^{-1}(\Gamma'P\Phi+\bar{M}')$ $P = \Phi'P\Phi - (\Gamma'P\Phi+\bar{M}')'(\bar{R}+\Gamma'P\Gamma)^{-1}(\Gamma'P\Phi+\bar{M}')+\bar{Q}_s$
Control-Rate-Weighted Regulator $x = \Phi x_n + \Gamma u_n$ $y = Cx + Du_n$	$J = \frac{1}{2}\sum_{n=0}^{\infty}(x_c'\bar{Q}_c x_c + 2x_c'\bar{M}_c u_c + u_c'\bar{R}_c u_c)_n$	$\dot{u}_n = -K_1 x_n - K_2 u_n$ $[K_1,K_2] = (\bar{R}_c+\Gamma_c'P\Gamma_c)^{-1}(\Gamma_c'P\Phi_c+\bar{M}_c')$ $P = \Phi_c'P\Phi_c - (\Gamma_c'P\Phi_c+\bar{M}_c')'(\bar{R}_c+\Gamma_c'P\Gamma_c)^{-1}(\Gamma_c'P\Phi_c+\bar{M}_c')+\bar{Q}_c$
Output-Weighted Regulator $x = \Phi x_n + \Gamma u_n$ $y = Cx + Du_n$	$J = \frac{1}{2}\sum_{n=0}^{\infty}(x_n'\bar{Q}_o x_n + 2x_n'\bar{M}_o u_n + u_n'\bar{R}_o u_n)$	$u_n = -Kx_n$ $K = (\bar{R}_o+\Gamma'P\Gamma)^{-1}(\Gamma'P\Phi+\bar{M}_o')$ $P = \Phi'P\Phi - (\Gamma'P\Phi+\bar{M}_o')'(\bar{R}_o+\Gamma'P\Gamma)^{-1}(\Gamma'P\Phi+\bar{M}_o')+\bar{Q}_o$

Table 3.2   Summary of Sampled Data Optimal Regulator Problems and Solutions (Reference 7)

where

$$\Phi(t,t_n) = \exp[A(t-t_n)]$$

$$\Gamma(t,t_n) = \{\int_{t_n}^{t} \Phi(t,\tau)d\tau\}B$$

$$\bar{Q} = \int_{0}^{T}\{\Phi'(t,0)Q\Phi(t,0)\}dt$$

$$\bar{R} = RT + \int_{0}^{T}\{\Gamma'(t,0)Q\Gamma(t,0)\}dt$$

$$\bar{M} = \int_{0}^{T}\{\Phi'(t,0)Q\Gamma(t,0)\}dt$$

$$Q_s = C'QC$$

$$\bar{Q}_s = \int_{0}^{T}\{\Phi'(t,0)Q_s\Phi(t,0)\}dt$$

$$\bar{R} = RT + \int_{0}^{T}\{\Gamma'(t,0)Q_s\Gamma(t,0)\}dt$$

$$\bar{M} = \int_{0}^{T}\{\Phi'(t,0)Q_s\Gamma(t,0)\}dt$$

Table 3.2   Summary of Sampled Data Optimal Regulator
Problems and Solutions (Continued)

28

and

$$\Phi_C(t) = \exp(A_C t)$$

$$\Gamma_C(t) = \int_0^T \{\Phi_C(t)dt\}B_C$$

$$\bar{Q}_C = \int_0^T \{\Phi_C'(t)Q_C\Phi_C(t)\}dt$$

$$\bar{R}_C = R_C T + \int_0^T \{\Gamma_C'(t)Q_C\Gamma_C(t)\}dt$$

$$\bar{M}_C = \int_0^T \{\Phi_C'(t)Q_C\Gamma_C(t)\}dt$$

$$\bar{Q}_O = \int_0^T \{\Phi'(t)[C'QC]\Phi(t)\}dt$$

$$\bar{M}_O = \int_0^T \{\Phi'(t)[C'QC]\int_0^t \Phi(\tau)B(\tau)d\tau + \Phi'(t)C'QD\}dt$$

$$\bar{R}_O = (D'QD+R) + \int_0^T \{\int_0^t B'(\tau)\Phi'(\tau)d\tau (C'QC)\int_0^t \Phi(\tau)B(\tau)d\tau + N' + N\}dt$$

$$N = D'QC\int_0^t \Phi(\tau)B(\tau)d\tau$$

Table 3.2   Summary of Sampled Data Optimal Regulator
Problems and Solutions (Concluded)

3.2 SUMMARY OF SAMPLED-DATA OPTIMAL CONTROL DESIGNS

Using the techniques of Appendix A and Reference 3, the Cessna 402B equations of motion were modeled in state-space form for five flight conditions spanning the basic operating envelope of the aircraft. These conditions are

1. Take-off at sea-level conditions

2. Climb at sea-level

3. Climb at 5000 feet

4. Cruise at 20,000 feet

5. Approach at sea-level.

Both the longitudinal and lateral directional models for all five flight conditions are included in Appendix B. Using the ICAD program, the sampled-data control-rate-weighting and output-weighting design techniques presented in Section 3.1 were applied to these linearized models.

To illustrate the basic process and controller design, the optimal design of the RQAS for the sea-level climb flight condition will be presented in the next two sections. First, the control-rate-weighting designs will be presented, and then the output-weighting designs. A complete set of designs for all of the flight conditions is included in Appendix B.

3.2.1 CONTROL-RATE-WEIGHTING DESIGNS

The RQAS performance using the sampled-data control-rate-weighting design technique for the sea-level climb condition is presented. Performance is indicated by the maximum values and RMS values of the components of the output vector. Included are the open loop response, i.e. the response of the unaugmented aircraft to the gust field, and the response of the RQAS controlled aircraft. The system eigenvalues for both the unaugmented and augmented aircraft are given. The augmented aircraft eigenvalues are given in terms of W'-plane frequency and damping ratios. To evaluate the W'-plane eigenvalues, the controller is designed in the Z-plane. The Z-plane eigenvalues are then transformed into the W'-plane. The equivalence of the S-plane and the W'-plane is valid due to the small sample time used (Ts = 0.02 seconds). Also included are the final diagonal elements of the weighting matrices Q, R, and S, and the resulting optimal gain matrix K, used to implement the controller

$$u = - K x$$

where for the longitudinal motion

$$x' = (\alpha, u, q, \theta, \delta_{se}, \delta_f)$$

$$u' = (\dot{\delta}_{se}, \dot{\delta}_f)$$

31

and for the lateral-directional motion

$$x' = (\beta, p, r, \phi, \delta_{df}, \delta_{sr})$$
$$u' = (\dot{\delta}_{df}, \dot{\delta}_{sr}) \qquad .$$

3.2.1.1 LONGITUDINAL DESIGNS

The results of the longitudinal control-rate-weighting designs, as presented in Table 3.3 for a sea-level climb, display many features common to the results for all of the longitudinal RQAS designs. First of all, there is a subtantial reduction in the vertical accelerations, both peak value and RMS value. That is to be expected since that is the expressed purpose of the RQAS. There is, however, a substantial increase in the other values when viewed as a percentage. When viewed in terms of absolute change in magnitude, the increase is not seen to be significant. For example, the maximum forward velocity perturbation, u, increases by 116% when the RQAS is engaged, but that increase is actually only a change of 3.2 feet per second, from 1.9 to 4.1 feet per second. The other values behave similarly. The time domain response portion of the table also indicates the control activity for the augmented aircraft. It can be seen that the maximum deflections for the flaps and separate surface elevator are at or below the standards

Table 3.3 Summary of Longitudinal RQAS Response for a Sea-Level Climb -- Control-Rate-Weighting

Time Domain Response:

	Open Loop		Baseline RQAS		Percent Reduction	
	Max.	RMS	Max.	RMS	Max.	RMS
a_z (f/s2)	13.1	6.3	12.2	3.4	7%	46%
α (deg)	2.8	1.3	3.6	1.5	-29%	-15%
u (f/s)	1.9	1.1	4.1	2.4	-116%	-118%
q (deg/s)	1.8	0.9	2.7	1.4	-50%	-56%
θ (deg)	1.6	1.0	2.0	1.1	-25%	-10%
δ_{se} (deg)	-	-	4.3	2.3	-	-
δ_f (deg)	-	-	11.8	3.4	-	-
$\dot{\delta}_{se}$ (deg/s)	-	-	11.4	-	-	-
$\dot{\delta}_f$ (deg/s)	-	-	91.1	-	-	-

Table 3.3   Summary of Longitudinal RQAS Response
            for a Sea-Level Climb -- Control-Rate-Weighting
            (Continued)

System Eigenvalues:

	Open Loop		Baseline RQAS	
	Frequency	Damping	Frequency	Damping
Phugoid	0.15	0.04	0.09	0.79
Phugoid	0.15	0.04	0.09	0.79
Short Period	2.4	1.0	6.0	0.68
Short Period	7.1	1.0	6.0	0.68
Servo	10.0	1.0	3.5	1.0
Servo	10.0	1.0	11.8	1.0
Filter	-	-	15.3	1.0
Filter	-	-	63.8	1.0

Note 1: Baseline RQAS Frequency and Damping are based on
         roots of the W'-Plane.

Note 2: Control-Rate-Weighting introduces 2 filter states.

Optimal Gain Matrix:

$$K = \begin{bmatrix} 27.930 & 0.0123 & -2.5093 & -13.634 & 8.8770 & 6.1749 \\ 171.39 & 0.1719 & 14.655 & 24.772 & 3.0441 & 38.537 \end{bmatrix}$$

Weighting Matrices -- Diagonal Elements:

Q' = (0.05, 10.0, 0.0001, 3.0, 20.0)

R' = (0.12, 0.33)

S' = (0.02, 0.03)

of Table 2.4. The maximum control rates are also well below the designated maximum rates. This is to be expected for in control-rate-weighting, as the name implies, the control rates can be directly weighted making maximum rate limits easy to enforce. Reference 7 shows that the nature of the control-rate-weighting structure limits the maximum deflection rates. In that reference, the weighting of the rates was reduced to extremely small values but the actual deflection rates seem to approach an asymptotic value. This can be explained by the fact that the deflection rates are included in the cost functional, therefore, the deflection cannot go to infinity while the cost functional, which penalizes control rates, is still minimized.

The system eigenvalues are also presented in Table 3.3 for the longitudinal mode. The eigenvalues are presented in terms of frequencies and damping ratios. The open loop eigenvalues, i.e. the unaugmented aircraft eigenvalues, show that the aircraft phugoid mode is barely damped and the short period mode has separated into 2 real roots. The two servo eigenvalues are from the separate elevator and flap servos. The baseline RQAS augmented aircraft has very good characteristics. Both the phugoid and the short period have damping above

critical damping (0.707). There are two filter states introduced by control-rate-weighting in addition to the two servo states.

3.2.1.2 LATERAL-DIRECTIONAL DESIGNS

The lateral-directional RQAS design for the sea-level climb flight condition are representative of the characteristics of the lateral-directional designs for all five flight conditions. Good lateral-directional designs proved to be much easier to obtain than longitudinal designs. As can be seen in Table 3.4, there is over a 50% reduction in the RMS lateral acceleration when the baseline RQAS is implemented. Where this caused the remaining state values to increase in the longitudinal motion, all of the state values decrease in the lateral-directional motion. For example, the RMS value for the aircraft roll rate decreases by over 80%. The control surface deflections and deflection rates are also all well within the desired limits. These limits were actually the driving factor in the lateral-directional motion. The lateral acceleration could be reduced almost without limit if the deflections and rates were allowed to increase. The control-rate-weighting intrinsic rate limits, of course, held the control rates

in check.

The lateral-directional system eigenvalues included in Table 3.4 indicate some of the reasons for the ease of design mentioned above. The unaugmented aircraft has a slightly unstable spiral mode and a lightly damped Dutch Roll mode. The instability of the spiral mode is not of much consequence as long as the eigenvalue is near the origin. The baseline RQAS augmented aircraft has considerably different eigenvalues which is expected. The spiral has been substantially stabilized. The Dutch Roll mode has also been very well damped. There are also two filter states introduced. The excellent time domain response can be explained by the damping of the augmented Dutch Roll over the unaugmented Dutch Roll.

A tabular summary of the baseline control-rate-weighting RQAS designs for all of the remaining flight conditions can be found in Appendix B.

Table 3.4   Summary of Lateral-Directional RQAS Response for a Sea-Level Climb -- Control-Rate-Weighting

Time Domain Response:

	Open Loop		Baseline RQAS		Percent Reduction	
	Max.	RMS	Max.	RMS	Max.	RMS
a_y (f/s2)	6.1	2.7	3.5	1.3	43%	52%
β (deg)	6.2	2.8	5.8	1.9	6%	32%
p (deg/s)	6.4	2.7	1.5	0.5	77%	81%
r (deg/s)	10.6	4.8	7.1	2.8	33%	42%
ϕ (deg)	3.2	1.3	1.0	0.4	69%	69%
δ_{df} (deg)	-	-	4.8	2.1	-	-
δ_{sr} (deg)	-	-	14.7	5.8	-	-
$\dot{\delta}_{df}$ (deg/s)	-	-	30.0	-	-	-
$\dot{\delta}_{sr}$ (deg/s)	-	-	30.8	-	-	-

Table 3.4 Summary of Lateral-Directional RQAS Response for a Sea-Level Climb -- Control-Rate-Weighting (Continued)

System Eigenvalues:

	Open Loop		Baseline RQAS	
	Frequency	Damping	Frequency	Damping
Spiral Mode	0.02	-1.0	0.59	1.0
Roll Mode	2.7	1.0	3.3	1.0
Dutch Roll	2.1	0.12	2.8	0.51
Dutch Roll	2.1	0.12	2.8	0.51
Servo	10.0	1.0	5.5	0.88
Servo	10.0	1.0	5.5	0.88
Filter	-	-	12.6	1.0
Filter	-	-	21.3	1.0

Note 1: Baseline RQAS Frequency and Damping are based on roots of the W'-Plane.

Note 2: Control-Rate-Weighting introduces 2 filter states.

Optimal Gain Matrix:

$$K = \begin{bmatrix} 22.429 & -9.4558 & -6.6832 & -12.139 & 16.148 & -0.6806 \\ -1.9138 & 3.7262 & -14.873 & 3.5634 & -0.4145 & 7.2291 \end{bmatrix}$$

Weighting Matrices -- Diagonal Elements:

$Q' = (0.01, 15.0, 0.07, 0.5, 1.5)$

$R' = (2.007, 0.52)$

$S' = (0.007, 0.02)$

3.2.2 OUTPUT-WEIGHTING DESIGNS

The results of applying the sampled-data output-weighing design technique to the sea-level climb condition are presented in Tables 3.5 and 3.6 for the lonitudinal and lateral-directional motions, respectively. These tables include all of the same items as the corresponding tables for the control-rate-weighting designs. The feedback gain matrix, K, along with the two weighting matrices, Q and R, are also included. There is no equivalent to the S weighting matrix in output-weighting. The state and control vectors for the longitudinal output- weighting designs are

$$x' = (\alpha, u, q, \theta)$$

$$u' = (\delta_{se}, \delta_f)$$

and for the lateral-directional design are

$$x' = (\beta, p, r, \phi)$$

$$u' = (\delta_{df}, \delta_{sr})$$

The state vector only has 4 elements for output-weighting as compared to 6 for control-rate-weighting. This difference can make output-weighting easier to implement because the control deflections are not part of the state vector and do not have to be measured.

3.2.2.1 LONGITUDINAL DESIGNS

The results of the longitudinal output-weighting designs (Table 3.5) compare favorably to the control-rate-weighting designs. (Table 3.3) The RMS vertical acceleration is subtantially reduced over the unaugmented aircraft acceleration. The remaining values increase over the unaugmented aircraft values just as the control-rate-weighting designs did. Again, the percent increases are rather large, but the magnitude to the results are not particular large. The control surface activity for the RQAS augmented aircraft also meets all of the design specifications. The activity of the output-weighting design is slightly greater than the activity of the control-rate-weighting designs. The separate surface elevator is used more extensively, while the maximum control rates are both higher. This difference can be attributed to two separate sources. First, the intrinsic rate control of control-rate-weighting holds those control rates down. Also, the design process is not unique, i.e. the designs both satisfy the design requirements, but the method by which the acceleration reduction is achieved can vary considerably.

The eigenvalues of the RQAS baseline output-weighting show good general characteristics. They are

Table 3.5   Summary of Longitudinal RQAS Response for a Sea-Level Climb -- Output-Weighting

Time Domain Response:

	Open Loop		Baseline RQAS		Percent Reduction	
	Max.	RMS	Max.	RMS	Max.	RMS
a_z (f/s2)	13.1	6.3	11.8	3.3	10%	48%
α (deg)	2.8	1.3	3.7	1.6	-32%	-23%
u (f/s)	1.9	1.1	4.0	2.3	-111%	-110%
q (deg/s)	1.8	0.9	2.5	1.2	-39%	-33%
θ (deg)	1.6	1.0	1.8	1.1	-13%	-10%
δ_{se} (deg)	-	-	5.0	2.5	-	-
δ_f (deg)	-	-	11.7	5.4	-	-
$\dot{\delta}_{se}$ (deg/s)	-	-	22.3	-	-	-
$\dot{\delta}_f$ (deg/s)	-	-	98.8	-	-	-

Table 3.5   Summary of Longitudinal RQAS Response
            for a Sea-Level Climb -- Output-Weighting
            (Continued)

System Eigenvalues:

	Open Loop		Baseline RQAS	
	Frequency	Damping	Frequency	Damping
Phugoid	0.15	0.04	0.09	0.89
Phugoid	0.15	0.04	0.09	0.89
Short Period	2.4	1.0	11.6	0.66
Short Period	7.1	1.0	11.6	0.66
Servo	10.0	1.0	1.9	1.0
Servo	10.0	1.0	11.3	1.0

Note 1:   Baseline RQAS Frequency and Damping are based on
          roots of the W'-Plane.

Optimal Gain Matrix:

$$K = \begin{bmatrix} -0.5014 & -0.0018 & -1.5609 & -2.5312 \\ 4.5062 & 0.0046 & 0.5469 & 0.9847 \end{bmatrix}$$

Weighting Matrices -- Diagonal Elements:

Q' = (0.05, 10.0, 0.0001, 18.0, 40.0)

R' = (2.2, 1.0)

43

very stable and the oscillatory motion is well damped. The guaranteed stability is, of course, one of the benefits of optimal control. The phugoid mode is over critically damped and the short period mode is nearly so. The frequency of the short period is rather high. This is one of the characteristics observed in all of the output-weighting designs. The control-rate-weighting designs also have a high short period frequency, but not as high as the output-weighting designs.

3.2.2.2 LATERAL-DIRECTIONAL DESIGNS

The results of the lateral-directional output-weighting designs of Table 3.6 have the same good characteristics as the control-rate-weighting designs. In addition to the marked decrease in the side accelerations, the other perturbation variables are also decreased, sometimes by a large percentage. The RMS acceleration is reduced by 59%, which is much better than the 50% design criteria. This is achieved without any harm to the other variables. The only limit is the control surface deflection and rate limits. Since the control rates could not be directly weighted, the rate limits had to be enforced by using some engineering and increasing or decreasing the weights on some of the

**Table 3.6 Summary of Lateral-Directional RQAS Response
for a Sea-Level Climb -- Ouput-Weighting**

Time Domain Response:

	Open Loop		Baseline RQAS		Percent Reduction	
	Max.	RMS	Max.	RMS	Max.	RMS
a_y (f/s2)	6.1	2.7	3.4	1.1	44%	59%
β (deg)	6.2	2.8	6.0	1.9	3%	32%
p (deg/s)	6.4	2.7	1.8	0.6	72%	78%
r (deg/s)	10.6	4.8	6.8	2.7	36%	44%
ϕ (deg)	3.2	1.3	1.7	0.7	47%	46%
δ_{df} (deg)	-	-	6.2	2.8	-	-
δ_{sr} (deg)	-	-	14.7	5.7	-	-
$\dot{\delta}_{df}$ (deg/s)	-	-	51.4	-	-	-
$\dot{\delta}_{sr}$ (deg/s)	-	-	27.1	-	-	-

Table 3.6 Summary of Lateral-Directional RQAS Response
for a Sea-Level Climb -- Output-Weighting
(Continued)

System Eigenvalues:

	Open Loop		Baseline RQAS	
	Frequency	Damping	Frequency	Damping
Spiral Mode	0.02	-1.0	0.78	1.0
Roll Mode	2.7	1.0	7.4	1.0
Dutch Roll	2.1	0.12	2.2	0.58
Dutch Roll	2.1	0.12	2.2	0.58
Servo	10.0	1.0	6.8	0.87
Servo	10.0	1.0	6.8	0.87

Note 1: Baseline RQAS Frequency and Damping are based on
roots of the W'-Plane.

Optimal Gain Matrix:

$$K = \begin{bmatrix} 2.0004 & -0.8556 & -0.6140 & -1.0563 \\ -0.0932 & 1.1370 & -2.4060 & 1.1638 \end{bmatrix}$$

Weighting Matrices -- Diagonal Elements:

$Q' = (0.05, 10.0, 0.1, 0.75, 10.0)$

$R' = (7.0, 1.8)$

other variables, most importantly the acceleration. The output-weighting designs did get slightly better acceleration reductions, but the differential flap deflection rate was increased by about 60%. These factors must be balanced out in the final selection of an algorithm for implementation.

The system eigenvalues of Table 3.6 are all well behaved. The Dutch Roll damping has been increased by a large margin over the unaugmented aircraft. The unstable spiral mode has been strongly stabilized. A question might arise if this is too stable for the pilots. That is a subject recommended for future investigations. The roll mode eigenvalue also has been pushed far into the left half of the W'-plane. This is comparable to the high frequencies developed in the short period mode by output-weighting.

The output-weighting designs and performance summaries for all flight conditions can be found in Appendix B.

3.3 GAIN SCHEDULING

The topic of gain scheduling for aircraft control systems is always a complex one. The need for gain scheduling arises from the variation of the aircraft open loop dynamics throughout its operation envelope. The feedback gains developed by optimal control techniques mirror the aircraft dynamics variation due to the dependence of the optimal regulator solution on the aircraft state equation. Therefore, many distinct sets of gains are needed to cover the flight envelope. There are two ways of solving this problem. One is to only use one set of gains for the entire flight envelope, and the other is to schedule the gains to coincide with the current flight condition.

One set of fixed gains, constant for all flight conditions would be very easy to implement. The questions that need to be addressed for fixed gain implementations are related to the degradation of performance by the fixed gains over the optimal gains and the stability of the fixed gain controlled aircraft in the entire flight envelope. If a fixed gain design is desired, the question of how to choose the gains arises. They may be chosen by averaging the gains for all of the available flight conditions, or, more likely, they may

be chosen by some sort of weighted average because all available designs may not be deemed equally important.

The other method of handling the multiple sets of gains is gain scheduling. If gain scheduling is chosen, the scheduled gains must still be determined. Two major questions arise. What parameter (or parameters) should the gains be scheduled on and how should the gains be fit between design points? Common parameters used for gain scheduling include aircraft velocity, center of gravity location, and trimmed control surface position. The gains are usually fit between design points by some sort of curve fitting technique. This can introduce non-optimal gains though, i.e. the scheduled gains at the design points are not equal to the optimal gains. The questions of performance degradation and stability become important for these non-optimal gains.

The baseline optimal designs for the Cessna 402B (Appendix B) were all optimized for a particular flight condition. Due to the variation of the 402B dynamics, the controller gains do vary "significantly" with flight condition. On the other hand, they are designs for a particular aircraft so the corresponding row and column positions in the gain matrices take on values that are in general of the same sign and order of magnitude although this is not universally true. All of these

items may be seen by comparing the optimal design gains in Tables B.21 through B.40 which cover all flight conditions for both the longitudinal and lateral-directional controllers using control-rate-weighting and output-weighting.

Initially it was thought that gain scheduling for the 402B would be necessary. The implementation problems would be somewhat alleviated by the large amount of computing power available in the proposed onboard flight computer. If scheduled, the gains would be based upon a combination of forward velocity, trimmed flap deflection, and center of gravity location. These parameters would distinctly identify each basic flight condition allowing for appropriate gain scheduling.

For the initial work on the RQAS gain scheduling problem, four sets of fixed gains were chosen and tested for feasibility. The four sets are

1. Longitudinal Control-Rate-Weighting Fixed Gains

2. Lateral-Direction Control-Rate-Weighting
   Fixed Gains

3. Longitudinal Output-Weighting Fixed Gains

4. Lateral-Directional Output-Weighting
   Fixed Gains.

These fixed gains were determined by comparing all of the optimal gains for the five flight conditions and choosing a gain for each matrix position which would

come closest to most of the values. An average was not directly taken because the five flight conditions were not felt to be equally important. The take-off and approach conditions generally had optimal gains which were considerably different than the other three conditions. This was due to the aircraft forward velocity in these conditions and especially the trim flap deflection in the approach condition.

The results of applying the fixed gain designs to the five flight conditions and the three longitudinal center of gravity locations follows in the next five sections. Included in these sections are figures which depict the accelerations and control surface activity for the baseline optimal designs and for the fixed gain designs. The fifth section investigates the stability of the fixed gain designs as compared to the baseline designs.

The general results of this analysis indicate that no gain scheduling is needed. It is recommended that the issue be reexamined as refinements are made to the vehicle model. This would include models of the test aircraft with the modified controls.

3.3.1 LONGITUDINAL CONTROL-RATE-WEIGHTING FIXED GAINS

The results of the longitudinal control-rate-weighting fixed gain tests are presented in Figures 3.1, 3.2, and 3.3. Each plot contains the results of time simulation for three center of gravity locations. These are the quarter chord c.g., which is representative of the mid portion of the c.g. travel range, the forward most c.g. location, and the aft most c.g. location. All basic designs were done at the mid c.g. location. For the longitudinal designs, plots of the vertical RMS acceleration and the control surface activity, i.e. maximum deflections and rates, were made.

The fixed gain matrix for the control-rate-weighting longitudinal design is

$$K = \begin{bmatrix} 28.0 & 0.0 & -3.0 & -13.0 & 9.0 & 6.0 \\ 170.0 & 0.0 & 14.5 & 24.5 & 3.0 & 38.5 \end{bmatrix} .$$

Several points should be noticed. First, the column of zero elements corresponds to the velocity feedback column. The actual elements existed in the optimal gains, but they were several orders of magnitude smaller than all of the other elements of the matrix. Therefore, they were set to zero. It might be argued that the velocity is several orders of magnitude larger than the other variables, but this velocity is a perturbation

around the steady state, so it should never be large, especially if the linear models are to hold. It is also obvious that all of the elements were rounded to "nice" values. This is true, but the method of determining these gains didn't warrant any more accuracy. These gains could be directly compared to the baseline optimal gains. For some flight conditions, the gains are nearly identical, and for other conditions there are large differences. It remains to be seen how the differences affect the outcome.

The RMS vertical acceleration is plotted in Figure 3.1 for the fixed gain design, the baseline design and the unaugmented, open loop, aircraft. All results are generated with the same gust field so all results are directly comparable. The fixed gain designs perform nearly the same as the baseline designs. In the take-off flight condition, the fixed gain controller works better. The 0.11g line is the RQAS upper design limit for acceptable vertical accelerations. The 0.055g line indicates a lower limit below which further reductions are deemed unnecessary and cost prohibitive.

The excellent acceleration reduction of the fixed gain designs is not without its downfalls. These may be seen in the control surface activity shown in Figures 3.2 and 3.3. All flight conditions except the take-off
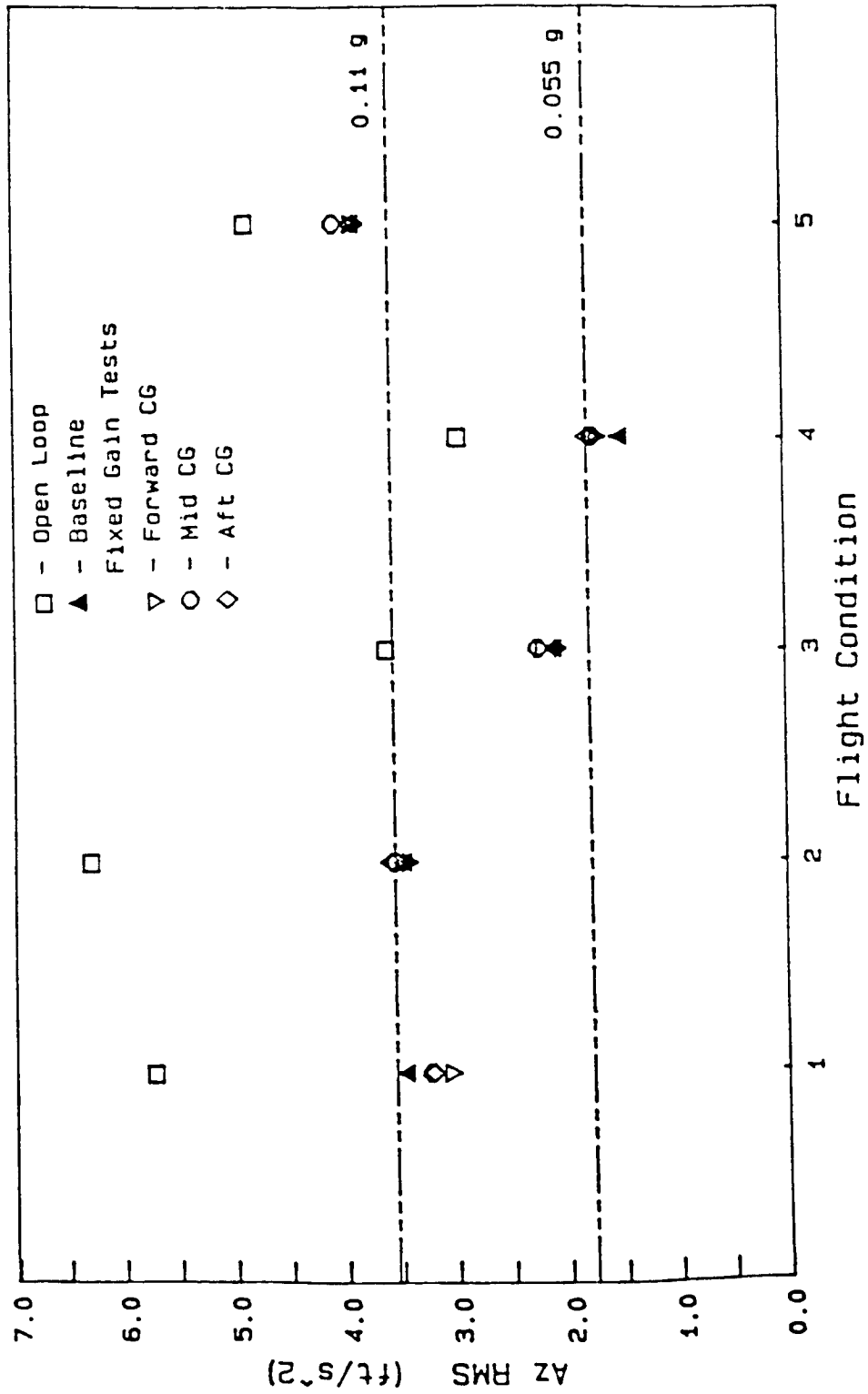
Figure 3.1   Longitudinal Control-Rate-Weighting
             Fixed Gain Acceleration Performance

54

perform reasonably well. All values are near enough to the baseline to call them equal within the given accuracy of the models. Maximum rates and deflections for both the flaps and the separate surface elevator increase for the take-off flight condition. That is the reason for the larger acceleration reduction. The rates, although larger, are still within the design limits. The surface deflections, though, are not within their limits. If the deflection limits were enforced, the vertical acceleration performance would deteriorate, but it is felt that it would not be too substantial. The same sort of argument could be made for the separate surface elevator deflection for the approach flight condition.

The effect of center of gravity location is not particularly strong for the control-rate-weighting designs. The RMS accelerations are nearly identical for all of the flight conditions. The center of gravity location is a little more apparent on the surface activity. The aft center of gravity location requires more flap deflection and rate than the other locations. The forward center of gravity location, on the other hand, uses the separate surface elevator more.

Figure 3.2   Longitudinal Control-Rate-Weighting
             Fixed Gain Direct Lift Flap Activity

Figure 3.3   Longitudinal Control-Rate-Weighting Fixed
Gain Separate Surface Elevator Activity

3.3.2 LATERAL-DIRECTIONAL CONTROL-RATE-WEIGHTING FIXED GAINS

The lateral-directional fixed gain design response can be seen in Figures 3.4 through 3.6. The control-rate-weighting fixed gains are

$$
K = \begin{bmatrix} 25.0 & -10.0 & -7.5 & -12.0 & 16.5 & -0.7 \\ -2.0 & 3.5 & -14.5 & 3.5 & -0.4 & 7.0 \end{bmatrix}.
$$

The lateral accelerations are plotted in Figure 3.4 for the open loop aircraft, the baseline optimal design, and the fixed gain designs. The results of the baseline and fixed gain designs are nearly identical. Only in the approach flight condition is there any difference in the RMS acceleration. For that case, the fixed gain design decreases the acceleration slightly. The reason for that reduction can be seen in the control surface activity show in Figures 3.5 and 3.6. While the differential flap and separate surface rudder deflections and rates of the other four conditions remain nearly the same, the deflections and deflection rates increase slightly in the approach condition. In the longitudinal case an increase is not good because the surfaces are working near their RQAS design limits. Here the increases are not important because the surfaces are below
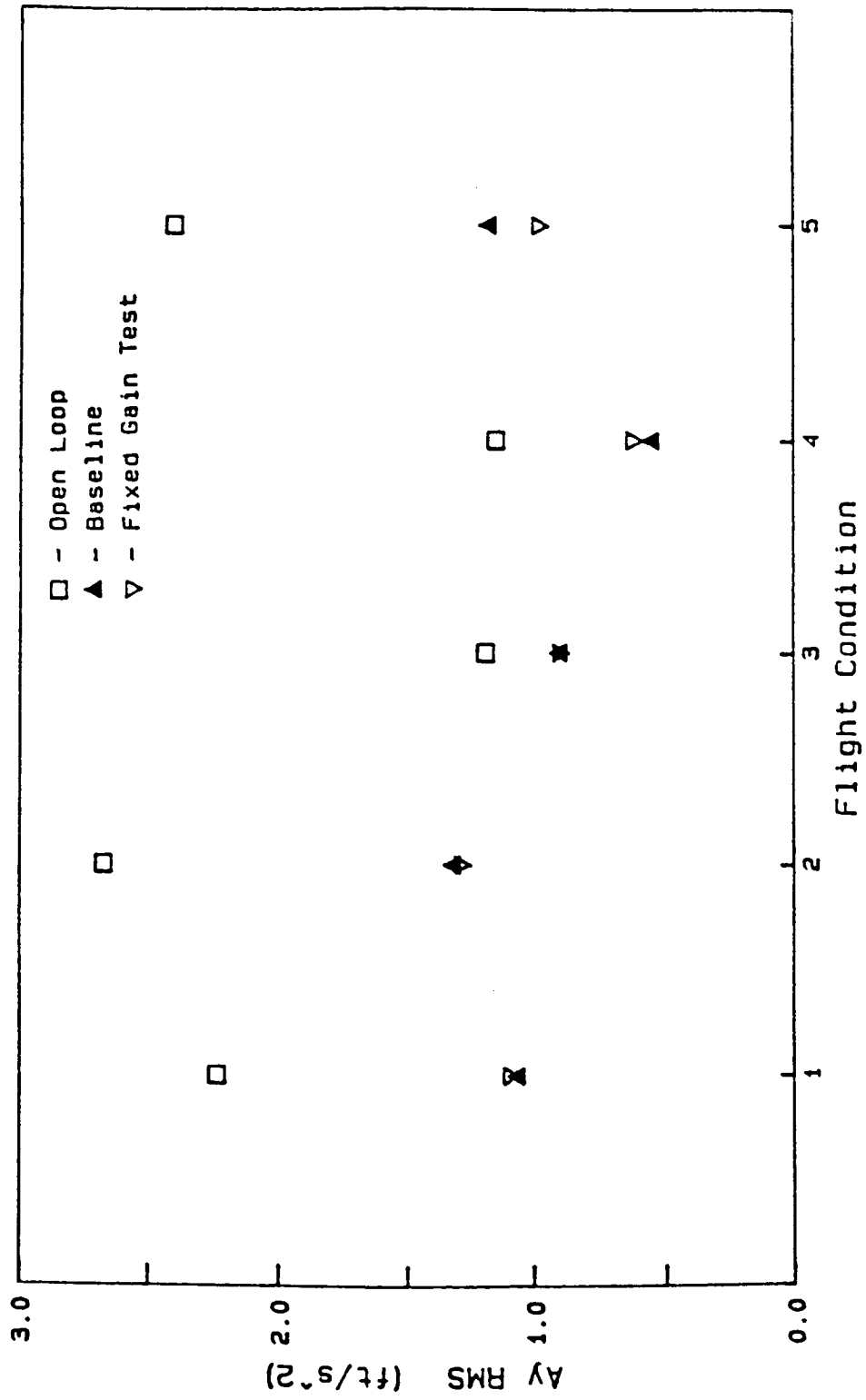
Figure 3.4   Lateral-Directional Control-Rate-Weighting
            Fixed Gain Acceleration Performance

59

Figure 3.5   Lateral-Directional Control-Rate-Weighting
Fixed Gain Differential Flap Activity

60
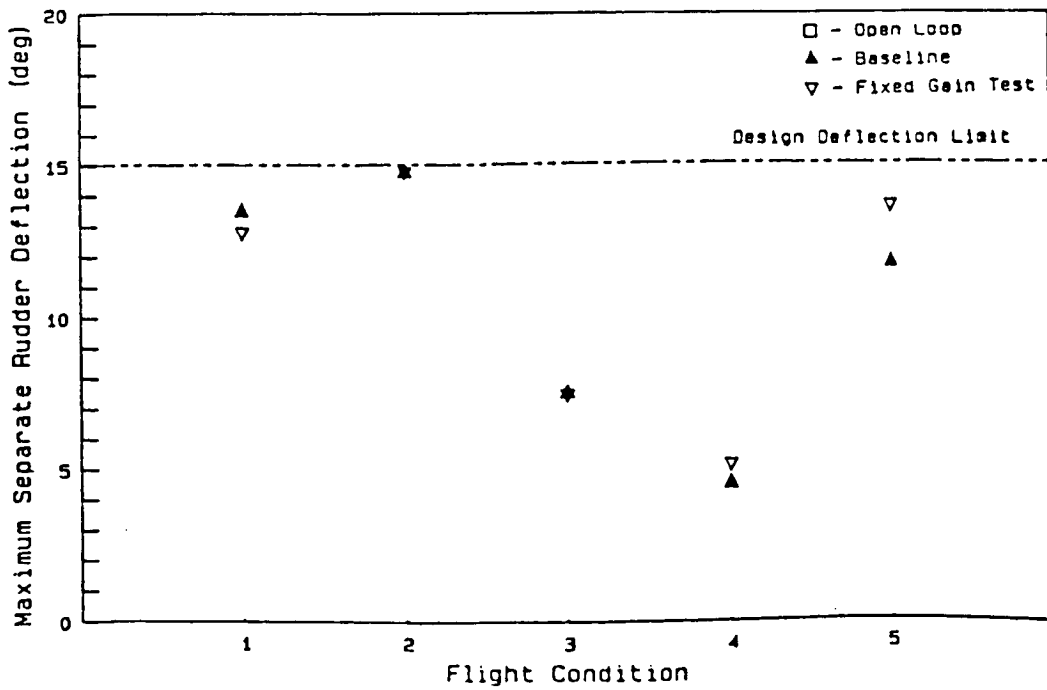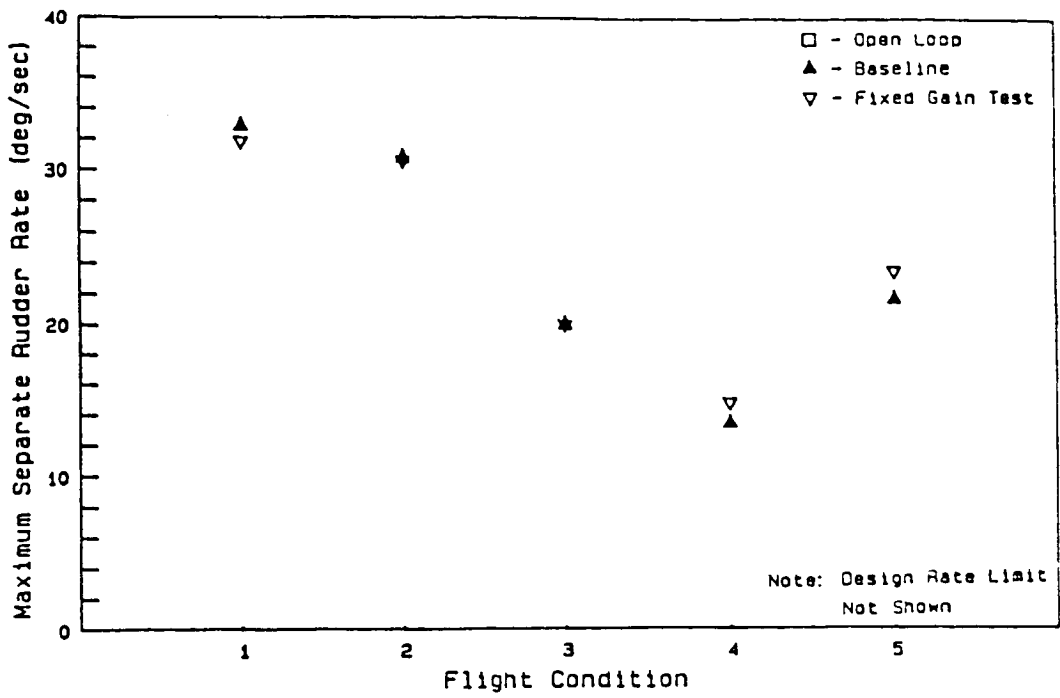
Figure 3.6 Lateral-Directional Control-Rate-Weighting Fixed
Gain Separate Surface Rudder Activity

their rate and deflection limits. The lateral-directional motion does not seem to be affected by flight condition as much as the longitudinal motion.

3.3.3 LONGITUDINAL OUTPUT-WEIGHTING FIXED GAINS

The results of the application of the longitudinal output-weighting fixed gain designs were very similar to the control-rate-weighting designs. The results can be seen in Figures 3.7 through 3.9. The fixed gain that was used for this analysis was

$$K = \begin{bmatrix} -0.5 & 0.0 & -1.6 & -2.5 \\ 4.5 & 0.0 & 0.5 & 1.0 \end{bmatrix} .$$

A quick comparison of these gains to the longitudinal control-rate-weighting fixed gains of Section 3.3.1 shows these gains to be quite a bit smaller in magnitude. There are of course only 4 feedback variables here as compared to 6 for the control-rate-weighting designs. The perturbation velocity feedback terms have again been set to zero since the were generally two or more orders of magnitude smaller than the other gains.

The acceleration response of the fixed gain designs is nearly the same as the baseline designs for all flight conditions. As can be seen in Figure 3.7, only the acceleration of the approach flight condition
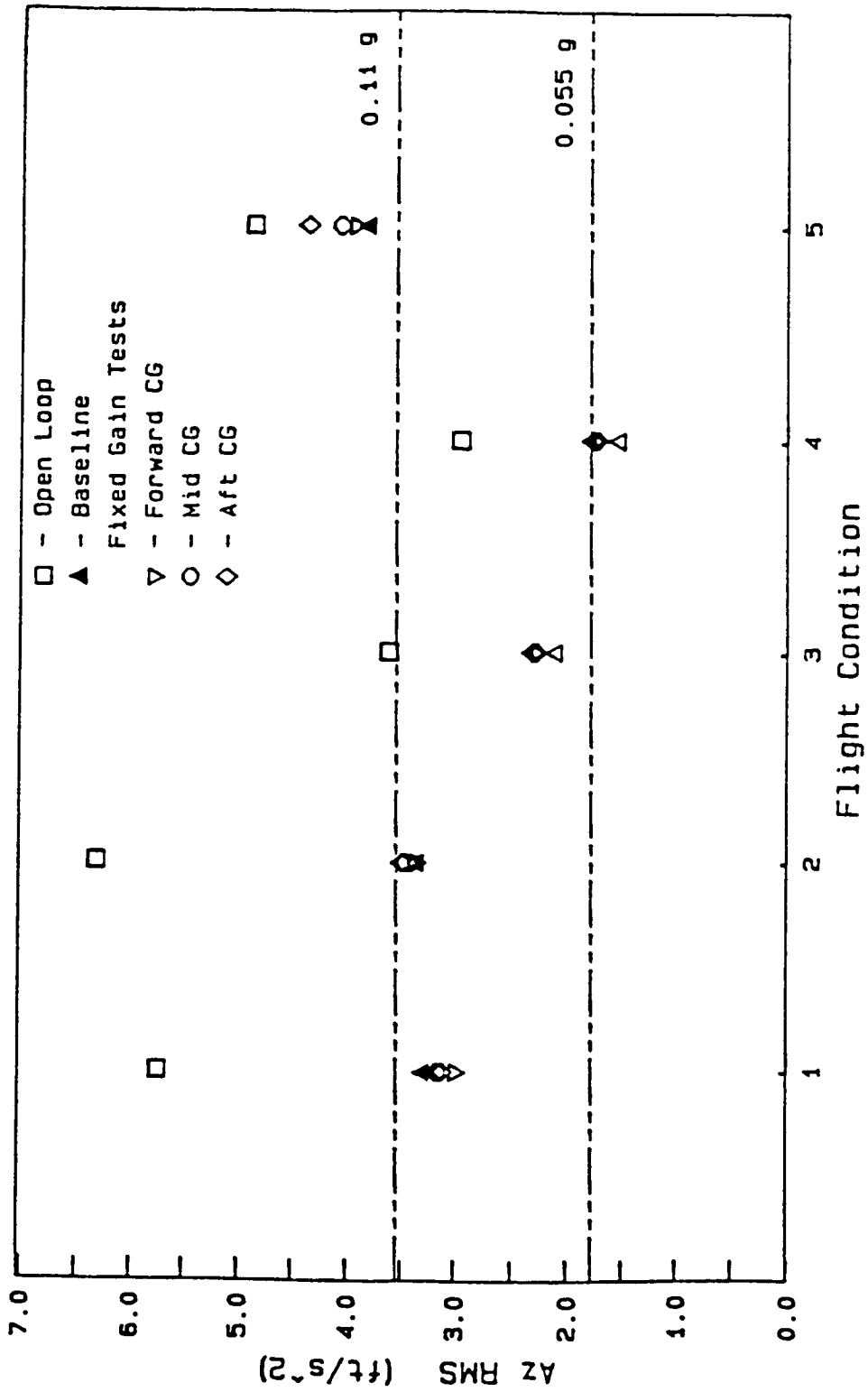
Figure 3.7   Longitudinal Output-Weighting
Fixed Gain Acceleration Performance

changes. Here there is a small increase over the baseline design. Although the fixed gain design has RMS accelerations that are above the RQAS design limit, so does the baseline design. The approach flight condition was very difficult to design to because the trim flap deflection reduced the effectiveness of the flaps as direct lift devices.

The direct lift flap and separate surface elevator activity is shown in Figures 3.8 and 3.9. There is a wide variation of the surface deflections and rates between the baseline designs and the fixed gain designs. Both the flap rates and the separate elevator rates were within the design limits even with the increases caused by the fixed gain designs. The maximum deflections for the flaps and separate elevators were not within the prescribed limits for several of the flight conditions tested. Although this is not good, at the present time it is felt that these deflections are tolerable for the current aircraft models. If the deflections were limited, the acceleration would most likely increase.
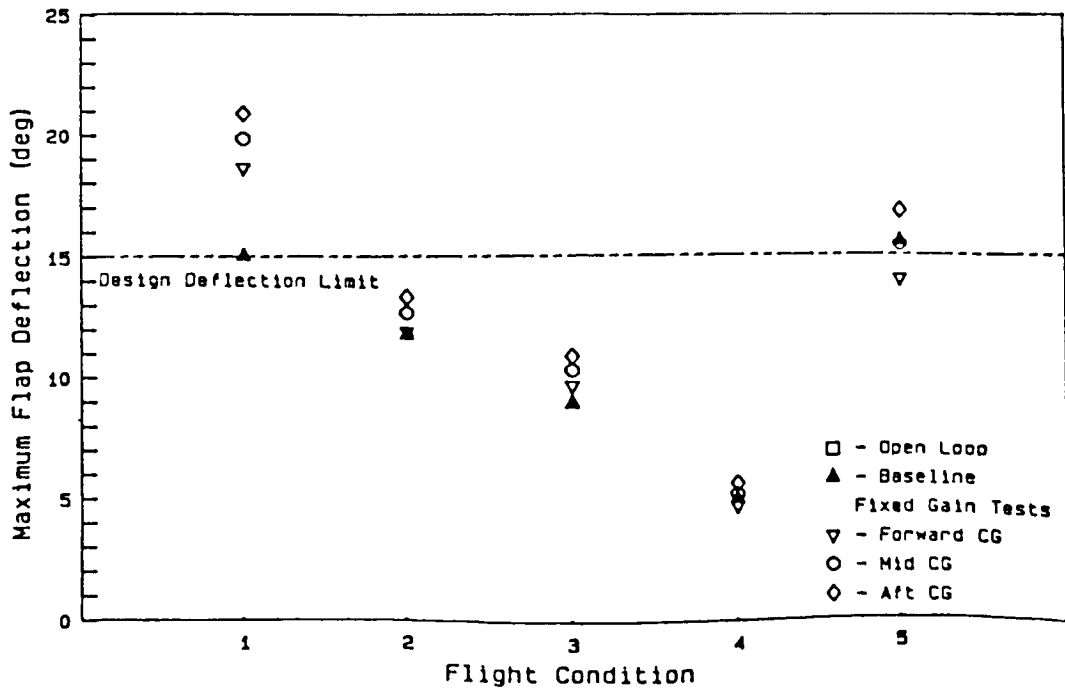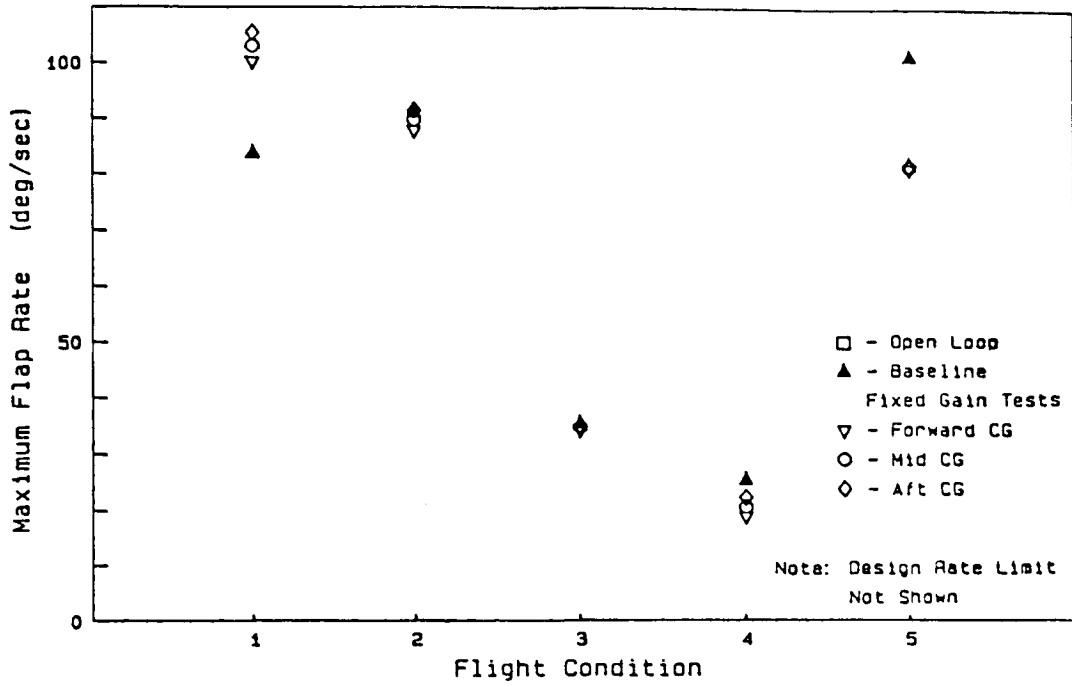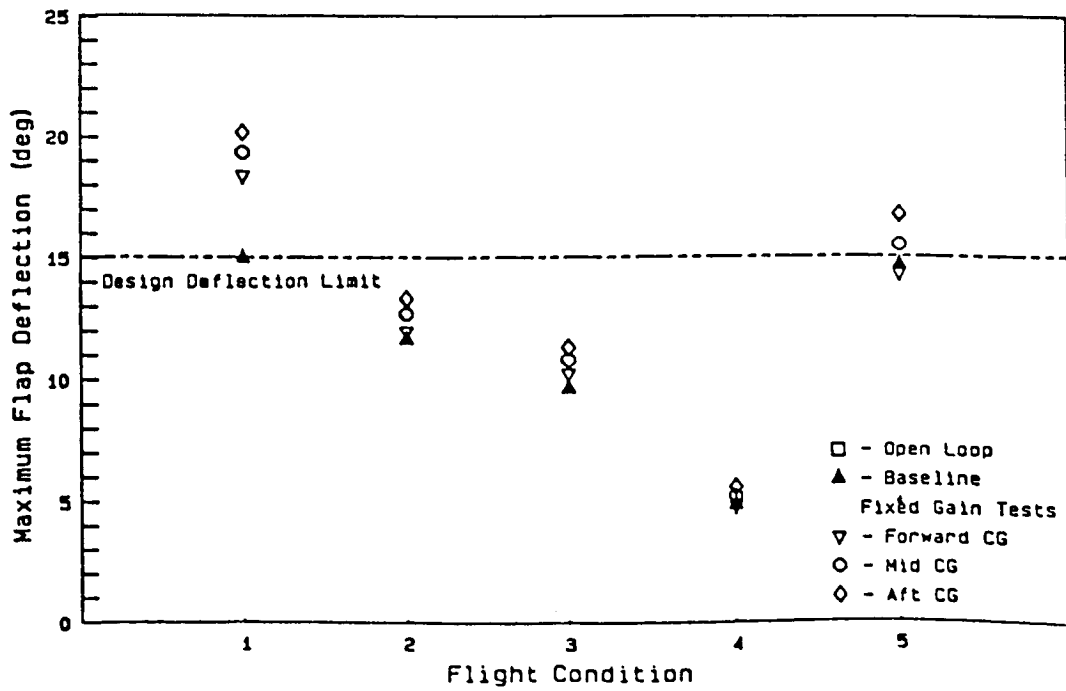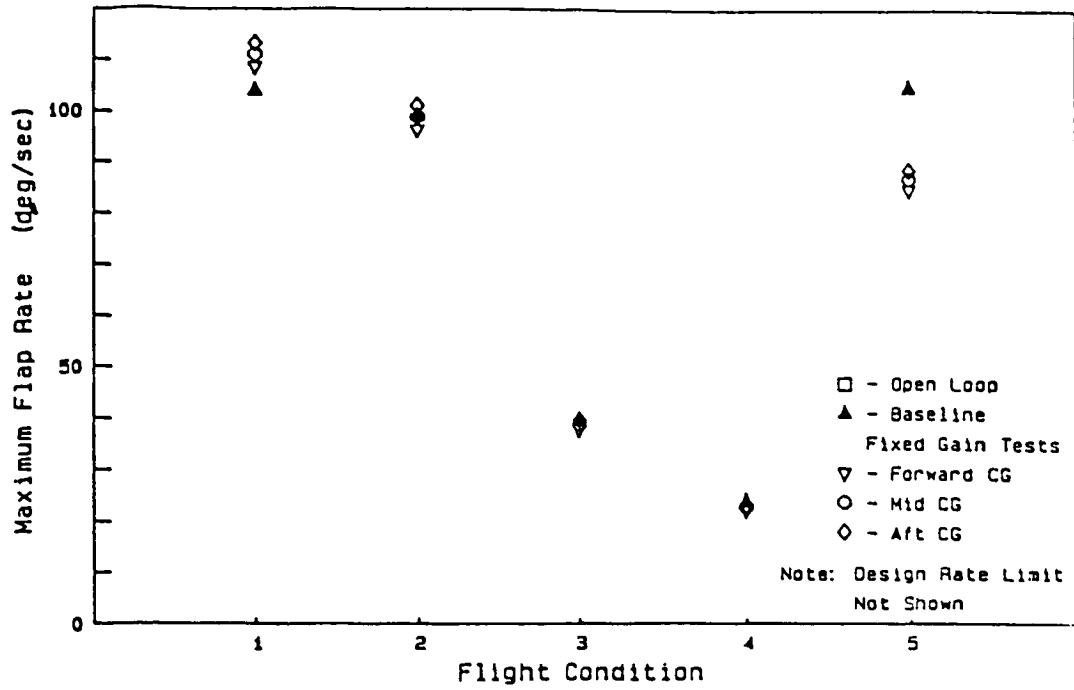
Figure 3.8   Longitudinal Output-Weighting
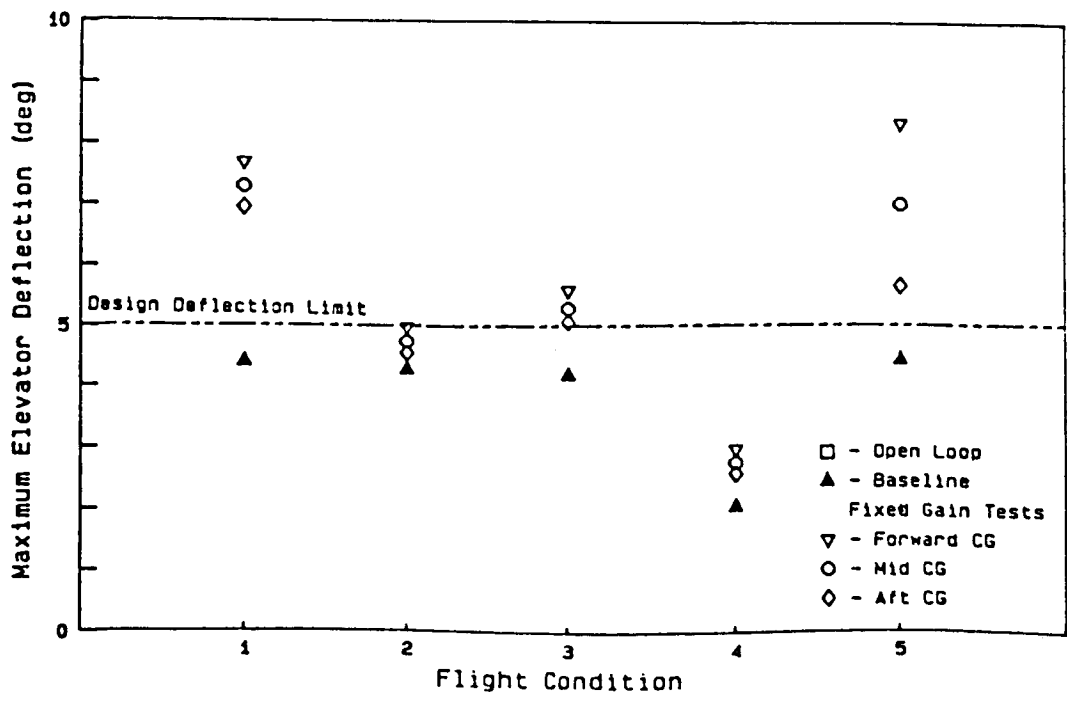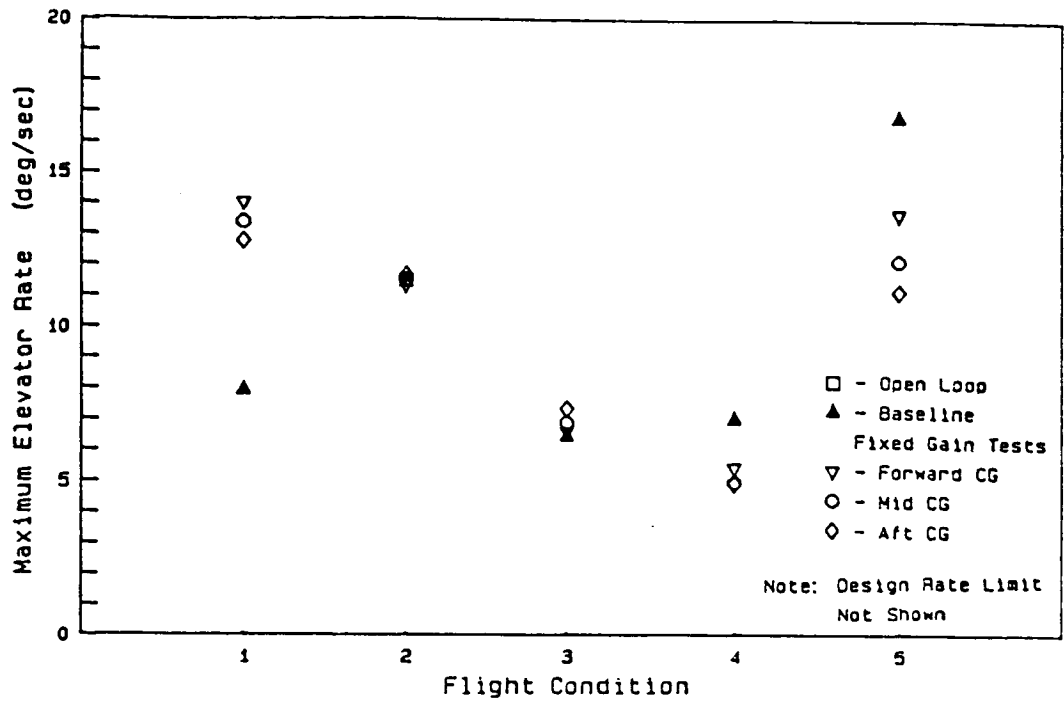   Fixed Gain Direct Lift Flap Activity
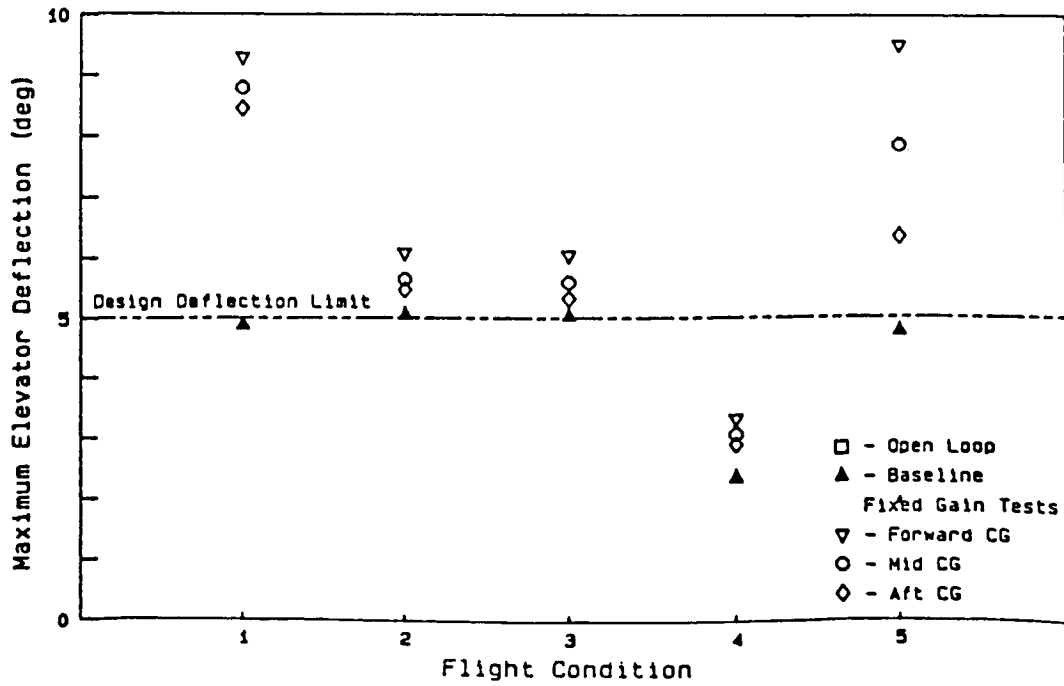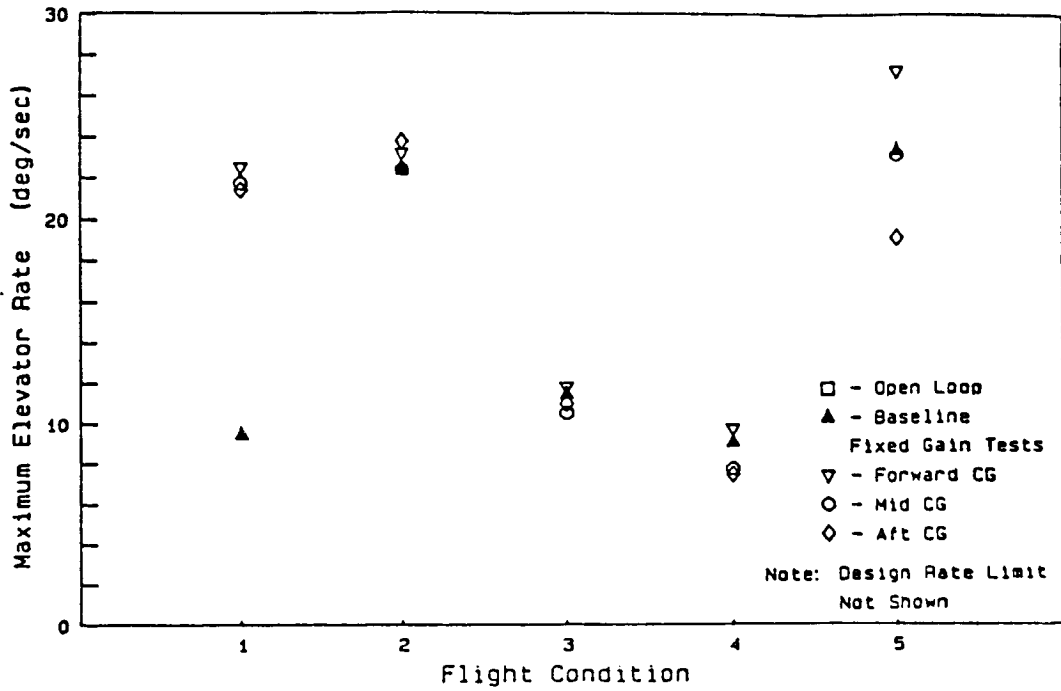
Figure 3.9   Longitudinal Output-Weighting Fixed
              Gain Separate Surface Elevator Activity

3.3.4 LATERAL-DIRECTIONAL OUTPUT-WEIGHTING FIXED GAINS

Once again, the lateral-directional designs were much easier to design, and consequently, the fixed gain design behave much nicer. The output-weighting lateral-directional fixed gain results are given in Figures 3.10 through 3.12. The fixed gains used are

$$K = \begin{bmatrix} 2.0 & -1.0 & -0.7 & -1.0 \\ 0.0 & 1.5 & -2.5 & 1.5 \end{bmatrix} .$$

The zero element in this matrix results from different circumstances than the zero elements in the longitudinal fixed gain designs. The zero element is the feedback of sideslip angle, β, to the separate surface rudder. This would seem to be an important term, and it is. But, in this case, the matrix elements from the five baseline optimal designs vary around zero giving an average of approximately zero.

The lateral RMS acceleration, given in Figure 3.10, shows that the fixed gain designs perform as well or better than the baseline optimal designs. The extra performance in the approach flight condition once again results from increased control surface activity. That activity can be seen in Figures 3.11 and 3.12. Although there is an increase in differential flap or separate surface rudder rates and deflections in some cases, all

67
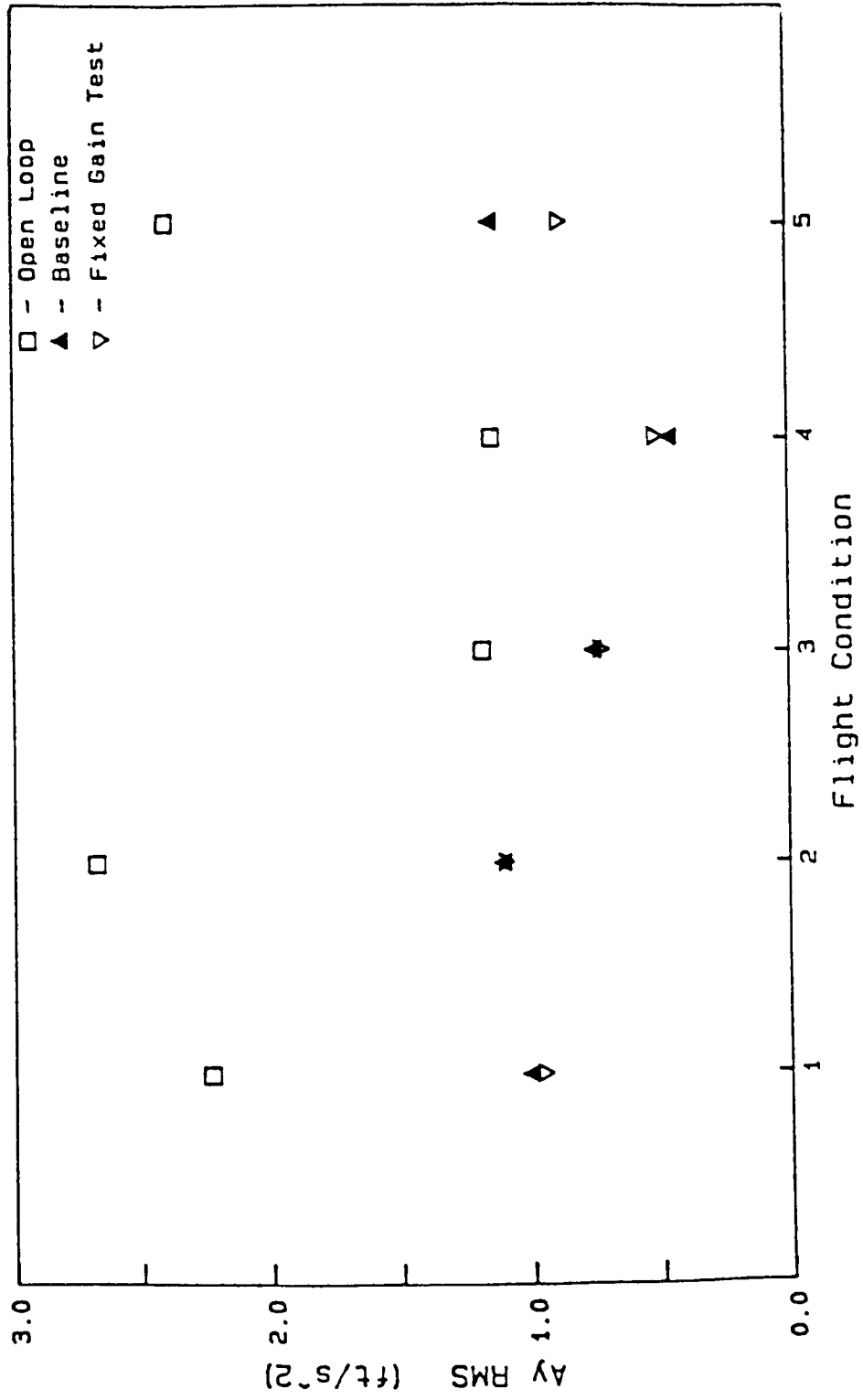
Figure 3.10   Lateral-Directional Output-Weighting
Fixed Gain Acceleration Performance

activity is below the specified RQAS design limits. All of the results for the sea-level climb conditions are closely matched between the baseline design and the fixed gain design. This happens because the fixed gains that were chosen happen to be very close to the baseline gains for all of the gain matrix positions.

3.3.5 FIXED GAIN STABILITY

While the time response of the fixed gain designs is very good, there are no assurances that the aircraft will be stable under all circumstances. The time simulations that were performed may not indicate any potentially dangerous dynamic modes of the aircraft. As a further check of the fixed gain response, the eigenvalues for the closed loop fixed gain aircraft were investigated. In addition to indicating the stability of the fixed gain controllers for all flight conditions and center of gravity locations, the eigenvalues can be compared to the eigenvalues of the baseline design to give another indication of performance degradation caused by the fixed gains. The eigenvalues for the sea-level climb flight condition will be discussed below. The fixed gain eigenvalues for the remaining flight conditions may be found in Appendix B.
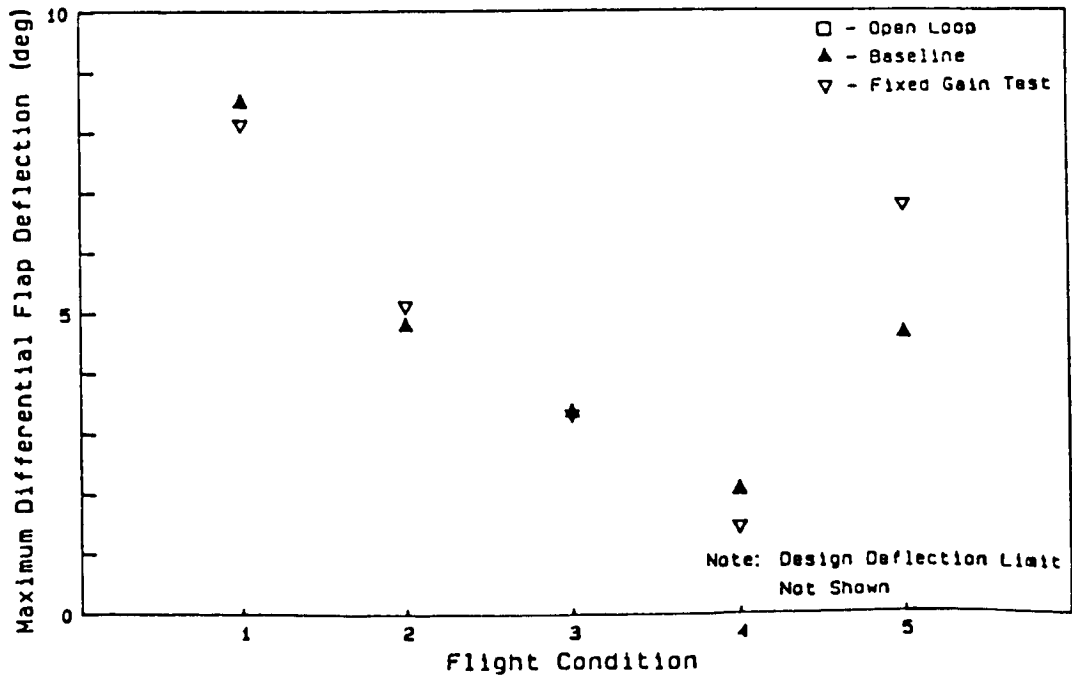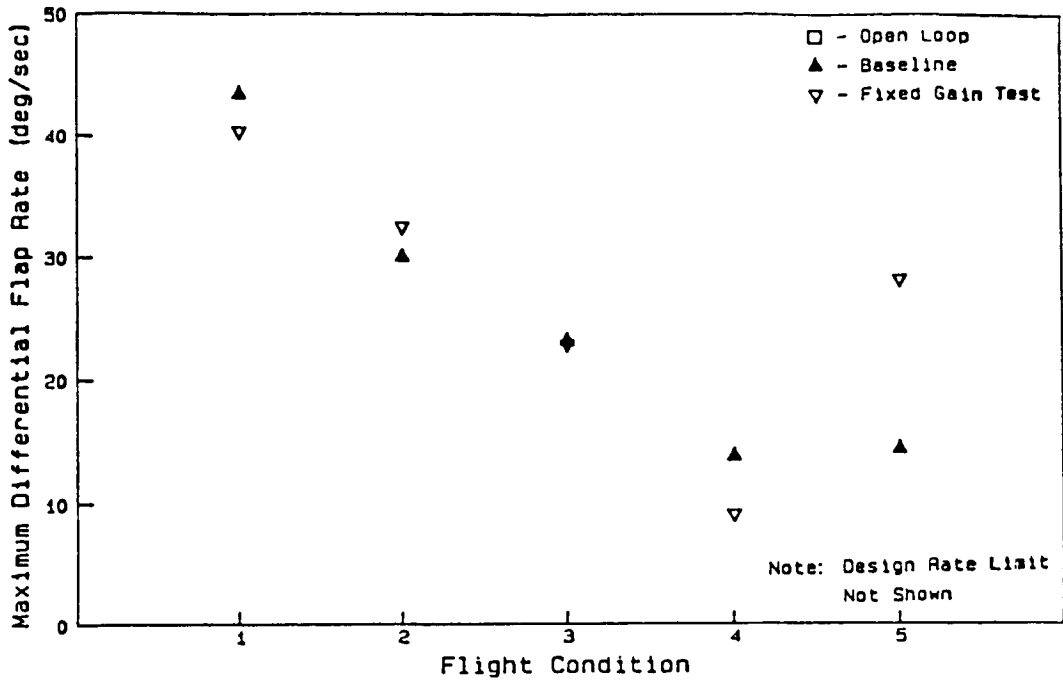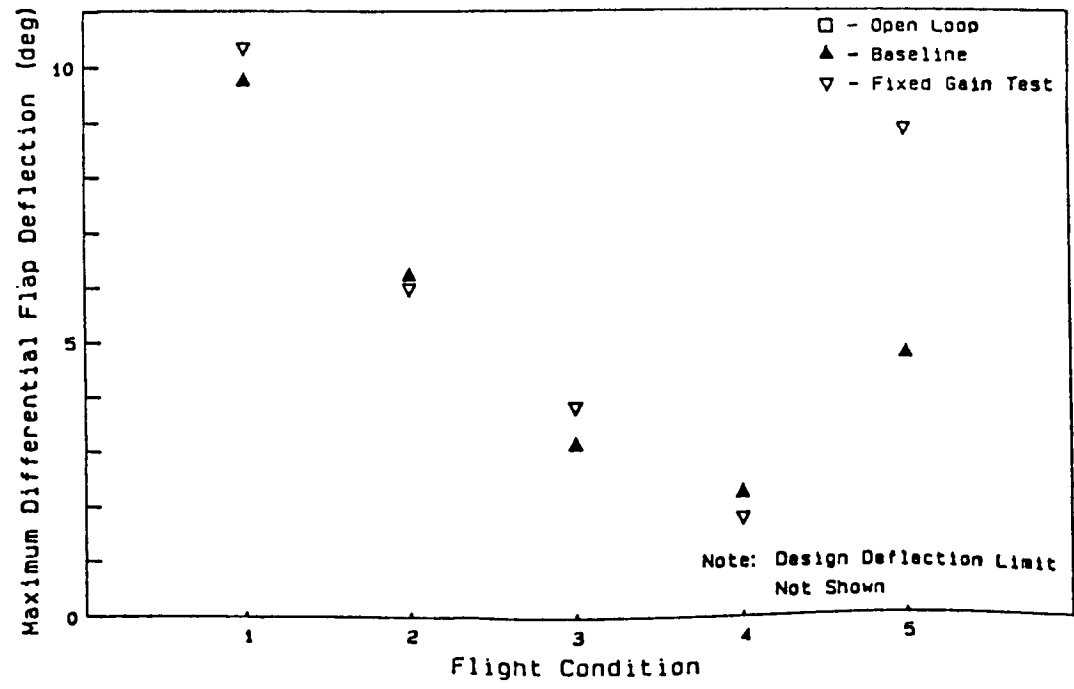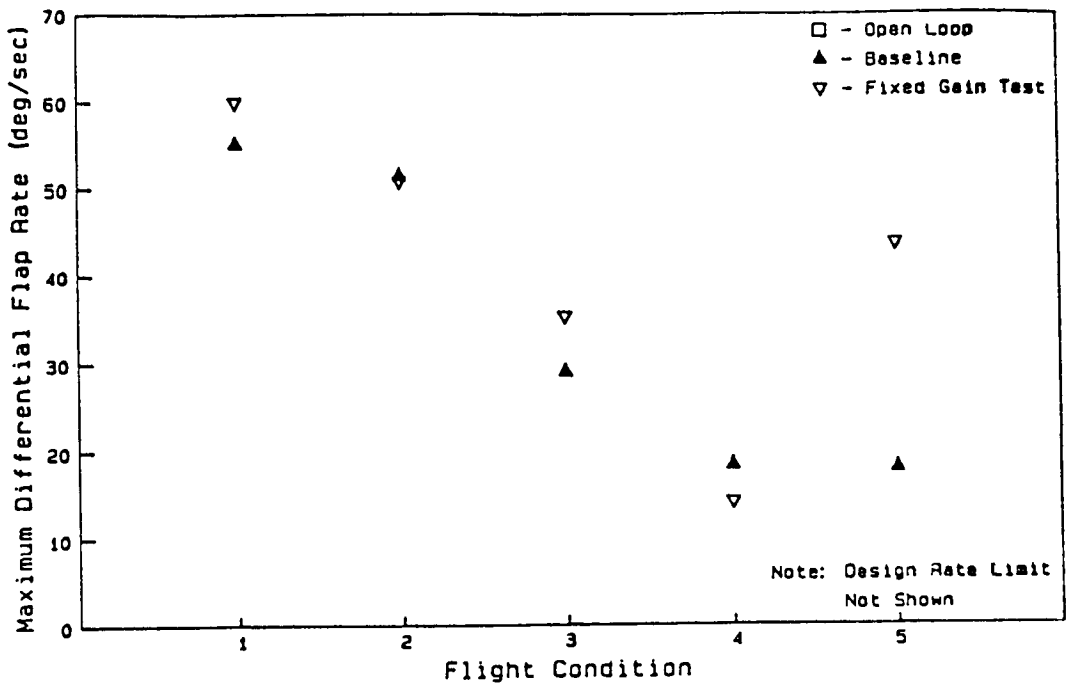
Figure 3.11   Lateral-Directional Output-Weighting
Fixed Gain Differential Flap Activity
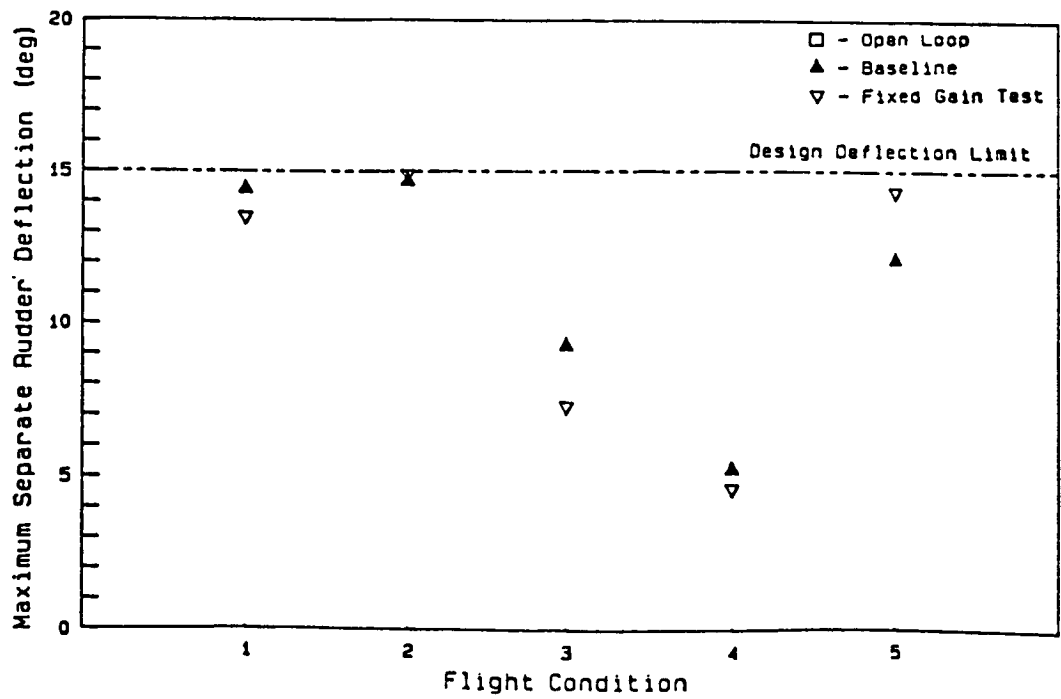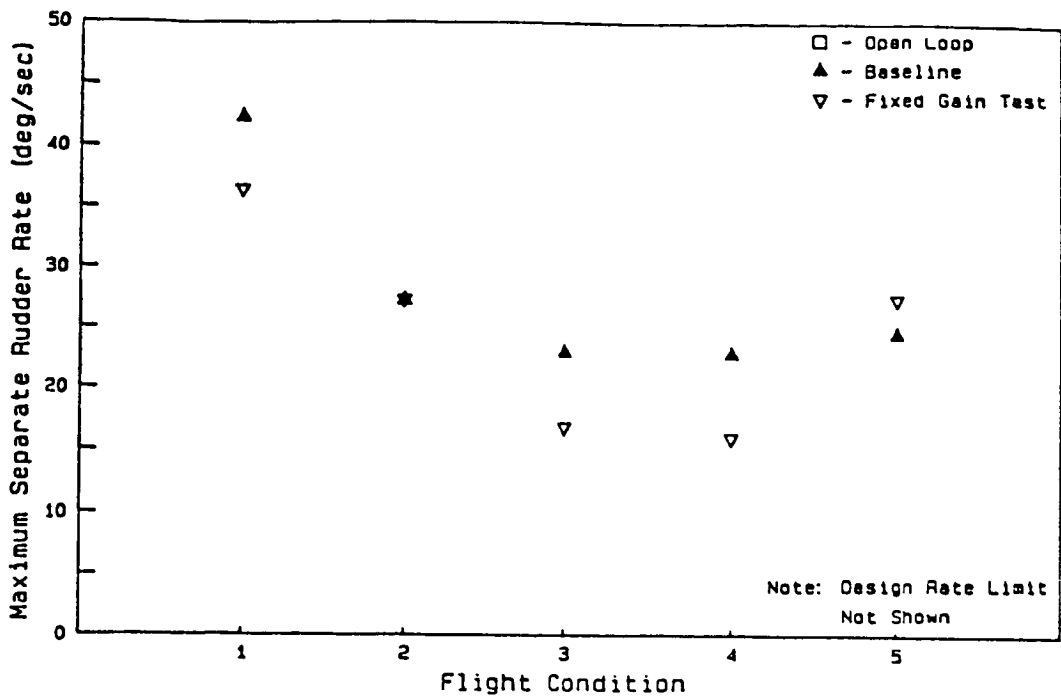
Figure 3.12   Lateral-Directional Output-Weighting Fixed
Gain Separate Surface Rudder Activity

The longitudinal control-rate-weighting fixed gain eigenvalues are given in Table 3.7 for the sea-level climb flight conditon. The eigenvalues for the fixed gain system at three center of gravity locations are included. While there is some variation of frequencies and damping ratios among the center of gravity locations, the changes are not large. That is why the time simulations for the three center of gravity locations all performed nearly identically. The fixed gain phugoid eigenvalues are considerably different than the phugoid eigenvalues of the baseline design, but the others remain similar. Although the damping on the phugoid has been decreased, it is still well damped, especially in comparison to the open loop damping.

Table 3.8 contains the eigenvalue summary for the longitudinal output-weighting fixed gain design. Again, there is nearly no difference in the eigenvalues when the fixed gain designs are implemented at the three center of gravity locations. The comparison between the baseline eigenvalues and the fixed gain eigenvalues is exactly as before. The phugoid increases in frequency and decreases in damping when the fixed gains are used. The other eigenvalues remain nearly the same.

The lateral-directional eigenvalues for the sea-level climb are given in Table 3.9 for the control-rate-

Table 3.7 Longitudinal Control-Rate-Weighting
Fixed Gain Stability for Sea-Level Climb

Baseline Eigenvalues:

Mode	Frequency	Damping
Phugoid	0.0874	0.791
Phugoid	0.0874	0.791
Short Period	6.02	0.682
Short Period	6.02	0.682
Servo	3.47	1.0
Servo	11.8	1.0
Filter	15.3	1.0
Filter	63.8	1.0

Fixed Gain Eigenvalues:

Foward c.g.		Mid c.g.		Aft c.g.	
Freq.	Damp.	Freq.	Damp.	Freq.	Damp.
0.213	0.368	0.214	0.370	0.214	0.372
0.213	0.368	0.214	0.370	0.214	0.372
6.80	0.699	6.44	0.671	6.14	0.643
6.80	0.699	6.44	0.671	6.14	0.643
2.56	1.0	2.88	1.0	3.17	1.0
11.7	1.0	11.7	1.0	11.7	1.0
15.9	1.0	15.7	1.0	15.8	1.0
63.5	1.0	63.7	1.0	63.9	1.0

Table 3.8 Longitudinal Output-Weighting Fixed
Gain Stability for Sea-Level Climb

Baseline Eigenvalues:

Mode	Frequency	Damping
Phugoid	0.0887	0.886
Phugoid	0.0887	0.886
Short Period	11.6	0.661
Short Period	11.6	0.661
Servo	1.94	1.0
Servo	11.3	1.0

Fixed Gain Eigenvalues:

Foward c.g.		Mid c.g.		Aft c.g.	
Freq.	Damp.	Freq.	Damp.	Freq.	Damp.
0.216	0.420	0.216	0.419	0.217	0.418
0.216	0.420	0.216	0.419	0.217	0.418
12.1	0.668	11.7	0.658	11.4	0.649
12.1	0.668	11.7	0.658	11.4	0.649
1.77	1.0	1.89	1.0	1.99	1.0
11.3	1.0	11.3	1.0	11.3	1.0

weighting fixed gain designs, and in Table 3.10 for the output-weighting fixed gain designs. The eigenvalues for the fixed gain designs and the baseline designs are nearly identical for both the control-rate-weighting and the output-weighting. Only the servo frequencies for the output-weighting show any change. This reinforces the findings of the time simulation. There it was noted that the fixed gain time response for this flight conditions was very close to the baseline response.

3.3.6 GAIN SCHEDULING SUMMARY

In the preceeding five sections, the time response and the stability of fixed gain controllers were investigated for five flight conditions and three center of gravity locations in both the longitudinal and lateral directions. All of the results indicate that the fixed gains will perform well enough to prevent the need for gain scheduling. There are several things which might change these conclusions. If control surface rate and deflection limits were strictly enforced, the performance of the fixed gains may be degraded beyond acceptable levels. There may be an alternative way in which to pick gains so that the performance is not degraded by the surface limits. Since all of the gains and results

Table 3.9   Lateral Directional Control-Rate-Weighting
            Fixed Gain Stability for Sea-Level Climb

	Baseline		Fixed Gain	
	Frequency	Damping	Frequency	Damping
Spiral	0.594	1.0	0.570	1.0
Roll	3.25	1.0	3.06	1.0
Dutch Roll	2.75	0.514	2.77	0.507
Dutch Roll	2.75	0.514	2.77	0.507
Servo	5.47	0.882	5.59	0.871
Servo	5.47	0.882	5.59	0.871
Filter	12.6	1.0	12.4	1.0
Filter	21.3	1.0	21.8	1.0

Table 3.10 Lateral Directional Output-Weighting
            Fixed Gain Stability for Sea-Level Climb

	Baseline		Fixed Gain	
	Frequency	Damping	Frequency	Damping
Spiral	0.776	1.0	0.683	1.0
Roll	7.39	1.0	7.06	1.0
Dutch Roll	2.22	0.578	2.30	0.586
Dutch Roll	2.22	0.578	2.30	0.586
Servo	6.84	0.874	7.31	0.833
Servo	6.84	0.874	7.31	0.833

depend so directly on the aircraft models, the entire topic of gain scheduling and fixed gain designs needs to be reinvestigated when the aircraft models are improved. If the performance of the fixed gains is close but not quite within acceptable levels, it may be possible to scheduled a single gain while all of the others remain fixed. This is a subject which has not yet been examined.

3.4 SUMMARY

Using the standard optimal regulator solution as a basis, the continuous and sampled-data solutions for two extended optimal control structures were presented. The equations necessary for the solution of these structures, control-rate-weighting and output-weighting, were presented in a summarized form. Using the design routines of ORACLS that have been implemented in the ICAD program, the two control structures were applied to a Cessna 402B aircraft for five basic flight conditions in both the longitudinal and lateral-directional modes. A discussion of the complete results for one flight condition is included here. Based upon the optimal designs, a set of fixed gains were chosen and tested. These fixed gains were checked for their feasibilty as a

simple solution for the problem of gain scheduling. The time response of these fixed gains was compared against the response of the baseline designs. With a few exceptions, the fixed gains performed well. The exceptions arose from the enforcement of deflection limits. The stability of the fixed gains was checked by examining the eigenvalues of the closed loop system. The fixed gains were all stable and the oscillatory modes were all well damped. Based upon these results, the fixed gains are a good alternative to gain scheduling. This topic will have to reinvestigated as better models of the aircraft become available.

C-2

CHAPTER 4.

SYSTEM MODIFICATIONS

To continue the investigation of the RQAS, the next step is implementation and flight testing of the proposed control laws. Several hardware related areas need to be investigated first. This chapter presents the preliminary design of the hardware required to implement a RQAS. First, an experimental system, including sensors and a flight control law computer, is defined. Next, an investigation into the possible control surface configurations is discussed. The proposed modifications to the aircraft control surfaces of the Cessna 402B aircraft are then detailed. The control surface actuator requirements are also discussed.

4.1 EXPERIMENTAL SYSTEM

The basic proposed experimental system, Figure 4.1, includes onboard sensors, a digital flight computer, a set of analog-to-digital (A/D) and digital-to-analog (D/A) converters, an onboard flight engineering station and a set of electro-hydraulic actuators, and an onboard digital data recording system. No telemetry data recording equipment is proposed.
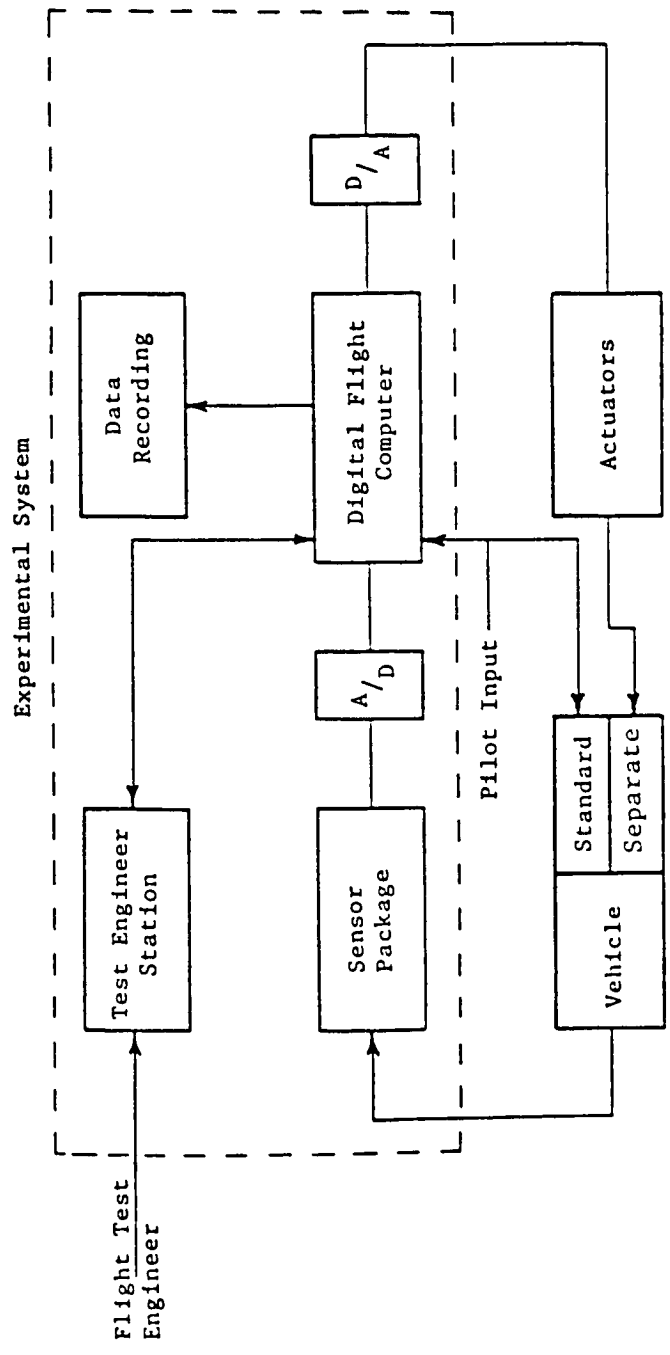
Figure 4.1   Ride Quality Experimental System

80

4.1.1 SENSOR PACKAGE

A full set of aircraft motion variable sensors is required. These include

1. Accelerometers for vertical and lateral axes

2. Angle of attack and sideslip angle booms

3. Vertical gyros for pitch and roll angle

4. Rate gyros for pitch, roll, and yaw rates

5. Sensors for temperature and both static and dynamic pressure.

The proposed package includes an angle of attack and sideslip angle boom for documentation purposes only. This angle data will not be used as control law feedback due to the inaccuracy of these types of sensors. Instead, the α and β feedback signals will be based on vertical and lateral acceleration data. The temperature and pressure sensors are used for, among other things, forward velocity determination. Pilot stick positon sensors may also be included to aid in the implementation of a controller which eliminates problems associated with the RQAS feedback during maneuvers. This is an area currently under research. Table 4.1 indicates some suggested accuracy and range limits for the sensors. These values were chosen based upon currently available sensors and preliminary estimates of necessary data limits. Detailed analysis has yet to be performed.

Table 4.1 Suggested Sensor Requirements

Variable	Sensor	Resolution or Accuracy *	Range
A_y	Accelerometer	0.0020 g's	$\pm$0.5 g's
A_z	Accelerometer	0.0024 g's	$\pm$5.0 g's
θ,ϕ	Vertical Gyro	0.5 deg.	$\pm$30 deg.
P,Q,R	Rate Gyro	0.5 deg/sec	$\pm$50 deg/sec
Temperature	Transducer	2.0 deg. F	-65 to 120 deg. F
Static Pressure Trans.		0.010 psia (25 ft)	0 to 25,000 feet
Dynamic Pressure Trans.		0.005 psia (4 knots)	40 to 150 knots

* Whichever value is larger.

4.1.2 FLIGHT ENGINEERING STATION

The proposed flight engineering station is composed of a mode control panel for controlling the various control laws to be implemented and a real time system monitoring system. Also, this station will contain the digital data recording system. The detailed design and selection of equipment for the flight engineering station has yet to be performed.

4.1.3 DIGITAL FLIGHT COMPUTER

The proposed digital flight computer is the ROLM 1666. This computer is a state-of-the art general purpose minicomputer designed for airborne applications. It is proposed due to its ability to use higher order language (FORTRAN) and floating point arithmetic. This capability can greatly reduce the time required to develop and checkout flight coding. The ROLM 1666 has been used succesfully in other flight test programs (Reference 9). The characteristics of the ROLM 1666 are summarized in Table 4.2.

Table 4.2   ROLM 1666 Characteristics (Reference 9)

Description: General purpose 16-bit minicomputer
                         designed to MIL-E-5400 specifications

Memory: 32,768 words of 1 μsec ferrite core

Instruction Execution Time:

(Time in μsec, register-to-register operations)

	Fixed Point (16 bit)	Floating Point (32 bit)
Add	1.0	1.8 to 4.8
Multiply	5.2 to 5.4	3.6 to 4.8
Divide	9.2 to 9.6	8.0 to 8.8
Load, Store	2.0	4.8

Support
Software: Real-Time Disk Operating System (RDOS)
                         supports   text   editors,   a   FORTRAN
                         compiler, and a linking loader, all
                         used in constructing executable save
                         files. Application programs use the
                         Real-Time Operating System (RTOS) for
                         flight tests.

4.2 CONTROL SURFACE MODIFICATIONS

This section discusses the control surface modifications required to implement a ride quality augmentation system on a Cessna 402B airplane. The control surfaces investigated for the RQAS are a separate surface elevator and direct lift flaps for longitudinal control and a separate surface rudder and differential flaps for lateral-directional control. The following sections describe the modification options investigated and include preliminary structural drawings of the recommended options.

4.2.1 SEPARATE SURFACE ELEVATOR

To alleviate any feedback of the RQAS control surface motions to the pilot, an elevator separate from the primary elevator is used by the RQAS. The following characteristics were assumed as requirements for the separate surface elevator (SSE):

1. SSE area approximately 20% of the existing elevator area.

2. One SSE surface on each side of the fuselage.

3. SSE surfaces linked by a single torque tube.

4. Torque tube driven by a single actuator.

85

Two options which meet these four criteria were investigated:

1. Concentric torque tubes: SSE hinged about the primary elevator torque tube (Figure 4.2).

2. Parallel torque tubes: SSE hinged about an axis parallel to and behind the primary elevator torque tube (Figure 4.3).

4.2.1.1 CONCENTRIC TORQUE TUBE ARRANGEMENT

Figure 4.2 illustrates the concentric torque tube arrangement. The SSE pivots about the primary elevator torque tube, aided by a system of bearings and brackets. This arrangement is similar to the separate surface elevator system used by Prins et. al. for a separate surface stability augmentation system controlled Beechcraft Model 99 (Reference 10).

Although this arrangement offers flexibility in the location and size of the separate surface elevator, the existing elevator must be modified and the modifications are complex. Also, the thickness limitations of the primary elevator may require a redesign of the primary elevator torque tube.

Separate Surface Elevator

Primary Elevator

Trim Tab

1. Primary Torque Tube
2. Separate Surface Torque Tube
3. Bearing Bracket
4. Bracket
5. Trim Tab Push Rod Channel
6. Primary Elevator Hinge

Original Elevator
Inboard Station
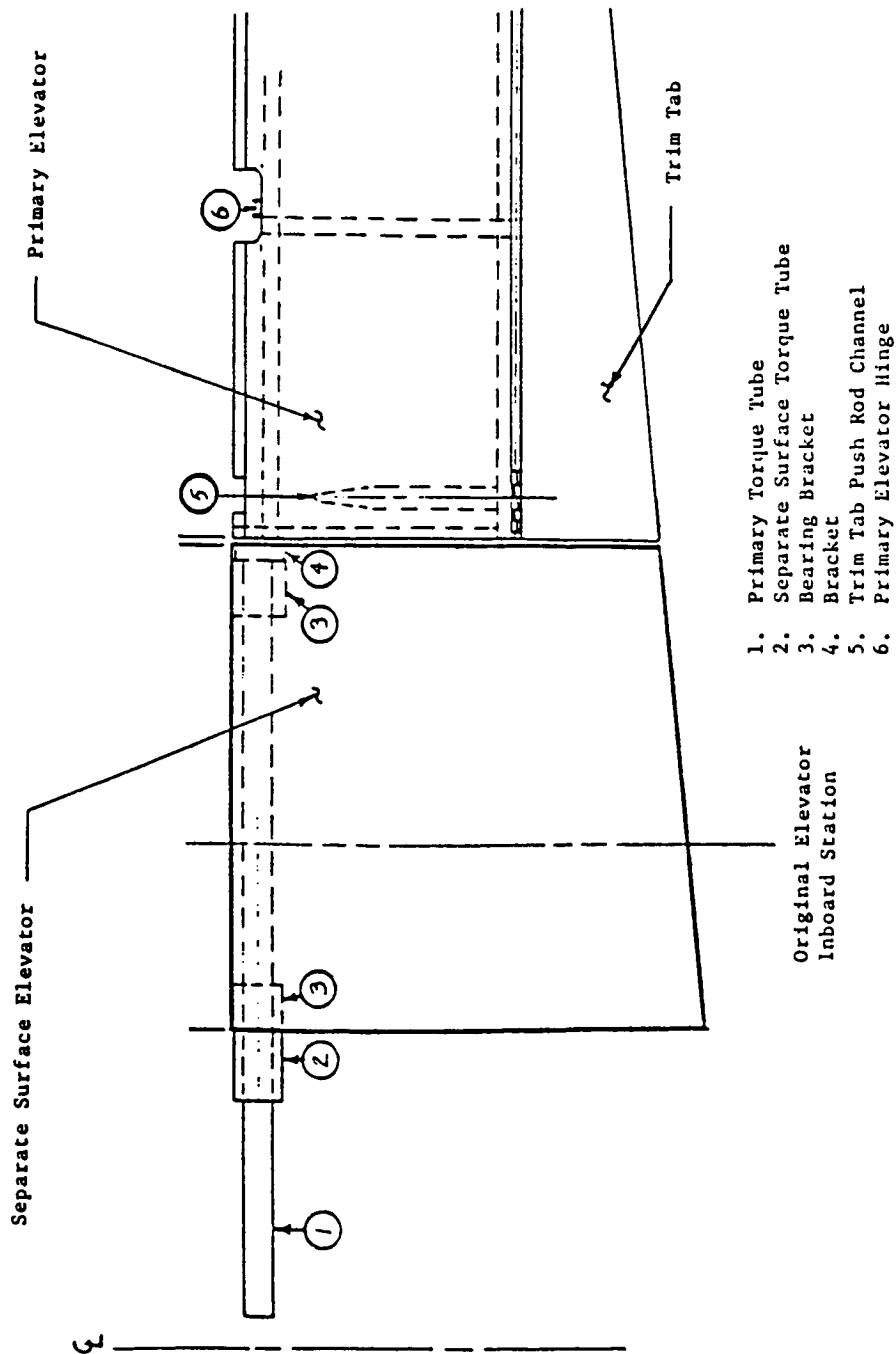
Figure 4.2   Separate Surface Elevator: Concentric Torque
Tube Arrangement

87
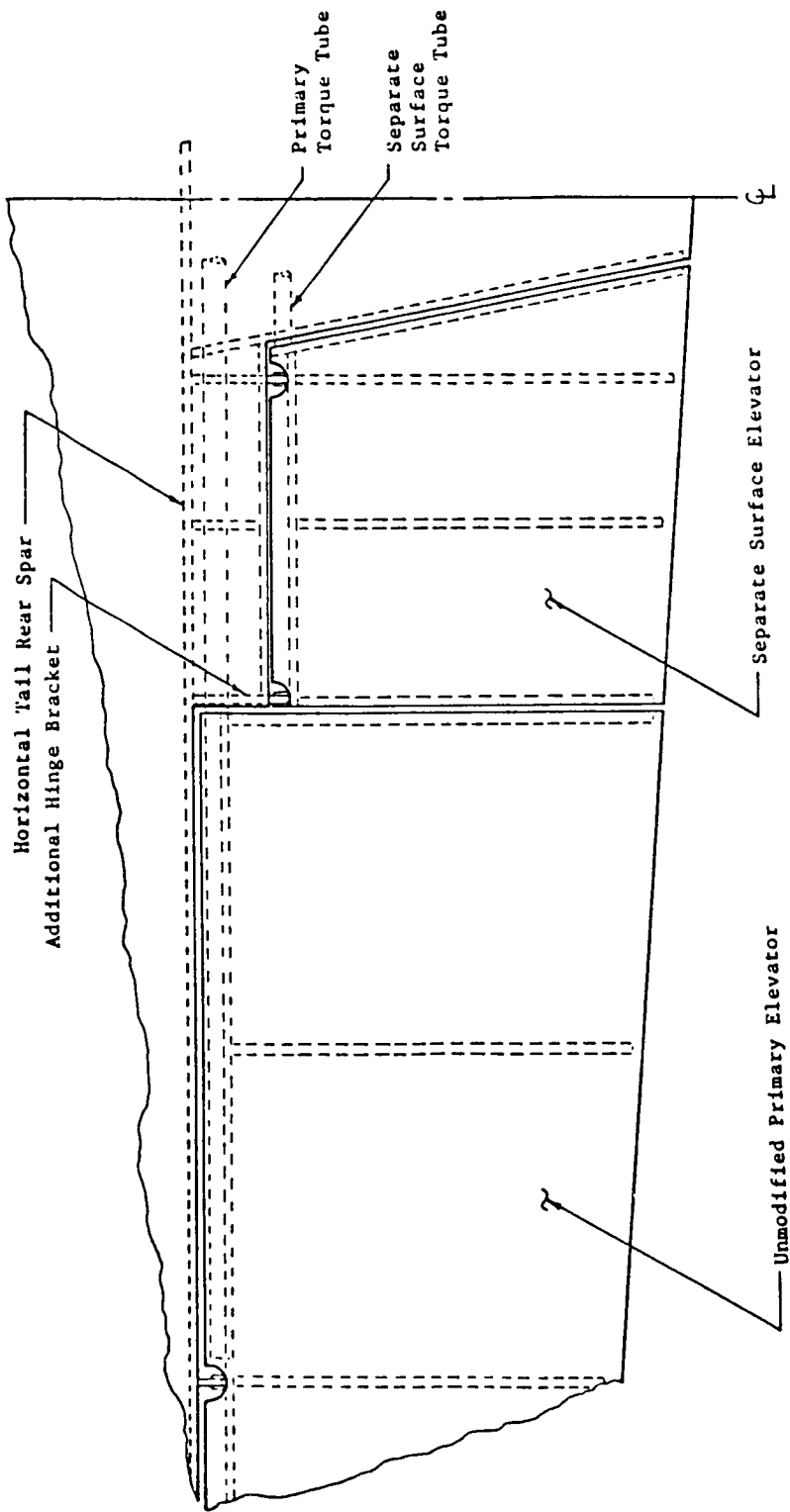
Figure 4.3 Separate Surface Elevator: Parallel Torque Tube Arrangement

4.2.1.2 PARALLEL TORQUE TUBE ARRANGEMENT

Figure 4.3 illustrates the parallel torque tube arrangement for the separate surface elevator. The main advantage of this arrangement is that the primary elevator remains unchanged. The modifications are not complex and the hinge moments can be tailored through the positioning of the SSE hinge line. However, the size and location of the separate surface elevator is restricted in this arrangement.

4.2.1.3 SEPARATE SURFACE ELEVATOR PLACEMENT AND SIZING

Due to the complexity and ultimate cost of the concentric torque tube arrangement, the parallel torque tube arrangement is considered the most favorable. So as not to interfere with the existing elevator, the separate surface elevator is placed in the aft, inboard section of the horizontal stabilizer (Figure 4.4). This area is unused on the basic 402B.

Figure 4.5 is an initial structural drawing for this arrangement. This drawing is for the SSE section on the left side of the fuselage. The total SSE area for
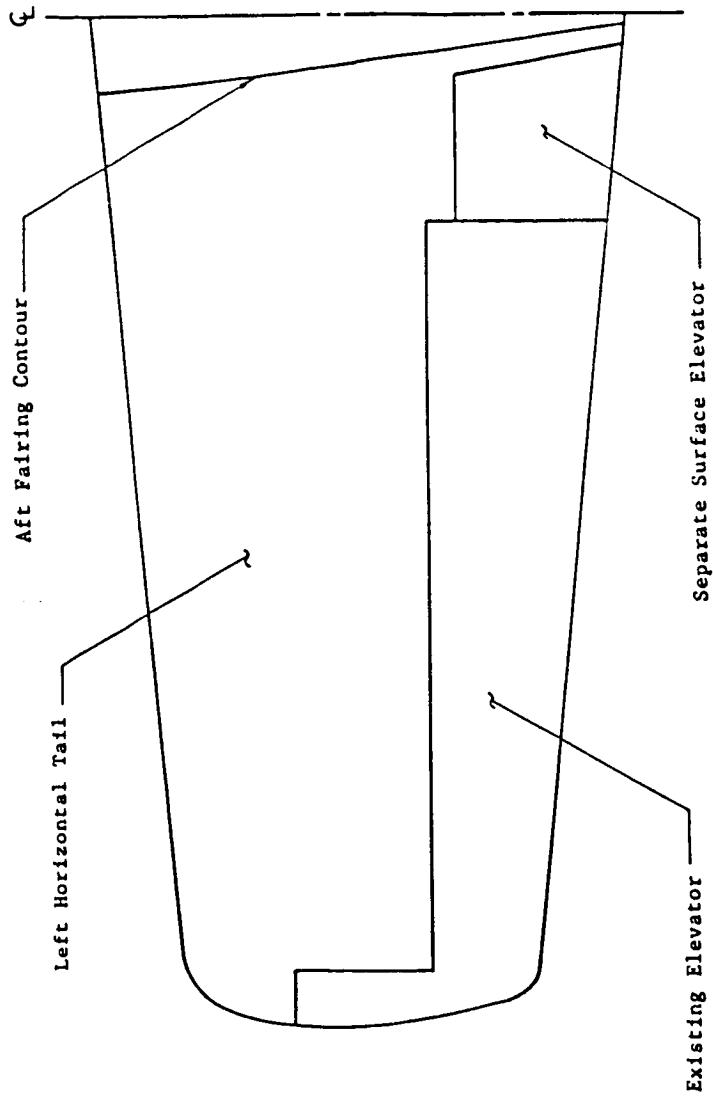
Figure 4.4 Chosen Separate Surface Elevator Position

The figure labels include: Aft Fairing Contour, Left Horizontal Tail, Separate Surface Elevator, Existing Elevator.
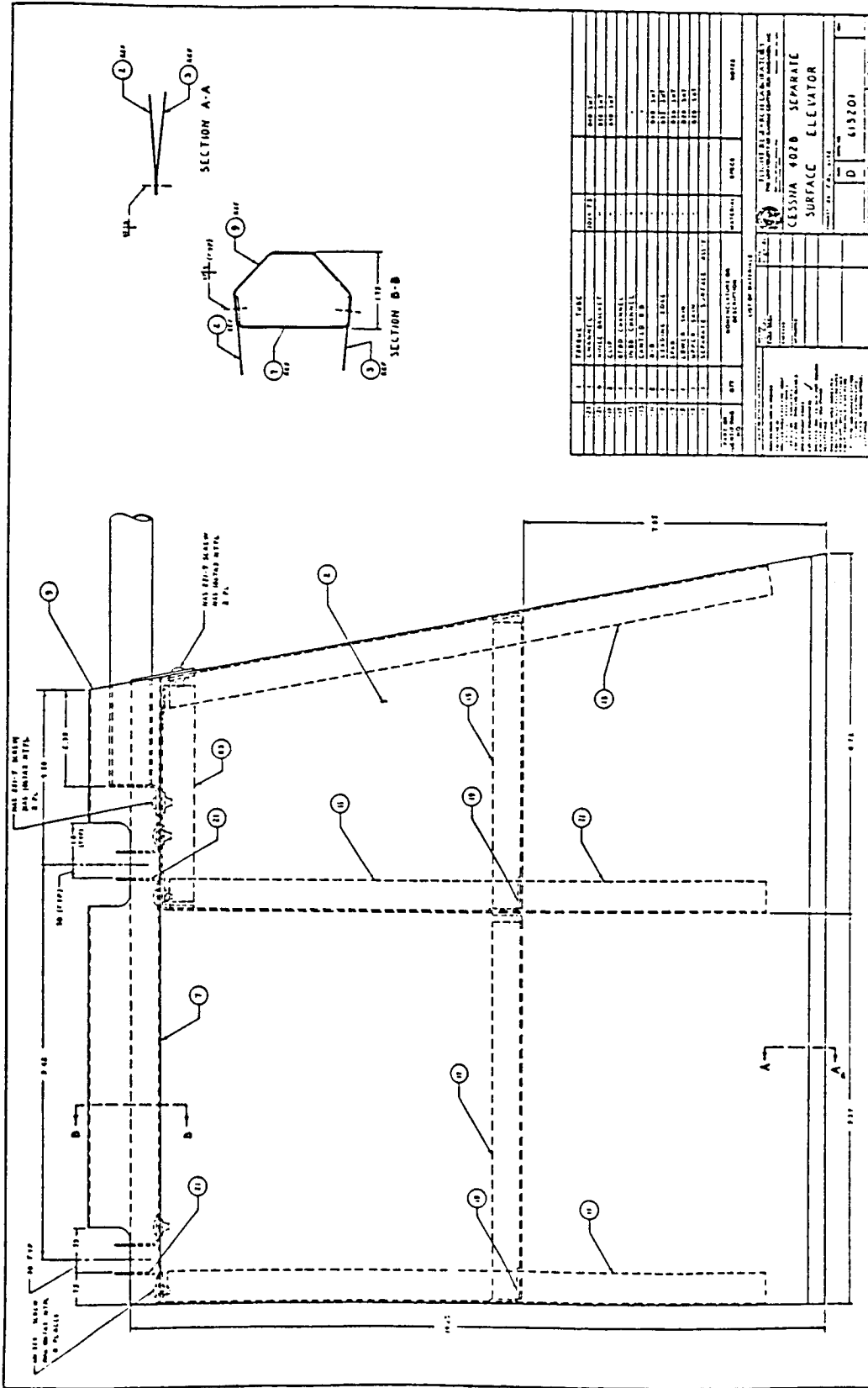
Figure 4.5   Preliminary Structural Arrangement of the
Left Separate Surface Elevator Section

this configuration is 3.16 square feet or approximately 21% of the primary elevator surface area.

The maximum deflection of the separate surface elevator is ±5 degrees. With the elevator in the maximum up position, there will be interference with the rudder when it has been deflected approximately 5 degrees in either direction. To eliminate this problem, 0.75 inches must be trimmed from the bottom of the rudder tab. Detailed part drawings for the separate surface elevator are included in Appendix C.

4.2.2 RUDDER MODIFICATIONS

This section summarizes the design decisions made regarding the implementaion of the rudder for use in the ride quality augmentation system. The design options investigated are:

1. Separate surface rudder (SSR).

2. Ventral fin arrangement.

3. Twin separate surface rudders located on the horizontal stabilizer.

4. Use of the entire rudder (no structural modification).

The following sections point out the characteristics of each option and discuss the final decision.

4.2.2.1 SEPARATE SURFACE RUDDER

The separate surface rudder was investigated as an option which, like the separate surface elevator option, would not feedback the ride quality augmentaion system motions to the pilot. It was found in the RQAS designs that a separate surface rudder with an area equal to approximately 33% of the area of the existing rudder is needed for adequate control power for the RQAS.

Two locations of the SSR were investigated. The first placed the SSR at the top of the primary elevator; the second placed the SSR at the bottom of the primary rudder.

Figure 4.6 depicts the placement of the SSR at the top of the primary rudder. This arrangement is comparable to the arrangement used in the SSSA airplane of Reference 10. An actuator in the vertical tail drives the SSR through an arm fixed to the SSR. This arrangement would be relatively easy to actuate and implement but would require a redesign of the mass balance of the primary rudder.

Figure 4.7 depicts the placement of the SSR at the bottom of the primary rudder. This arrangement requires no modification to the primary rudder mass balance but would require modifications to the rudder trim system.
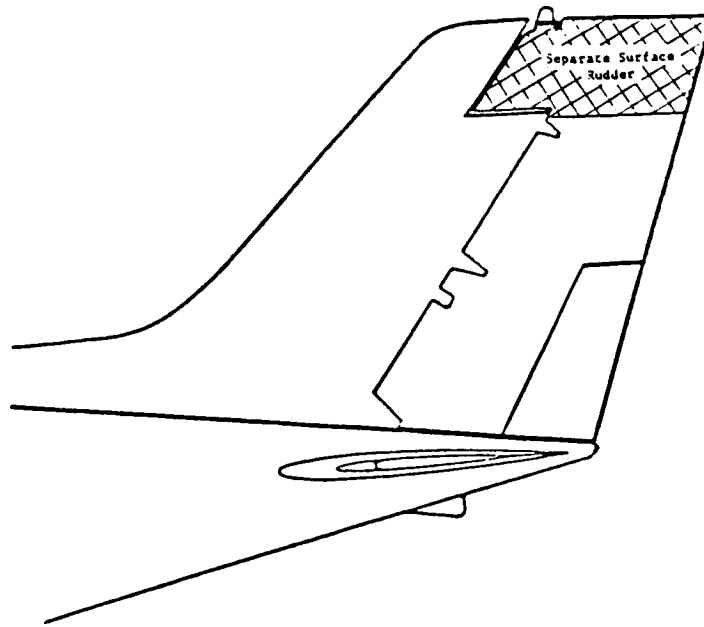
Figure 4.6 Upper Separate Surface Rudder
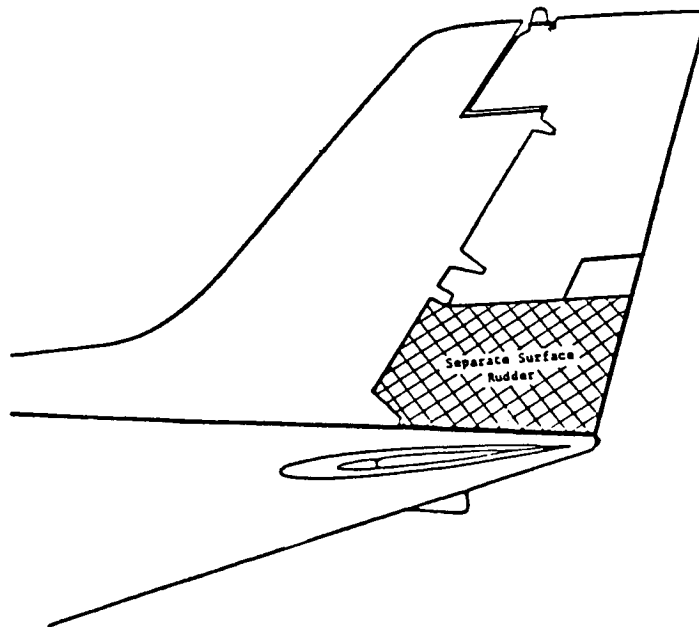
Figure 4.7 Lower Separate Surface Rudder

Also, mounting would be difficult since the primary rudder torque tube translates as it rotates.

In both location options, a large portion of the primary rudder would be lost to the separate surface rudder. This could cause problems with directional control and may require the addition of some mechanism to allow the use of the SSR in conjunction with the primary rudder during takeoff and landing.

4.2.2.2 VENTRAL FIN ARRANGEMENT

Another configuration which would provide a surface for directional control which is separate from the primary rudder is a ventral fin arrangement. Figure 4.8 illustrates this type of configuration. The low aspect ratio of the fin results from a compromise in required fin area (approximately 33% of the rudder area) and take-off rotation angle. The aft fuselage angle is reduced by 2 degrees.

The main advantage of this arrangement is the fact that it requires no modification to the existing rudder. The disadvantages are that the fin would be cumbersome to deflect in flight and the low aspect ratio would provide uncertain control power. Also, as noted above, the ventral fin reduces the take-off rotation angle.

Ventral Fin (deflects $\pm$ 5 degrees)
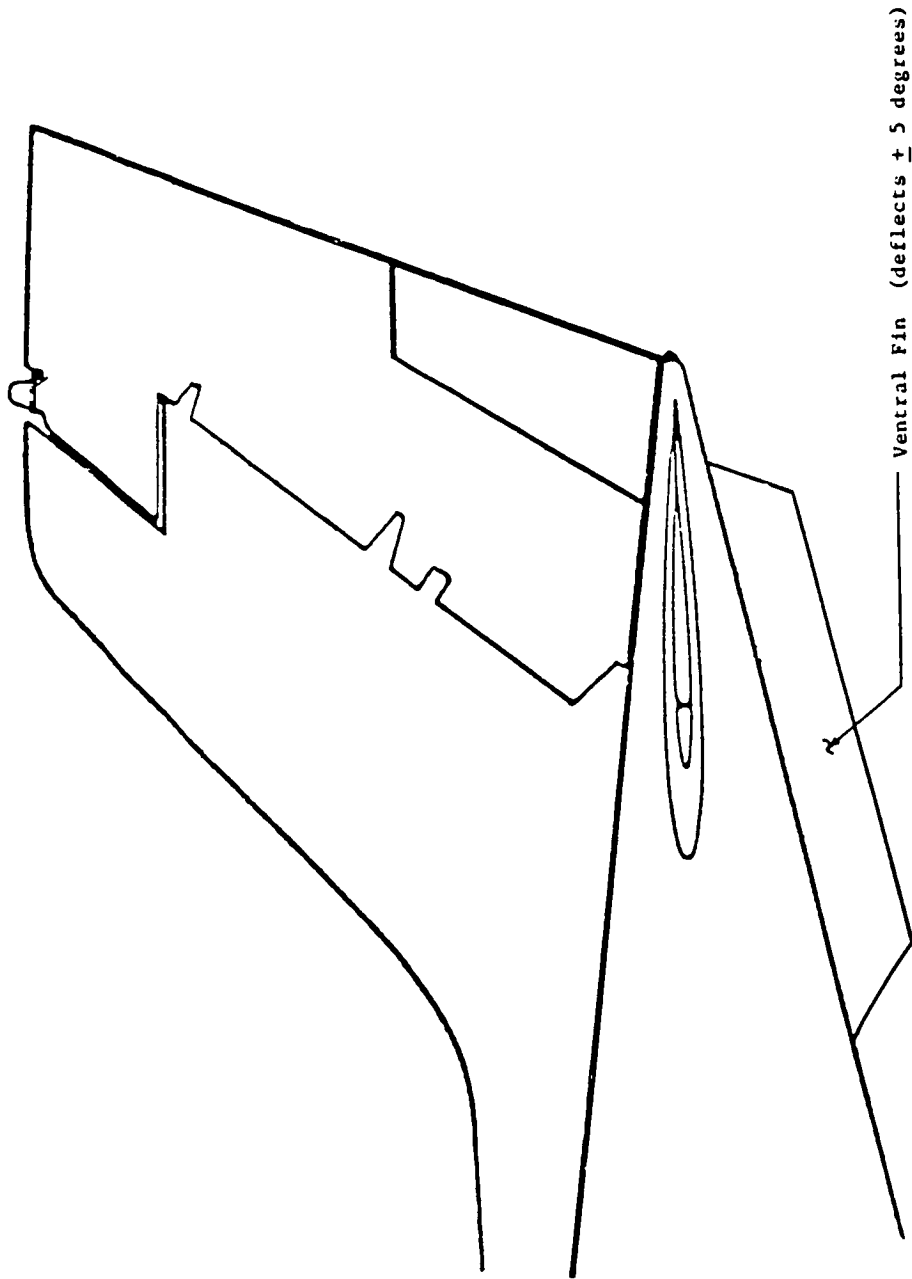
Figure 4.8 Ventral Fin Arrangement

4.2.2.3 TWIN SEPARATE SURFACE RUDDERS

The twin separate surface rudder arrangement is illustrated in Figure 4.9. This arrangement is again designed to provide directional control separate from the primary rudder. The twin "rudders" act like variable incidence vertical stabilizers.

This arrangement again requires no modification to the existing rudder. However, it does require the stiffening of the horizontal stabilizer structure and may cause interference with the airflow over the existing elevator making the elevator control power unpredictable.

4.2.2.4 USE THE ENTIRE EXISTING RUDDER

After examining the options which provide directional control for the RQAS separate from the primary rudder system, it is seen that each has major drawbacks. For this reason, it was decided to devote the entire existing rudder to the RQAS. The fact that this option requires no modifications to the rudder is the prime factor in this decision. The negative aspect is that the pilot will now have to deal with the feedback from the RQAS.
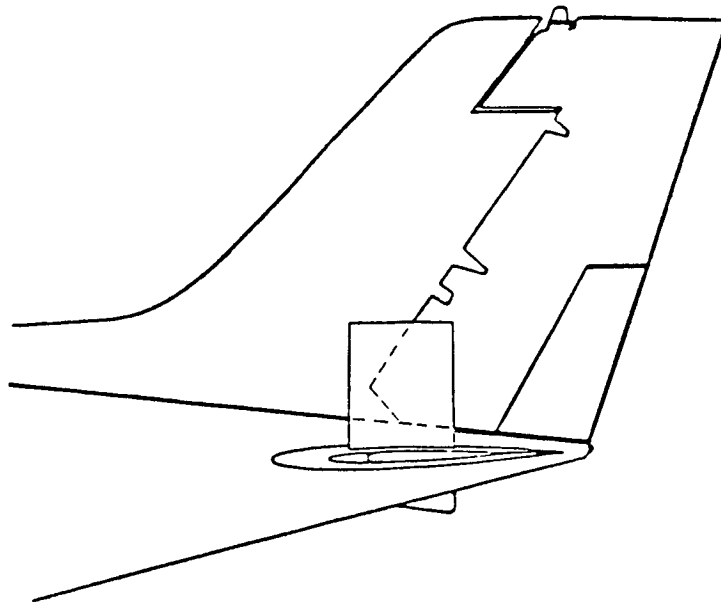
SIDE VIEW OF VERTICAL SEPARATE SURFACE RUDDER

Vertical Separate Surface (deflects ±5 degrees)
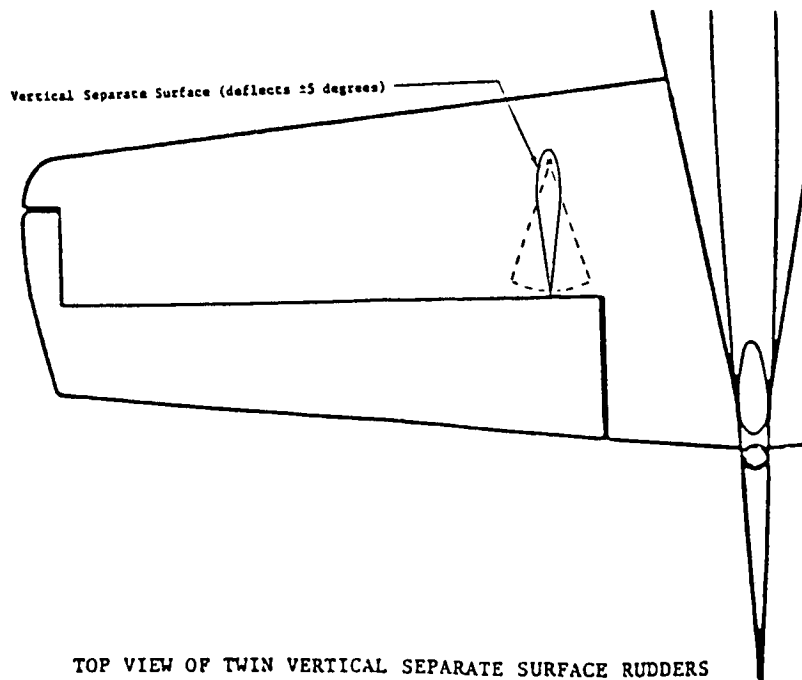
TOP VIEW OF TWIN VERTICAL SEPARATE SURFACE RUDDERS

Figure 4.9   Twin Separate Surface Rudder Arrangement

Since this is a research project, it is felt that the feedback will not be a major problem since the pilot will be warned of the problem and much of the flight testing will be performed with the pilots feet on the floor. Also, the RQAS rudder deflections will be limited to ± 5 degrees. If the RQAS were to be incorporated into the design of a new aircraft, the separate surface rudder option could be easily implemented and would be recommended.

4.2.3 FLAP MODIFICATIONS

As stated earlier, the flap must perform two operations. The entire flap is driven in the longitudinal mode. In addition, the outboard halves of the flap are driven in the lateral-directional mode. Also, the flap must be modified to deflect up 15 degrees and down 45 degrees. The present flap sytem on the Cessna 402B is a split flap system and only deflects down. Two basic arrangements were investigated:

1. Modify the wing to include plain flaps.

2. Use a trailing flap system (external airfoil). The following sections describe each of these options in more detail.

4.2.3.1 PLAIN FLAP MODIFICATION

The plain flap modification option requires reworking the trailing edge of the wing, aft of the rear spar. The piano hinge on the lower spar cap is used to attach the flap to the spar (Figure 4.10). No major structural modification is required and the inboard and outboard sections of the flap can easily be actuated separately. Actuating the outboard section separately is a requirement due to the dual role of this section. The disadvantage of this modification is the fact that the wing locker must be modified to allow the upward deflection of the flap. This leaves a section of the engine nacelle extending beyond the trailing edge of the flap (Figure 4.11) and makes it hard to predict the control power of the flap. Also, the actuation mechanism must be redesigned.
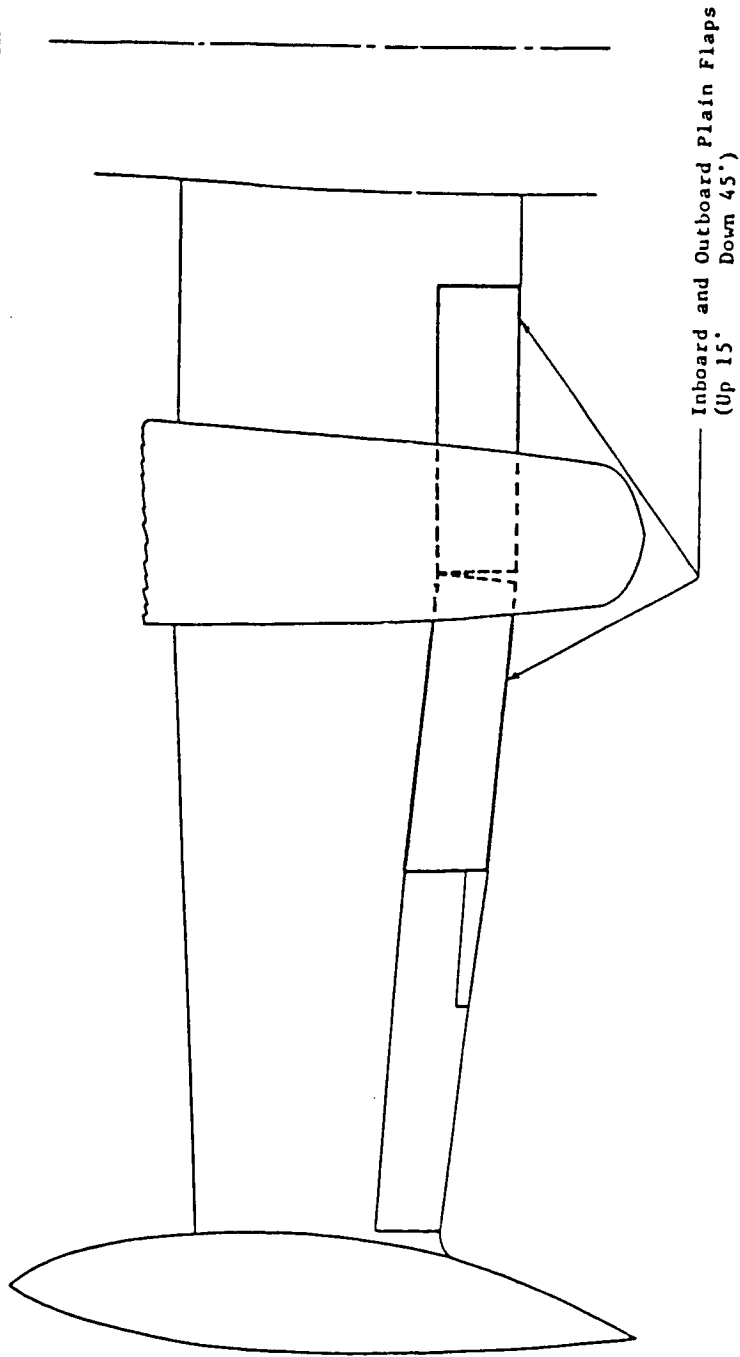
Figure 4.10   Plain Flap Configuration

101

4.2.3.2 TRAILING FLAP SYSTEM

As a simple alternative to the plain flap modification, a trailing flap (auxillary airfoil) could be mounted below and aft of the wing trailing edge (Figures 4.11 and 4.12). However, several problems arise from this arrangement. First, additional structural members are required for supporting the flap. Also, this arrangement may cause severe changes in the center of gravity and stability characteristics of the airplane.

4.2.3.3 FLAP DESIGN CHOICE

For this project, the wing mounted plain flap configuration was chosen. The basic configuration is illustrated in Figures 4.13 and 4.14. These figures illustrate the inboard and outboard sections of the proposed flap, respectively. This arrangement allows the outboard flap sections to be deflected differentialy and the inboard flap sections to be deflected symetrically.

As noted earlier, this configuration requires some modification to the wing locker portion of the engine nacelle. Figure 4.15 illustrates the required modifications. Detailed part drawings for the flap modifications are included in Appendix C.

Nacelle Modification Required for
Plain Flap Configuration

Relative Position of Airfoil for Trailing Plain Flap Option
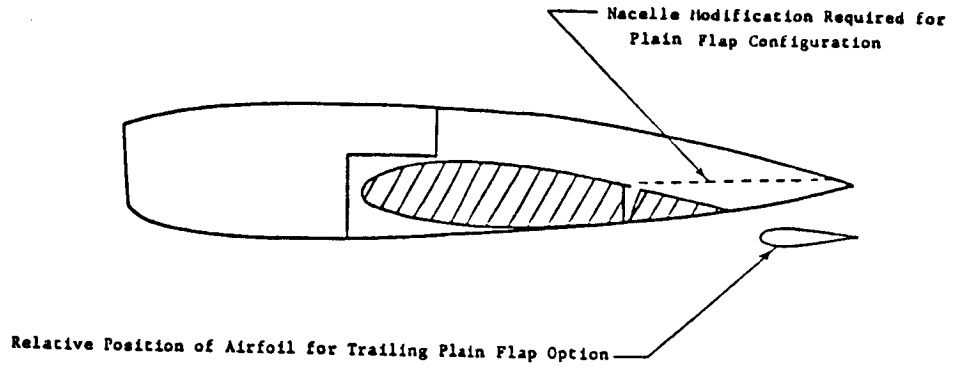
Figure 4.11   Nacelle/Wing Cross Section For The Flap
Configuration Options

Unmodified Split Flaps

Actuator

Torque Tube

Trailing Plain Flap (External Airfoil)
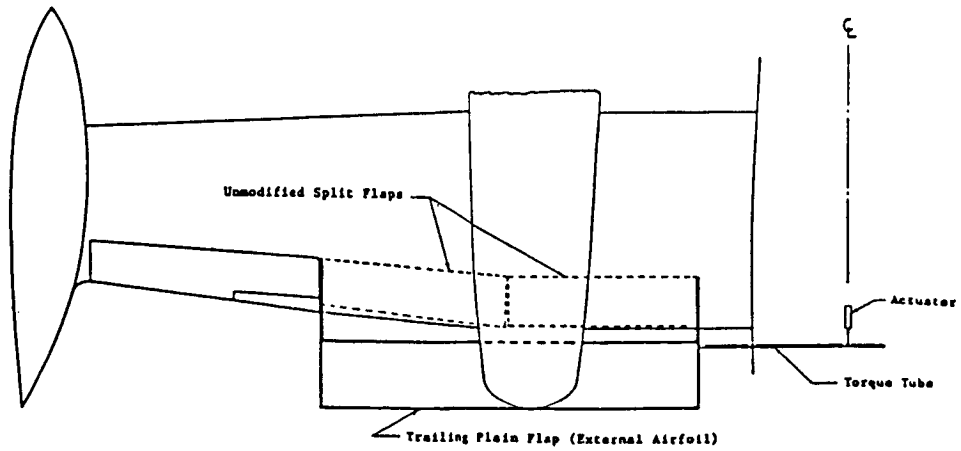
Figure 4.12   Trailing Flap System (External Airfoil)

103
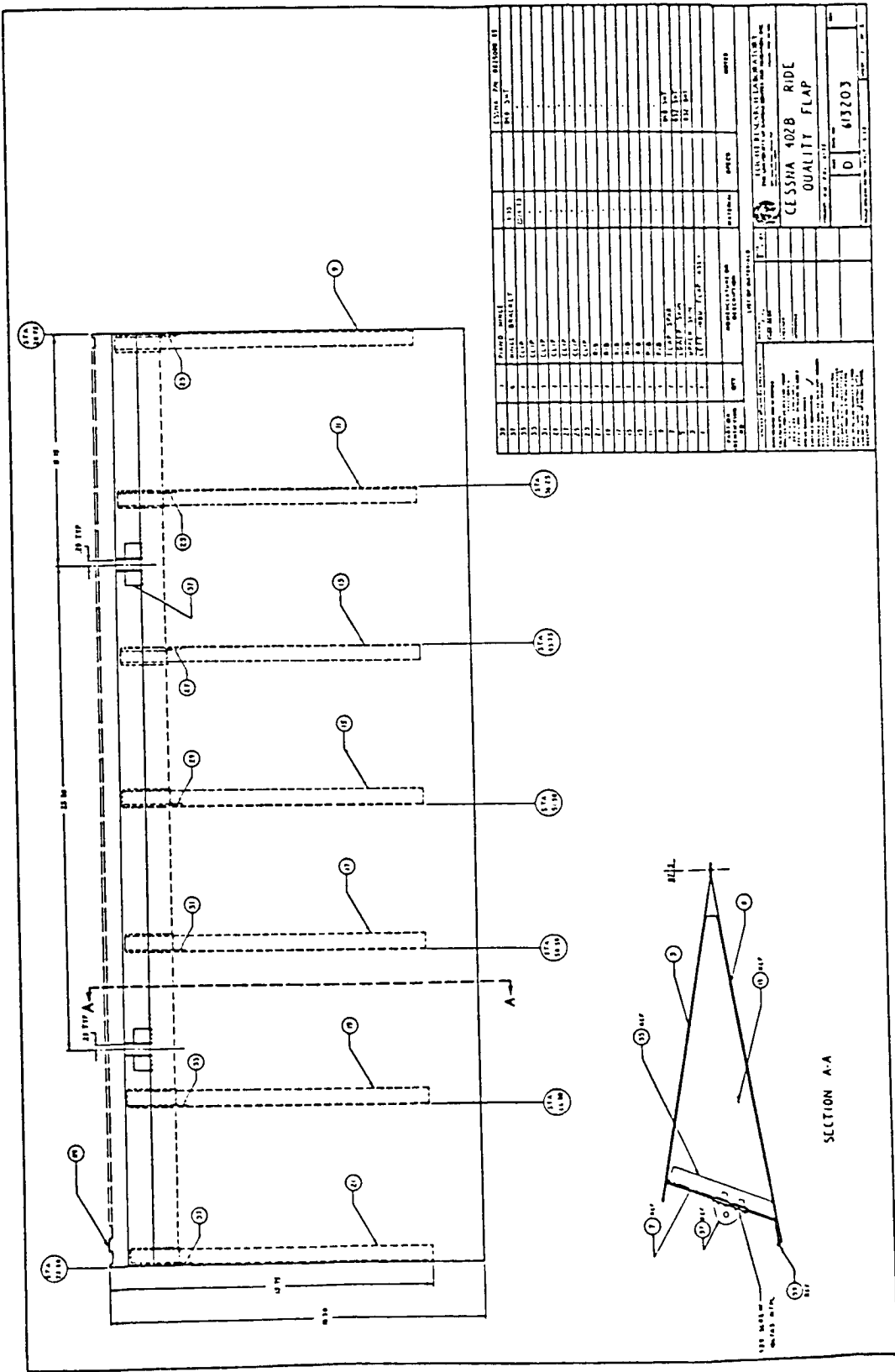
Figure 4.13   Inboard Flap Preliminary Structural Drawing

Figure 4.14 Outboard Flap Preliminary Structural Drawing
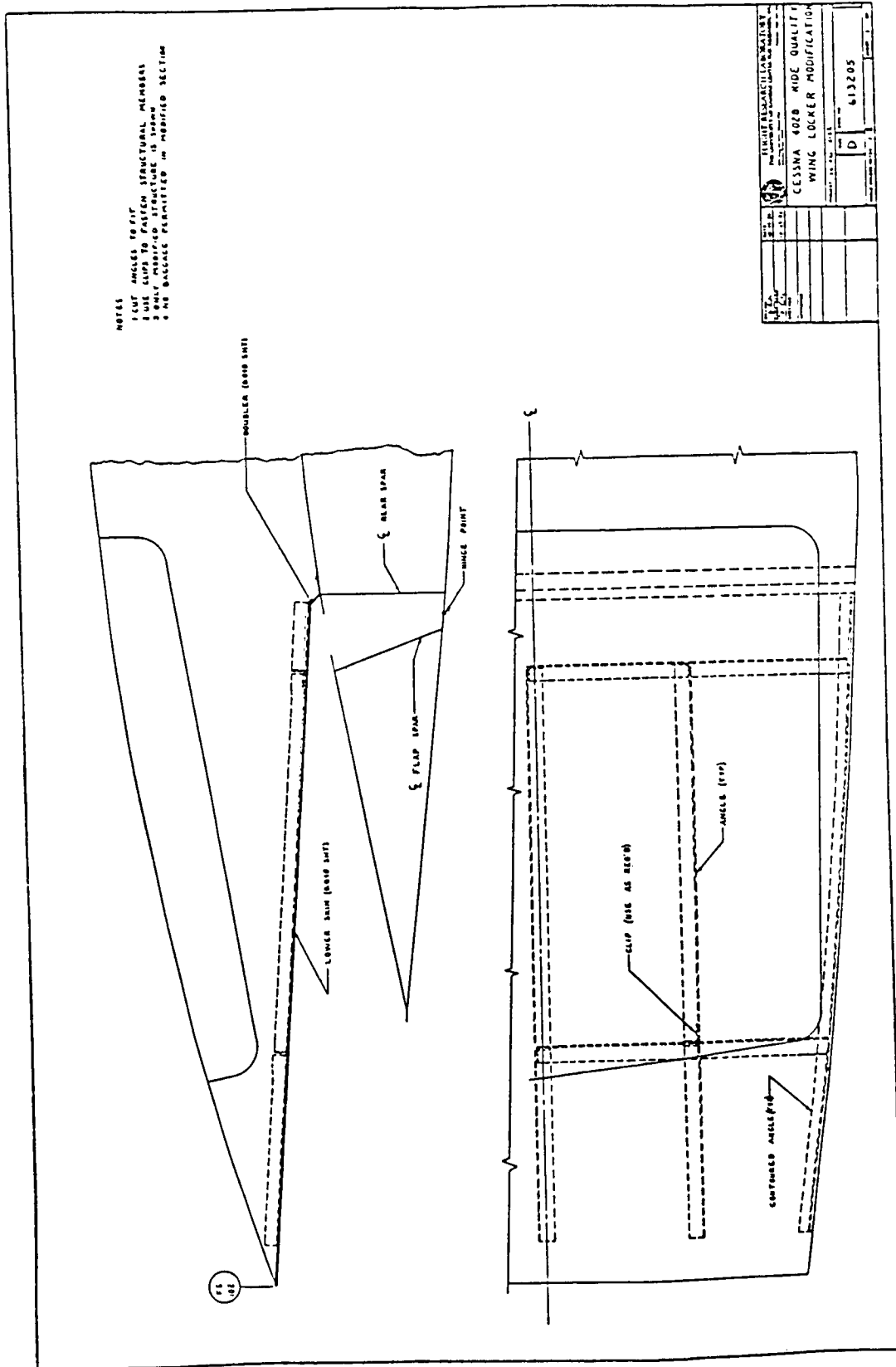
Figure 4.15 Required Wing Locker Modification

4.2.4 SUMMARY OF PROPOSED RQAS CONTROL SURFACE MODIFICATIONS

The proposed control surface modifications to the Cessna 402B for the purposes of the ride quality augmentation system are summarized as follows:

Longitudinal Mode

1. Separate surface elevator located in the aft, inboard section of the horizontal stabilizer with a deflection range of ±5 degrees.*

2. Plain flap replacing existing split flap with a differentialy deflecting outboard section and a symetrically deflecting inboard section. Each section can deflect +15 to -45 degrees.*

Lateral-Directional Mode

1. Outboard section of the plain flap described above.

2. Use the entire existing rudder (limiting the RQAS range of deflections to ±5 degrees).*

It should be remembered that the modifications proposed were motivated by providing the capability to evaluate the RQAS concept with minimum modification to the vehicle. The configuration could be significantly different in new aircraft designs.

*   If additional modes are required, e.g. engine out control, these limits may be changed.

4.3 CONTROL SURFACE ACTUATION

This section summarizes the preliminary actuator sizing for the Cessna 402B ride quality augmentation system. The sizing involves calculation of the maximum hinge moments for each control surface and the corresponding maximum actuator loads, stroke, and speed. A hydraulic actuation system is proposed with actuators controlled by electric servo valves. The components needed for this system are a hydraulic pump to be mounted on one of the engines, an accumulator and a set of electro-hydraulic actuators. The proposed system will operate at hydraulic pressures from 1,000 to 3,000 pounds per square inch.

4.3.1 RQAS CONTROL SURFACE GEOMETRY

The geometry of the control surfaces proposed for the ride quality augmentation system in Section 4.2 is summarized in Table 4.3. This information is needed in the hinge moment calculations. The separate surface elevator information is given for the sum of the two surfaces since they will be driven by a single actuator. The flap information is for the sum of the inboard sections which will also be driven by a single actuator.

The differential flap information is for a single surface since the left and right sections will be driven separately. The rudder requires a single actuator.

Table 4.3   RQAS Control Surface Geometry

Surface	Span $S(ft)$	Mean Chord $c(ft)$	Area $S(ft^2)$
SS Elevator	2.66	1.19	3.16
Flap(Inboard)	7.43	1.53	11.36
Differential Flap	4.95	1.50	7.41
Rudder	6.67	2.66	17.77

4.3.2 HINGE MOMENT CALCULATIONS

This section summarizes the hinge moment calculations used in the actuator sizing. The hinge moment coefficients were obtained from Reference 3 and were verified by DATCOM methods (Reference 11). The hinge moments were calculated using the equation:

$$HM = C_h \bar{q} b c^2 \qquad (4.1)$$

where HM is the hinge moment, C_h is the hinge moment coefficient for the given control surface, q is the

109

design dynamic pressure (for V_{max} at sea level), and b and c are the control surface span and mean chord respectively (Table 4.3). The hinge moment calculations are summarized in Table 4.4.

Table 4.4 Hinge Moment Summary

Surface	Hinge Moment Coefficient	Hinge Moment (in-lb) Equation (4.3)
SS Elevator	0.0219	178
Flap(inboard)	0.0450	1,691
Differential Flap	0.0450	1,083
Rudder	0.0145	1,478

4.3.3 ACTUATOR REQUIREMENTS

The characteristics of the required actuators are summarized in Table 4.5. The calculations were made assuming a 4 inch moment arm and a linear actuator for each control surface. The specifications given in Table 4.5 can be modified easily by varying this moment arm. The maximum load calculations were made using the following equation:

Max Load = 1.4 x HM(in-lb)/moment arm(in)   , (4.2)

where the 1.4 is a factor of safety. The speed and stroke are based on the maximum control surface rate and deflection respectively. The speed is calculated with the equation:

$$\text{Speed} = \dot{\delta}_{max} \times h \quad , \tag{4.3}$$

where $\dot{\delta}_{max}$ is the maximum control surface rate and h is the moment arm. The stroke is based on the geometry of the mechanism and the deflection range.

Table 4.5 Actuator Requirements

Control Surface Deflection and Rate Limits

Surface	Deflection Range(deg)	Maximum Rate(deg/sec)
SS Elevator	±5	50
Flap(inboard)	+15 to -45	120
Differential Flap	+15 to -45	120
Rudder[1]	±32	50

Actuator Requirements

Surface	Max Load (lbs)	Speed (in/sec)	Stroke (in)
SS Elevator	65	3.50	0.75
Flap(inboard)	750	8.50	4.25
Differential Flap	380	8.50	4.25
Rudder	520	3.50	4.50

[1] The deflection is for the standard rudder. The RQAS uses a deflection range of ±5 degrees.

CHAPTER 5.

SUMMARY, CONCLUSIONS, AND RECOMMENDED RESEARCH

5.1 SUMMARY

The primary goals of this phase of work have been the generation of detailed optimal designs for the longitudinal and lateral-directional RQAS. Another goal was the preliminary investigation of the necessary hardware modifications to the Cessna 402B to implement separate surface controllers and direct lift flaps. These goals have been achieved along with the groundwork for the implementation of the RQAS controller on an experimental aircraft. This groundwork included the preliminary definition of the experimental system and the determination of the necessary requirements for surface actuation.

The results of this (and previous) work show that substantial reductions can be made in the RMS values of the vertical and lateral accelerations caused by atmospheric turbulence by implementing an active control system. It was shown in Section 3.3 that the implementation of fixed gain designs, based on either the control-rate-weighting or output-weighting optimal design techniques, give good results across the basic flight envelope.

5.2 RECOMMENDED RESEARCH

The next steps in the RQAS project should involve all of the factors necessary to implement and experimental flight test the system. The following is a list of research topics which follow from the present project. Some are directly related to the implementation of the experimental system and others relate to furthering the basic design concept.

1. Continue with the hardware modification plans including the detailed structural design of the flaps and separate elevator. This includes a detailed structural analysis along with flutter analysis. Of special concern is the bending moments caused by the new, more active, control surfaces.

2. Proceed with detailed study of the experimental system and hardware requirements for implementation of the controller on the Cessna 402B. This includes investigation of sensor accuracy and placement, digital computer requirements, and data recording equipment.

3. Continue with the analytic designs using the RQAS concept. This might include investigations of

other control structures such as Limited State Feedback.

4. Investigate the response and interaction of the individually designed longitudinal and lateral-directional RQAS controllers on fully coupled linear models.

5. Investigate methods to prevent interference with the pilot induced accelerations. This might be achieved by including washout filters in the control circuits or by directly measuring the pilot commands and implementing a trim map to account for the accelerations requested.

5. Study the effects of unsteady aerodynamics on the RQAS performance. The effects include the lag of control response when the control surfaces are deflected at high rates, the effects of the unsteady flap wake on the tail surfaces and controls, and the structural interactions caused by the control activity.

7. Develop a piloted simulation using the C-402 B model operational at NASA Langley. This simulation would be used to evaluate RQAS designs, conduct failure mode analysis, and evaluate candidate techniques for RQAS operation during intentional maneuvering.

8. Perform parameter identification flight test of the modified vehicle. If major model variations occur, refine the RQAS algorithms.

9. Perform a flight test program of a digital RQAS.

CHAPTER 6.

REFERENCES

1. Downing, D.R., Hammond, T.A., and Amin, S.P., "Ride Quality Systems for Commuter Aircraft", NASA CR-16618, May 1983.

2. Hammond, T.A., Amin, S.P., Paduano, J., and Downing, D.R., "Design of a Digital Ride Quality Augmentation System for Commuter Aircraft", NASA CR-172419, October 1984. (Phase 1)

3. Hoh, R.H., Mitchell, D.G., and Myers, T.T., "Simulation Model of Cessna 402B", NASA CR-152176, July 1978.

4. Roskam, J., Airplane Flight Dynamics and Automatic Controls, Part I, Roskam Aviation and Engineering Corp., Ottawa, KS, 1982.

5. Roskam, J., Airplane Flight Dynamics and Automatic Controls, Part II, Roskam Aviation and Engineering Corp., Ottawa, KS, 1982.

6. Eijsink, J.F., "On the Use of Electro-Mechanical Actuators in Light General Aviation Aircraft", M.E. Thesis, The University of Kansas, Lawrence, KS, 1977.

7. Davis, D.J., "A Comparison of Two Optimal Regulator Design Techniques for the Weighting of Output Variables Which are Linear Combinations of States and Controls", M.S. Thesis, The University of Kansas, Lawrence, KS, 1986.

8. Armstrong, E.S., ORACLS - A Design System for Linear Multivariable Control, Marcel Dekker, Inc., New York, 1980.

9. Downing, D.R., and Bryant, W.H., "Flight Test Evaluation of a Digital Controller Used in a VTOL Automatic Approach and Landing System", presented at the IEEE Conference on Decision and Control, Fort Lauderdale, FL, 1979.

10. Prins, J.J.M., "Flight Hardware Design and an Analog Model of a SSSA Control System for a Beech Model 99 Aircraft", M.S. Thesis, The University of Kansas, Lawrence, KS, 1970.

11. Hoak, D.E., et al., "USAF Stability and Control DATCOM", Flight Control Division, Air Force Flight Dynamics Laboratory, Wright Patterson Air Force Base, OH, September 1970.

APPENDIX A

EQUATIONS OF MOTION WRITTEN IN STATE-SPACE FORM

This appendix gives the conversion of the standard aircraft small perturbation equations of motion found in Reference 4 to state-space form. The equations are written in the stability axis system and are modified slightly to account for the change in the acceleration vector due to its rotation through the angle of attack. The resulting equations are consistent with the models supplied by NASA LaRC for the Cessna 402B aircraft (Reference 3).

The equations are separated into the longitudinal and lateral-directional modes and the modified dimensional stability derivatives are defined.

Assuming steady-state straight and level trimmed flight:

$$V_1 = \phi_1 = W_1 = 0 \quad ;$$
$$P_1 = Q_1 = R_1 = 0 \quad ;$$
$$\dot{\psi}_1 = \dot{\theta}_1 = \dot{\phi}_1 = 0 \quad ;$$

the equations of motion as derived in Reference 4 can be written as:

$$m\dot{u} = -mg\gamma\cos\gamma_1 + f_{A_x} + f_{T_x}$$

$$m(\dot{v} + U_1 r) = mg\phi\cos\theta_1 + f_{A_y} + f_{T_y}$$

$$m(\dot{w} - U_1 q) = -mg\gamma\sin\gamma_1 + f_{A_z} + f_{T_z}$$

$$I_{xx}\dot{p} - I_{xz}\dot{r} = l_A + l_T$$

$$I_{yy}\dot{q} = m_A + m_T$$

$$I_{zz}\dot{r} - I_{xz}\dot{p} = n_A + n_T$$

$$p = \dot{\phi} - \dot{\psi}\sin\theta_1$$

$$q = \dot{\theta}$$

$$r = \dot{\psi}\cos\theta_1$$

A.2

The small perturbation equations of motion can then be written in the dimensional stability derivatives as follows.

Longitudinal:

$$\dot{w} - U_1 q = -g\gamma\sin\gamma_1 + Z_u u + Z_{\dot{\alpha}}\dot{\alpha} + Z_\alpha\alpha + Z_q q +$$
$$+ Z_{\delta_{se}}\delta_{se} + Z_{\delta_f}\delta_f$$

$$\dot{u} = -g\gamma\cos\gamma_1 + X_u u + X_\alpha\alpha + X_{\delta_{se}}\delta_{se} + X_{\delta_f}\delta_f$$

$$\text{(A.1)}$$

$$\dot{q} = M_u u + M_{\dot{\alpha}}\dot{\alpha} + M_\alpha\alpha + M_q q + M_{\delta_{se}}\delta_{se} + M_{\delta_f}\delta_f$$

$$\dot{\theta} = q$$

Lateral-Directional:

$$\dot{v} + U_1 r = g\phi\cos\theta_1 + Y_p p + Y_\beta\beta + Y_r r + Y_{\delta_{df}}\delta_{df} + Y_{\delta_{sr}}\delta_{sr}$$

$$\dot{p} - A_1\dot{r} = L_\beta\beta + L_p p + L_r r + L_{\delta_{df}}\delta_{df} + L_{\delta_{sr}}\delta_{sr}$$

$$\text{(A.2)}$$

$$\dot{r} - B_1\dot{p} = N_p p + N_\beta\beta + N_r r + N_{\delta_{df}}\delta_{df} + N_{\delta_{sr}}\delta_{sr}$$

$$\dot{\phi} = p + \tan\theta_1 r$$

where the $\dot{\psi}$ equation has been neglected and

$$A_1 = I_{xz}/I_{xx} \quad \text{and} \quad B_1 = I_{xz}/I_{zz} \quad .$$

The dimensional stability derivatives as defined in Reference 4 are presented in Tables A.1 and A.2.

Introducing the equations

$$\dot{w} = U_1 \dot{\alpha}$$

$$\dot{v} = U_1 \dot{\beta}$$

$$\gamma = \theta - \alpha$$

into Equations (A.1) and (A.2) and rearranging results in the following state-space representation of the small perturbation equations of motion where the modified dimensional stability derivatives are defined in Tables A.3 and A.4.

Longitudinal:

$$
\begin{bmatrix} \dot{\alpha} \\ \dot{u} \\ \dot{q} \\ \dot{\theta} \end{bmatrix} =
\begin{bmatrix} Z'_\alpha & Z'_u & Z'_q & Z'_\theta \\ X'_\alpha & X'_u & 0 & X'_\theta \\ M'_\alpha & M'_u & M'_q & M'_\theta \\ 0 & 0 & 0 & 0 \end{bmatrix}
\begin{bmatrix} \alpha \\ u \\ q \\ \theta \end{bmatrix} +
\begin{bmatrix} Z'_{\delta_{se}} & Z'_{\delta_f} \\ X'_{\delta_{se}} & X'_{\delta_f} \\ M'_{\delta_{se}} & M'_{\delta_f} \\ 0 & 0 \end{bmatrix}
\begin{bmatrix} \delta_{se} \\ \delta_f \end{bmatrix}
$$

(A.3)

Lateral-Directional:

$$
\begin{bmatrix} \dot{\beta} \\ \dot{p} \\ \dot{r} \\ \dot{\phi} \end{bmatrix} = \begin{bmatrix} Y'_\beta & Y'_p & Y'_r & Y'_\phi \\ L'_\beta & L'_p & L'_r & 0 \\ N'_\beta & N'_p & N'_r & 0 \\ 0 & 1 & \tan\theta_1 & 0 \end{bmatrix} \begin{bmatrix} \beta \\ p \\ r \\ \phi \end{bmatrix} + \begin{bmatrix} Y'_{\delta_{df}} & Y'_{\delta_{sr}} \\ L'_{\delta_{df}} & L'_{\delta_{sr}} \\ N'_{\delta_{df}} & N'_{\delta_{sr}} \\ 0 & 0 \end{bmatrix} \begin{bmatrix} \delta_{df} \\ \delta_{sr} \end{bmatrix}
$$

$$(A.4)$$

$$X_u = \frac{-\bar{q}_1 S(C_{D_u} + 2C_{D_1})}{mU_1} \quad (\text{sec}^{-1})$$

$$X_{T_u} = \frac{\bar{q}_1 S(C_{T_{x_u}} + 2C_{T_{x_1}})}{mU_1} \quad (\text{sec}^{-1})$$

$$M_\alpha = \frac{\bar{q}_1 S \bar{c} C_{m_\alpha}}{I_{yy}} \quad (\text{sec}^{-2})$$

$$X_\alpha = \frac{-\bar{q}_1 S(C_{D_\alpha} - C_{L_1})}{m} \quad (\text{ft sec}^{-2})$$

$$M_{T_\alpha} = \frac{\bar{q}_1 S \bar{c} C_{m_{T_\alpha}}}{I_{yy}} \quad (\text{sec}^{-2})$$

$$X_{\delta_E} = \frac{-\bar{q}_1 S C_{D_{\delta_E}}}{m} \quad \begin{array}{l}(\text{ft sec}^{-2}\text{ or} \\ \text{ft sec}^{-2}\text{deg}^{-1})\end{array}$$

$$Z_u = -\frac{\bar{q}_1 S(C_{L_u} + 2C_{L_1})}{mU_1} \quad (\text{sec}^{-1})$$

$$M_{\dot{\alpha}} = \frac{\bar{q}_1 S \bar{c}^2 C_{m_{\dot{\alpha}}}}{2 I_{yy} U_1} \quad (\text{sec}^{-1})$$

$$Z_\alpha = -\frac{\bar{q}_1 S(C_{L_\alpha} + C_{D_1})}{m} \quad (\text{ft sec}^{-2})$$

$$M_q = \frac{\bar{q}_1 S \bar{c}^2 C_{m_q}}{2 I_{yy} U_1} \quad (\text{sec}^{-1})$$

$$Z_{\dot{\alpha}} = -\frac{\bar{q}_1 S C_{L_{\dot{\alpha}}} \bar{c}}{2mU_1} \quad (\text{ft sec}^{-1})$$

$$M_{\delta_E} = \frac{\bar{q}_1 S \bar{c} C_{m_{\delta_E}}}{I_{yy}} \quad \begin{array}{l}(\text{sec}^{-2}\text{ or} \\ \text{sec}^{-2}\text{deg}^{-1})\end{array}$$

$$Z_q = -\frac{\bar{q}_1 S C_{L_q} \bar{c}}{2mU_1} \quad (\text{ft sec}^{-1})$$

$$Z_{\delta_E} = -\frac{\bar{q}_1 S C_{L_{\delta_E}}}{m} \quad \begin{array}{l}(\text{ft sec}^{-2}\text{ or} \\ \text{ft sec}^{-2}\text{deg}^{-1})\end{array}$$

$$M_u = \frac{\bar{q}_1 S \bar{c}(C_{m_u} + 2C_{m_1})}{I_{yy} U_1} \quad (\text{ft}^{-1} \text{ sec}^{-1})$$

$$M_{T_u} = \frac{\bar{q}_1 S \bar{c}(C_{m_{T_u}} + 2C_{m_{T_1}})}{I_{yy} U_1} \quad (\text{ft}^{-1} \text{ sec}^{-1})$$

Table A.2 Lateral-Directional Dimensional Stability Derivatives (from Reference 4)

$$Y_\beta = \frac{\bar{q}_1 S C_{y_\beta}}{m} \quad (\text{ft sec}^{-2})$$

$$Y_p = \frac{\bar{q}_1 S b C_{y_p}}{2mU_1} \quad (\text{ft sec}^{-1})$$

$$Y_r = \frac{\bar{q}_1 S b C_{y_r}}{2mU_1} \quad (\text{ft sec}^{-1})$$

$$Y_{\delta_A} = \frac{\bar{q}_1 S C_{y_{\delta_A}}}{m} \quad \begin{array}{l}(\text{ft sec}^{-2} \text{ or} \\ \text{ft sec}^{-2} \text{ deg}^{-1})\end{array}$$

$$Y_{\delta_R} = \frac{\bar{q}_1 S C_{y_{\delta_R}}}{m} \quad \begin{array}{l}(\text{ft sec}^{-2} \text{ or} \\ \text{ft sec}^{-2} \text{ deg}^{-1})\end{array}$$

$$L_\beta = \frac{\bar{q}_1 S b C_{\ell_\beta}}{I_{xx}} \quad (\text{sec}^{-2})$$

$$L_p = \frac{\bar{q}_1 S b^2 C_{\ell_p}}{2I_{xx}U_1} \quad (\text{sec}^{-1})$$

$$L_r = \frac{\bar{q}_1 S b^2 C_{\ell_r}}{2I_{xx}U_1} \quad (\text{sec}^{-1})$$

$$L_{\delta_A} = \frac{\bar{q}_1 S b C_{\ell_{\delta_A}}}{I_{xx}} \quad \begin{array}{l}(\text{sec}^{-2} \text{ or} \\ \text{sec}^{-2} \text{ deg}^{-1})\end{array}$$

$$L_{\delta_R} = \frac{\bar{q}_1 S b C_{\ell_{\delta_R}}}{I_{xx}} \quad \begin{array}{l}(\text{sec}^{-2} \text{ or} \\ \text{sec}^{-2} \text{ deg}^{-1})\end{array}$$

$$N_\beta = \frac{\bar{q}_1 S b C_{n_\beta}}{I_{zz}} \quad (\text{sec}^{-2})$$

$$N_{T_\beta} = \frac{\bar{q}_1 S b C_{n_{T_\beta}}}{I_{zz}} \quad (\text{sec}^{-2})$$

$$N_p = \frac{\bar{q}_1 S b^2 C_{n_p}}{2I_{zz}U_1} \quad (\text{sec}^{-1})$$

$$N_r = \frac{\bar{q}_1 S b^2 C_{n_r}}{2I_{zz}U_1} \quad (\text{sec}^{-1})$$

$$N_{\delta_A} = \frac{\bar{q}_1 S b C_{n_{\delta_A}}}{I_{zz}} \quad \begin{array}{l}(\text{sec}^{-2} \text{ or} \\ \text{sec}^{-2} \text{ deg}^{-1})\end{array}$$

$$N_{\delta_R} = \frac{\bar{q}_1 S b C_{n_{\delta_R}}}{I_{zz}} \quad \begin{array}{l}(\text{sec}^{-2} \text{ or} \\ \text{sec}^{-2} \text{ deg}^{-1})\end{array}$$

Table A.3 Modified Longitudinal Dimensional Stability
Derivatives   (from Reference 7)

$Z'_\alpha = (g\sin\gamma_1 + Z_\alpha)/(U_1 - \dot{Z}_\alpha)$

$Z'_u = Z_u/(U_1 - \dot{Z}_\alpha)$

$Z'_q = (U_1 + Z_q)/(U_1 - \dot{Z}_\alpha)$

$Z'_\theta = -g\sin\gamma_1/(U_1 - \dot{Z}_\alpha)$

$Z'_{\delta_{se}} = Z_{\delta_{se}}/(U_1 - \dot{Z}_\alpha)$

$Z'_{\delta_f} = Z_{\delta_f}/(U_1 - \dot{Z}_\alpha)$

$X'_\alpha = g\cos\gamma_1 + X_\alpha$

$X'_u = X_u$

$X'_\theta = -g\cos\gamma_1$

$X'_{\delta_{se}} = X_{\delta_{se}}$

$X'_{\delta_f} = X_{\delta_f}$

$M'_\alpha = \dot{M}_\alpha Z'_\alpha + M_\alpha$

$M'_u = \dot{M}_\alpha Z'_u + M_u$

$M'_q = \dot{M}_\alpha Z'_q + M_q$

$M'_\theta = \dot{M}_\alpha Z'_\theta$

$M'_{\delta_{se}} = \dot{M}_\alpha Z'_{\delta_{se}} + M_{\delta_{se}}$

$M'_{\delta_f} = \dot{M}_\alpha Z'_{\delta_f} + M_{\delta_f}$

A.8

Table A.4 Modified Lateral-Directional Dimensional Stability Derivatives (from Reference 7)

$$Y'_\beta = Y_\beta/U_1$$

$$Y'_p = Y_p/U_1$$

$$Y'_r = (Y_r/U_1)-1$$

$$Y'_\phi = g\cos\theta_1/U_1$$

$$Y'_{\delta_{df}} = Y_{\delta_{df}}/U_1$$

$$Y'_{\delta_{sr}} = Y_{\delta_{sr}}/U_1$$

$$L'_\beta = (A_1 N_\beta + L_\beta)/(1-A_1 B_1)$$

$$L'_p = (A_1 N_p + L_p)/(1-A_1 B_1)$$

$$L'_r = (A_1 N_r + L_r)/(1-A_1 B_1)$$

$$L'_{\delta_{df}} = (A_1 N_{\delta_{df}} + L_{\delta_{df}})/(1-A_1 B_1)$$

$$L'_{\delta_{sr}} = (A_1 N_{\delta_{sr}} + L_{\delta_{sr}})/(1-A_1 B_1)$$

$$N'_\beta = (B_1 L_\beta + N_\beta)/(1-A_1 B_1)$$

$$N'_p = (B_1 L_p + N_p)/(1-A_1 B_1)$$

$$N'_r = (B_1 L_r + N_r)/(1-A_1 B_1)$$

$$N'_{\delta_{df}} = (B_1 L_{\delta_{df}} + N_{\delta_{df}})/(1-A_1 B_1)$$

$$N'_{\delta_{sr}} = (B_1 L_{\delta_{sr}} + N_{\delta_{sr}})/(1-A_1 B_1)$$

APPENDIX B.

MATHEMATICAL MODELS AND OPTIMAL DESIGN RESULTS

This appendix presents the basic math models of the Cessna 402B. These are perturbation models that have been linearized about five basic flight conditions as described previously. The models are presented here in terms of four basic matrices which satisfy the following linearized equations

$$\dot{x} = Ax + Bu$$

$$y = Cx + Du$$

The models for 3 center of gravity locations in the longitudinal direction are presented as are the basic lateral-directional models.

Following the tables of the aircraft design models are the tables of design results. These tables give the complete results of the baseline designs for all flight conditions. The results for both control-rate-weighting and output-weighting are given. The tables, beginning at Table B.21, give the basic time response of each design along with the closed loop eigenvalues, the optimal gain matrix, and the diagonal elements of the optimal weighting matrices.

The stability of the fixed gain models is shown in Tables B.41 through B.60. The eigenvalues of the base-

line designs are compared to the eigenvalues for the fixed gain designs in all of the flight conditions and at all of the center of gravity locations previously investigated. Both the control-rate-weighting and output-weighting designs are checked for stability.

Table B.1 Cessna 402B Longitudinal Mathematical Model
          For Sea Level Take-off   (CG = 0.25)

$\dot{x} = Ax + Bu$

$$
\begin{bmatrix} \dot{\alpha} \\ \dot{u} \\ \dot{q} \\ \dot{\theta} \end{bmatrix}
=
\begin{bmatrix}
-1.1730 & -0.0017 & 0.9133 & -0.0249 \\
9.6588 & -0.0278 & 0.0000 & -31.7843 \\
-5.4978 & 0.0007 & -7.5327 & 0.0784 \\
0.0000 & 0.0000 & 1.0000 & 0.0000
\end{bmatrix}
\begin{bmatrix} \alpha \\ u \\ q \\ \theta \end{bmatrix}
$$

$$
+
\begin{bmatrix}
-0.0361 & -0.2262 \\
0.0000 & -4.5082 \\
-3.7650 & 1.1163 \\
0.0000 & 0.0000
\end{bmatrix}
\begin{bmatrix} \delta_{se} \\ \delta_f \end{bmatrix}
$$

$y = Cx + Du$

$$
\begin{bmatrix} a_z \\ \alpha \\ u \\ q \\ \theta \end{bmatrix}
=
\begin{bmatrix}
-220.3845 & -0.3190 & -15.9281 & 0.1377 \\
1.0000 & 0.0000 & 0.0000 & 0.0000 \\
0.0000 & 1.0000 & 0.0000 & 0.0000 \\
0.0000 & 0.0000 & 1.0000 & 0.0000 \\
0.0000 & 0.0000 & 0.0000 & 1.0000
\end{bmatrix}
\begin{bmatrix} \alpha \\ u \\ q \\ \theta \end{bmatrix}
$$

$$
+
\begin{bmatrix}
-6.6301 & -41.5912 \\
0.0000 & 0.0000 \\
0.0000 & 0.0000 \\
0.0000 & 0.0000 \\
0.0000 & 0.0000
\end{bmatrix}
\begin{bmatrix} \delta_{se} \\ \delta_f \end{bmatrix}
$$

B.3

Table B.2 Cessna 402B Longitudinal Mathematical Model
For Sea Level Climb   (CG = 0.25)

$\dot{x} = Ax + Bu$

$$
\begin{bmatrix} \dot{\alpha} \\ \dot{u} \\ \dot{q} \\ \dot{\theta} \end{bmatrix} = \begin{bmatrix} -1.3325 & -0.0014 & 0.9189 & -0.0120 \\ 12.7885 & -0.0228 & 0.0000 & -32.0688 \\ -6.4781 & 0.0023 & -8.1525 & 0.0406 \\ 0.0000 & 0.0000 & 1.0000 & 0.0000 \end{bmatrix} \begin{bmatrix} \alpha \\ u \\ q \\ \theta \end{bmatrix}
$$

$$
+ \begin{bmatrix} -0.0389 & -0.2595 \\ 0.0000 & -5.9354 \\ -4.6678 & 1.4135 \\ 0.0000 & 0.0000 \end{bmatrix} \begin{bmatrix} \delta_{se} \\ \delta_f \end{bmatrix}
$$

$y = Cx + Du$

$$
\begin{bmatrix} a_z \\ \alpha \\ u \\ q \\ \theta \end{bmatrix} = \begin{bmatrix} -283.5580 & -0.2857 & -17.1010 & 0.0780 \\ 1.0000 & 0.0000 & 0.0000 & 0.0000 \\ 0.0000 & 1.0000 & 0.0000 & 0.0000 \\ 0.0000 & 0.0000 & 1.0000 & 0.0000 \\ 0.0000 & 0.0000 & 0.0000 & 1.0000 \end{bmatrix} \begin{bmatrix} \alpha \\ u \\ q \\ \theta \end{bmatrix}
$$

$$
+ \begin{bmatrix} -8.2010 & -54.7130 \\ 0.0000 & 0.0000 \\ 0.0000 & 0.0000 \\ 0.0000 & 0.0000 \\ 0.0000 & 0.0000 \end{bmatrix} \begin{bmatrix} \delta_{se} \\ \delta_f \end{bmatrix}
$$

B.4

Table B.3 Cessna 402B Longitudinal Mathematical Model
For Climb at 5000 Feet   (CG = 0.25)

$\dot{x} = Ax + Bu$

$$
\begin{bmatrix} \dot{\alpha} \\ \dot{u} \\ \dot{q} \\ \dot{\theta} \end{bmatrix}
=
\begin{bmatrix}
-1.2413 & -0.0012 & 0.9304 & -0.0105 \\
12.5650 & -0.0212 & 0.0000 & -32.0750 \\
-7.1464 & 0.0016 & -7.5786 & 0.0330 \\
0.0000 & 0.0000 & 1.0000 & 0.0000
\end{bmatrix}
\begin{bmatrix} \alpha \\ u \\ q \\ \theta \end{bmatrix}
$$

$$
+
\begin{bmatrix}
-0.0361 & -0.2417 \\
0.0000 & -5.9354 \\
-4.6749 & 1.2914 \\
0.0000 & 0.0000
\end{bmatrix}
\begin{bmatrix} \delta_{se} \\ \delta_{f} \end{bmatrix}
$$

$y = Cx + Du$

$$
\begin{bmatrix} a_z \\ \alpha \\ u \\ q \\ \theta \end{bmatrix}
=
\begin{bmatrix}
-284.6474 & -0.2662 & -15.8299 & 0.0636 \\
1.0000 & 0.0000 & 0.0000 & 0.0000 \\
0.0000 & 1.0000 & 0.0000 & 0.0000 \\
0.0000 & 0.0000 & 1.0000 & 0.0000 \\
0.0000 & 0.0000 & 0.0000 & 1.0000
\end{bmatrix}
\begin{bmatrix} \alpha \\ u \\ q \\ \theta \end{bmatrix}
$$

$$
+
\begin{bmatrix}
-8.2155 & -54.9407 \\
0.0000 & 0.0000 \\
0.0000 & 0.0000 \\
0.0000 & 0.0000 \\
0.0000 & 0.0000
\end{bmatrix}
\begin{bmatrix} \delta_{se} \\ \delta_{f} \end{bmatrix}
$$

Table B.4 Cessna 402B Longitudinal Mathematical Model For Cruise at 20,000 Feet (CG = 0.25)

$$\dot{x} = Ax + Bu$$

$$
\begin{bmatrix} \dot{\alpha} \\ \dot{u} \\ \dot{q} \\ \dot{\theta} \end{bmatrix}
=
\begin{bmatrix}
-1.2343 & -0.0005 & 0.9583 & 0.0000 \\
18.3366 & -0.0178 & 0.0000 & -32.1733 \\
-11.7142 & 0.0008 & -7.1964 & 0.0000 \\
0.0000 & 0.0000 & 1.0000 & 0.0000
\end{bmatrix}
\begin{bmatrix} \alpha \\ u \\ q \\ \theta \end{bmatrix}
$$

$$
+
\begin{bmatrix}
-0.0343 & -0.2423 \\
0.0000 & -9.2750 \\
-6.9711 & 1.5455 \\
0.0000 & 0.0000
\end{bmatrix}
\begin{bmatrix} \delta_{se} \\ \delta_f \end{bmatrix}
$$

$$y = Cx + Du$$

$$
\begin{bmatrix} a_z \\ \alpha \\ u \\ q \\ \theta \end{bmatrix}
=
\begin{bmatrix}
-441.7867 & -0.1736 & -14.9157 & 0.0000 \\
1.0000 & 0.0000 & 0.0000 & 0.0000 \\
0.0000 & 1.0000 & 0.0000 & 0.0000 \\
0.0000 & 0.0000 & 1.0000 & 0.0000 \\
0.0000 & 0.0000 & 0.0000 & 1.0000
\end{bmatrix}
\begin{bmatrix} \alpha \\ u \\ q \\ \theta \end{bmatrix}
$$

$$
+
\begin{bmatrix}
-12.2596 & -86.7313 \\
0.0000 & 0.0000 \\
0.0000 & 0.0000 \\
0.0000 & 0.0000 \\
0.0000 & 0.0000
\end{bmatrix}
\begin{bmatrix} \delta_{se} \\ \delta_f \end{bmatrix}
$$

Table B.5 Cessna 402B Longitudinal Mathematical Model
For Sea Level Approach   (CG = 0.25)

$\dot{x} = Ax + Bu$

$$
\begin{bmatrix} \dot{\alpha} \\ \dot{u} \\ \dot{q} \\ \dot{\theta} \end{bmatrix} =
\begin{bmatrix}
-1.0456 & -0.0024 & 0.9192 & 0.0102 \\
21.0420 & -0.0525 & 0.0000 & -32.1253 \\
-3.7424 & 0.0049 & -6.2240 & -0.0264 \\
0.0000 & 0.0000 & 1.0000 & 0.0000
\end{bmatrix}
\begin{bmatrix} \alpha \\ u \\ q \\ \theta \end{bmatrix}
$$

$$
+ \begin{bmatrix}
-0.0297 & -0.0570 \\
0.0000 & -3.1464 \\
-2.7075 & 1.0004 \\
0.0000 & 0.0000
\end{bmatrix}
\begin{bmatrix} \delta_{se} \\ \delta_f \end{bmatrix}
$$

$y = Cx + Du$

$$
\begin{bmatrix} a_z \\ \alpha \\ u \\ q \\ \theta \end{bmatrix} =
\begin{bmatrix}
-165.8660 & -0.3822 & -12.9420 & -0.0511 \\
1.0000 & 0.0000 & 0.0000 & 0.0000 \\
0.0000 & 1.0000 & 0.0000 & 0.0000 \\
0.0000 & 0.0000 & 1.0000 & 0.0000 \\
0.0000 & 0.0000 & 0.0000 & 1.0000
\end{bmatrix}
\begin{bmatrix} \alpha \\ u \\ q \\ \theta \end{bmatrix}
$$

$$
+ \begin{bmatrix}
-4.7561 & -9.1360 \\
0.0000 & 0.0000 \\
0.0000 & 0.0000 \\
0.0000 & 0.0000 \\
0.0000 & 0.0000
\end{bmatrix}
\begin{bmatrix} \delta_{se} \\ \delta_f \end{bmatrix}
$$

B.7

Table B.6 Cessna 402B Longitudinal Mathematical Model
For Sea Level Take-off   (CG = 0.34)

$$\dot{x} = Ax + Bu$$

$$\begin{bmatrix} \dot{\alpha} \\ \dot{u} \\ \dot{q} \\ \dot{\theta} \end{bmatrix} = \begin{bmatrix} -1.1739 & -0.0017 & 0.9157 & -0.0249 \\ 9.6588 & -0.0278 & 0.0000 & -31.8268 \\ -1.8837 & 0.0004 & -7.1388 & 0.0743 \\ 0.0000 & 0.0000 & 1.0000 & 0.0000 \end{bmatrix} \begin{bmatrix} \alpha \\ u \\ q \\ \theta \end{bmatrix}$$

$$+ \begin{bmatrix} -0.0360 & -0.2264 \\ 0.0000 & -4.5082 \\ -3.6665 & 1.8218 \\ 0.0000 & 0.0000 \end{bmatrix} \begin{bmatrix} \delta_{se} \\ \delta_f \end{bmatrix}$$

$$y = Cx + Du$$

$$\begin{bmatrix} a_z \\ \alpha \\ u \\ q \\ \theta \end{bmatrix} = \begin{bmatrix} -215.8356 & -0.3126 & -15.4996 & 3.8543 \\ 1.0000 & 0.0000 & 0.0000 & 0.0000 \\ 0.0000 & 1.0000 & 0.0000 & 0.0000 \\ 0.0000 & 0.0000 & 1.0000 & 0.0000 \\ 0.0000 & 0.0000 & 0.0000 & 1.0000 \end{bmatrix} \begin{bmatrix} \alpha \\ u \\ q \\ \theta \end{bmatrix}$$

$$+ \begin{bmatrix} -6.6264 & -41.6264 \\ 0.0000 & 0.0000 \\ 0.0000 & 0.0000 \\ 0.0000 & 0.0000 \\ 0.0000 & 0.0000 \end{bmatrix} \begin{bmatrix} \delta_{se} \\ \delta_f \end{bmatrix}$$

Table B.7   Cessna 402B Longitudinal Mathematical Model
For Sea Level Climb   (CG = 0.34)

$\dot{x} = Ax + Bu$

$$
\begin{bmatrix} \dot{\alpha} \\ \dot{u} \\ \dot{q} \\ \dot{\theta} \end{bmatrix}
=
\begin{bmatrix}
-1.3335 & -0.0014 & 0.9210 & -0.0120 \\
12.7885 & -0.0228 & 0.0000 & -32.0688 \\
-1.7499 & 0.0021 & -7.7263 & 0.0385 \\
0.0000 & 0.0000 & 1.0000 & 0.0000
\end{bmatrix}
\begin{bmatrix} \alpha \\ u \\ q \\ \theta \end{bmatrix}
$$

$$
+
\begin{bmatrix}
-0.0389 & -0.2597 \\
0.0000 & -5.9354 \\
-4.5455 & 2.3424 \\
0.0000 & 0.0000
\end{bmatrix}
\begin{bmatrix} \delta_{se} \\ \delta_f \end{bmatrix}
$$

$y = Cx + Du$

$$
\begin{bmatrix} a_z \\ \alpha \\ u \\ q \\ \theta \end{bmatrix}
=
\begin{bmatrix}
-281.1698 & -0.2952 & -16.6572 & 2.8614 \\
1.0000 & 0.0000 & 0.0000 & 0.0000 \\
0.0000 & 1.0000 & 0.0000 & 0.0000 \\
0.0000 & 0.0000 & 1.0000 & 0.0000 \\
0.0000 & 0.0000 & 0.0000 & 1.0000
\end{bmatrix}
\begin{bmatrix} \alpha \\ u \\ q \\ \theta \end{bmatrix}
$$

$$
+
\begin{bmatrix}
-8.2063 & -54.7580 \\
0.0000 & 0.0000 \\
0.0000 & 0.0000 \\
0.0000 & 0.0000 \\
0.0000 & 0.0000
\end{bmatrix}
\begin{bmatrix} \delta_{se} \\ \delta_f \end{bmatrix}
$$

Table B.8 Cessna 402B Longitudinal Mathematical Model
For Climb at 5000 Feet   (CG = 0.34)

$$\dot{x} = Ax + Bu$$

$$
\begin{bmatrix} \dot{\alpha} \\ \dot{u} \\ \dot{q} \\ \dot{\theta} \end{bmatrix}
=
\begin{bmatrix}
-1.2421 & -0.0012 & 0.9322 & -0.0105 \\
12.5650 & -0.0212 & 0.0000 & -32.0808 \\
-2.3755 & 0.0014 & -7.1815 & 0.0313 \\
0.0000 & 0.0000 & 1.0000 & 0.0000
\end{bmatrix}
\begin{bmatrix} \alpha \\ u \\ q \\ \theta \end{bmatrix}
$$

$$
+
\begin{bmatrix}
-0.0361 & -0.2419 \\
0.0000 & -5.9355 \\
-4.5520 & 2.2285 \\
0.0000 & 0.0000
\end{bmatrix}
\begin{bmatrix} \delta_{se} \\ \delta_f \end{bmatrix}
$$

$$y = Cx + Du$$

$$
\begin{bmatrix} a_z \\ \alpha \\ u \\ q \\ \theta \end{bmatrix}
=
\begin{bmatrix}
-282.3740 & -0.2728 & -15.4134 & 2.8603 \\
1.0000 & 0.0000 & 0.0000 & 0.0000 \\
0.0000 & 1.0000 & 0.0000 & 0.0000 \\
0.0000 & 0.0000 & 1.0000 & 0.0000 \\
0.0000 & 0.0000 & 0.0000 & 1.0000
\end{bmatrix}
\begin{bmatrix} \alpha \\ u \\ q \\ \theta \end{bmatrix}
$$

$$
+
\begin{bmatrix}
-8.2205 & -54.9926 \\
0.0000 & 0.0000 \\
0.0000 & 0.0000 \\
0.0000 & 0.0000 \\
0.0000 & 0.0000
\end{bmatrix}
\begin{bmatrix} \delta_{se} \\ \delta_f \end{bmatrix}
$$

Table B.9 Cessna 402B Longitudinal Mathematical Model
For Cruise at 20,000 Feet   (CG = 0.34)

$$\dot{x} = Ax + Bu$$

$$\begin{bmatrix} \dot{\alpha} \\ \dot{u} \\ \dot{q} \\ \dot{\theta} \end{bmatrix} = \begin{bmatrix} -1.2348 & -0.0005 & 0.9594 & 0.0000 \\ 18.3366 & -0.0178 & 0.0000 & -32.1740 \\ -4.1742 & 0.0007 & -6.8172 & 0.0000 \\ 0.0000 & 0.0000 & 1.0000 & 0.0000 \end{bmatrix} \begin{bmatrix} \alpha \\ u \\ q \\ \theta \end{bmatrix}$$

$$+ \begin{bmatrix} -0.0343 & -0.2424 \\ 0.0000 & -9.2750 \\ -6.7860 & 3.0365 \\ 0.0000 & 0.0000 \end{bmatrix} \begin{bmatrix} \delta_{se} \\ \delta_f \end{bmatrix}$$

$$y = Cx + Du$$

$$\begin{bmatrix} a_z \\ \alpha \\ u \\ q \\ \theta \end{bmatrix} = \begin{bmatrix} -441.9510 & -0.1790 & -14.5313 & 1.5492 \\ 1.0000 & 0.0000 & 0.0000 & 0.0000 \\ 0.0000 & 1.0000 & 0.0000 & 0.0000 \\ 0.0000 & 0.0000 & 1.0000 & 0.0000 \\ 0.0000 & 0.0000 & 0.0000 & 1.0000 \end{bmatrix} \begin{bmatrix} \alpha \\ u \\ q \\ \theta \end{bmatrix}$$

$$+ \begin{bmatrix} -12.2693 & -86.7581 \\ 0.0000 & 0.0000 \\ 0.0000 & 0.0000 \\ 0.0000 & 0.0000 \\ 0.0000 & 0.0000 \end{bmatrix} \begin{bmatrix} \delta_{se} \\ \delta_f \end{bmatrix}$$

Table B.10 Cessna 402B Longitudinal Mathematical Model
For Sea Level Approach   (CG = 0.34)

$$\dot{x} = Ax + Bu$$

$$
\begin{bmatrix} \dot{\alpha} \\ \dot{u} \\ \dot{q} \\ \dot{\theta} \end{bmatrix} =
\begin{bmatrix}
-1.0464 & -0.0024 & 0.9213 & 0.0102 \\
21.0420 & -0.0525 & 0.0000 & -32.1299 \\
-0.9632 & 0.0046 & -5.8986 & -0.0250 \\
0.0000 & 0.0000 & 1.0000 & 0.0000
\end{bmatrix}
\begin{bmatrix} \alpha \\ u \\ q \\ \theta \end{bmatrix}
$$

$$
+
\begin{bmatrix}
-0.0297 & -0.0570 \\
0.0000 & -3.1464 \\
-2.6365 & 1.1559 \\
0.0000 & 0.0000
\end{bmatrix}
\begin{bmatrix} \delta_{se} \\ \delta_f \end{bmatrix}
$$

$$y = Cx + Du$$

$$
\begin{bmatrix} a_z \\ \alpha \\ u \\ q \\ \theta \end{bmatrix} =
\begin{bmatrix}
-167.6825 & -0.3846 & -12.6114 & -0.5161 \\
1.0000 & 0.0000 & 0.0000 & 0.0000 \\
0.0000 & 1.0000 & 0.0000 & 0.0000 \\
0.0000 & 0.0000 & 1.0000 & 0.0000 \\
0.0000 & 0.0000 & 0.0000 & 1.0000
\end{bmatrix}
\begin{bmatrix} \alpha \\ u \\ q \\ \theta \end{bmatrix}
$$

$$
+
\begin{bmatrix}
-4.7593 & -9.1341 \\
0.0000 & 0.0000 \\
0.0000 & 0.0000 \\
0.0000 & 0.0000 \\
0.0000 & 0.0000
\end{bmatrix}
\begin{bmatrix} \delta_{se} \\ \delta_f \end{bmatrix}
$$

Table B.11 Cessna 402B Longitudinal Mathematical Model
For Sea Level Take-off   (CG = 0.14)

$$\dot{x} = Ax + Bu$$

$$
\begin{bmatrix} \dot{\alpha} \\ \dot{u} \\ \dot{q} \\ \dot{\theta} \end{bmatrix}
=
\begin{bmatrix}
-1.1719 & -0.0017 & 0.9106 & -0.0249 \\
9.6588 & -0.0278 & 0.0000 & -31.8268 \\
-9.9359 & 0.0011 & -8.0298 & 0.0836 \\
0.0000 & 0.0000 & 1.0000 & 0.0000
\end{bmatrix}
\begin{bmatrix} \alpha \\ u \\ q \\ \theta \end{bmatrix}
$$

$$
+
\begin{bmatrix}
-0.0360 & -0.2260 \\
0.0000 & -4.5082 \\
-3.8859 & 0.2500 \\
0.0000 & 0.0000
\end{bmatrix}
\begin{bmatrix} \delta_{se} \\ \delta_{f} \end{bmatrix}
$$

$$y = Cx + Du$$

$$
\begin{bmatrix} a_z \\ \alpha \\ u \\ q \\ \theta \end{bmatrix}
=
\begin{bmatrix}
-215.4679 & -0.3126 & -16.4373 & 3.8543 \\
1.0000 & 0.0000 & 0.0000 & 0.0000 \\
0.0000 & 1.0000 & 0.0000 & 0.0000 \\
0.0000 & 0.0000 & 1.0000 & 0.0000 \\
0.0000 & 0.0000 & 0.0000 & 1.0000
\end{bmatrix}
\begin{bmatrix} \alpha \\ u \\ q \\ \theta \end{bmatrix}
$$

$$
+
\begin{bmatrix}
-6.6154 & -41.5528 \\
0.0000 & 0.0000 \\
0.0000 & 0.0000 \\
0.0000 & 0.0000 \\
0.0000 & 0.0000
\end{bmatrix}
\begin{bmatrix} \delta_{se} \\ \delta_{f} \end{bmatrix}
$$

B.13

Table B.12 Cessna 402B Longitudinal Mathematical Model For Sea Level Climb (CG = 0.14)

$$\dot{x} = Ax + Bu$$

$$
\begin{bmatrix} \dot{\alpha} \\ \dot{u} \\ \dot{q} \\ \dot{\theta} \end{bmatrix}
=
\begin{bmatrix}
-1.3313 & -0.0014 & 0.9163 & -0.0120 \\
12.7885 & -0.0228 & 0.0000 & -32.0688 \\
-12.2848 & 0.0026 & -8.6919 & 0.0433 \\
0.0000 & 0.0000 & 1.0000 & 0.0000
\end{bmatrix}
\begin{bmatrix} \alpha \\ u \\ q \\ \theta \end{bmatrix}
$$

$$
+
\begin{bmatrix}
-0.0389 & -0.2593 \\
0.0000 & -5.9354 \\
-4.8180 & 0.2727 \\
0.0000 & 0.0000
\end{bmatrix}
\begin{bmatrix} \delta_{se} \\ \delta_f \end{bmatrix}
$$

$$y = Cx + Du$$

$$
\begin{bmatrix} a_z \\ \alpha \\ u \\ q \\ \theta \end{bmatrix}
=
\begin{bmatrix}
-280.7059 & -0.2952 & -17.6482 & 2.8614 \\
1.0000 & 0.0000 & 0.0000 & 0.0000 \\
0.0000 & 1.0000 & 0.0000 & 0.0000 \\
0.0000 & 0.0000 & 1.0000 & 0.0000 \\
0.0000 & 0.0000 & 0.0000 & 1.0000
\end{bmatrix}
\begin{bmatrix} \alpha \\ u \\ q \\ \theta \end{bmatrix}
$$

$$
+
\begin{bmatrix}
-8.1937 & -54.6737 \\
0.0000 & 0.0000 \\
0.0000 & 0.0000 \\
0.0000 & 0.0000 \\
0.0000 & 0.0000
\end{bmatrix}
\begin{bmatrix} \delta_{se} \\ \delta_f \end{bmatrix}
$$

Table B.13 Cessna 402B Longitudinal Mathematical Model
For Climb at 5000 Feet   (CG = 0.14)

$\dot{x} = Ax + Bu$

$$
\begin{bmatrix} \dot{\alpha} \\ \dot{u} \\ \dot{q} \\ \dot{\theta} \end{bmatrix}
=
\begin{bmatrix}
-1.2403 & -0.0012 & 0.9282 & -0.0105 \\
12.5650 & -0.0212 & 0.0000 & -32.0808 \\
-13.0067 & 0.0019 & -8.0812 & 0.0352 \\
0.0000 & 0.0000 & 1.0000 & 0.0000
\end{bmatrix}
\begin{bmatrix} \alpha \\ u \\ q \\ \theta \end{bmatrix}
$$

$$
+
\begin{bmatrix}
-0.0361 & -0.2415 \\
0.0000 & -5.9355 \\
-4.8260 & 0.1403 \\
0.0000 & 0.0000
\end{bmatrix}
\begin{bmatrix} \delta_{se} \\ \delta_f \end{bmatrix}
$$

$y = Cx + Du$

$$
\begin{bmatrix} a_z \\ \alpha \\ u \\ q \\ \theta \end{bmatrix}
=
\begin{bmatrix}
-281.9648 & -0.2728 & -16.3227 & 2.8603 \\
1.0000 & 0.0000 & 0.0000 & 0.0000 \\
0.0000 & 1.0000 & 0.0000 & 0.0000 \\
0.0000 & 0.0000 & 1.0000 & 0.0000 \\
0.0000 & 0.0000 & 0.0000 & 1.0000
\end{bmatrix}
\begin{bmatrix} \alpha \\ u \\ q \\ \theta \end{bmatrix}
$$

$$
+
\begin{bmatrix}
-8.2114 & -54.9016 \\
0.0000 & 0.0000 \\
0.0000 & 0.0000 \\
0.0000 & 0.0000 \\
0.0000 & 0.0000
\end{bmatrix}
\begin{bmatrix} \delta_{se} \\ \delta_f \end{bmatrix}
$$

Table B.14 Cessna 402B Longitudinal Mathematical Model
For Cruise at 20,000 Feet   (CG = 0.14)

$$\dot{x} = Ax + Bu$$

$$
\begin{bmatrix} \dot{\alpha} \\ \dot{u} \\ \dot{q} \\ \dot{\theta} \end{bmatrix}
=
\begin{bmatrix}
-1.2336 & -0.0005 & 0.9569 & 0.0000 \\
18.3366 & -0.0178 & 0.0000 & -32.1740 \\
-20.9806 & 0.0009 & -7.6766 & 0.0000 \\
0.0000 & 0.0000 & 1.0000 & 0.0000
\end{bmatrix}
\begin{bmatrix} \alpha \\ u \\ q \\ \theta \end{bmatrix}
$$

$$
+
\begin{bmatrix}
-0.0342 & -0.2422 \\
0.0000 & -9.2750 \\
-7.1985 & 0.2869 \\
0.0000 & 0.0000
\end{bmatrix}
\begin{bmatrix} \delta_{se} \\ \delta_f \end{bmatrix}
$$

$$y = Cx + Du$$

$$
\begin{bmatrix} a_z \\ \alpha \\ u \\ q \\ \theta \end{bmatrix}
=
\begin{bmatrix}
-441.5215 & -0.1790 & -15.4261 & 1.5492 \\
1.0000 & 0.0000 & 0.0000 & 0.0000 \\
0.0000 & 1.0000 & 0.0000 & 0.0000 \\
0.0000 & 0.0000 & 1.0000 & 0.0000 \\
0.0000 & 0.0000 & 0.0000 & 1.0000
\end{bmatrix}
\begin{bmatrix} \alpha \\ u \\ q \\ \theta \end{bmatrix}
$$

$$
+
\begin{bmatrix}
-12.2549 & -86.6865 \\
0.0000 & 0.0000 \\
0.0000 & 0.0000 \\
0.0000 & 0.0000 \\
0.0000 & 0.0000
\end{bmatrix}
\begin{bmatrix} \delta_{se} \\ \delta_f \end{bmatrix}
$$

Table B.15 Cessna 402B Longitudinal Mathematical Model
For Sea Level Approach   (CG = 0.14)

$\dot{x} = Ax + Bu$

$$
\begin{bmatrix} \dot{\alpha} \\ \dot{u} \\ \dot{q} \\ \dot{\theta} \end{bmatrix} =
\begin{bmatrix}
-1.0446 & -0.0024 & 0.9166 & 0.0102 \\
21.0420 & -0.0525 & 0.0000 & -32.1299 \\
-7.1555 & 0.0053 & -6.6358 & -0.0281 \\
0.0000 & 0.0000 & 1.0000 & 0.0000
\end{bmatrix}
\begin{bmatrix} \alpha \\ u \\ q \\ \theta \end{bmatrix}
$$

$$
+ \begin{bmatrix}
-0.0297 & -0.0569 \\
0.0000 & -3.1464 \\
-2.7946 & 0.8094 \\
0.0000 & 0.0000
\end{bmatrix}
\begin{bmatrix} \delta_{se} \\ \delta_f \end{bmatrix}
$$

$y = Cx + Du$

$$
\begin{bmatrix} a_z \\ \alpha \\ u \\ q \\ \theta \end{bmatrix} =
\begin{bmatrix}
-167.3940 & -0.3846 & -13.3646 & 2.7529 \\
1.0000 & 0.0000 & 0.0000 & 0.0000 \\
0.0000 & 1.0000 & 0.0000 & 0.0000 \\
0.0000 & 0.0000 & 1.0000 & 0.0000 \\
0.0000 & 0.0000 & 0.0000 & 1.0000
\end{bmatrix}
\begin{bmatrix} \alpha \\ u \\ q \\ \theta \end{bmatrix}
$$

$$
+ \begin{bmatrix}
-4.7529 & -9.1181 \\
0.0000 & 0.0000 \\
0.0000 & 0.0000 \\
0.0000 & 0.0000 \\
0.0000 & 0.0000
\end{bmatrix}
\begin{bmatrix} \delta_{se} \\ \delta_f \end{bmatrix}
$$

Table B.16 Cessna 402B Lateral-Directional
Mathematical Model For Sea Level Take-off

$\dot{x} = Ax + Bu$

$$
\begin{bmatrix} \dot{\beta} \\ \dot{p} \\ \dot{r} \\ \dot{\phi} \end{bmatrix} = \begin{bmatrix} -0.1547 & 0.1178 & -0.9939 & 0.1688 \\ -2.9322 & -2.4155 & 0.3692 & -0.0062 \\ 2.5862 & -0.3308 & -0.3206 & -0.0063 \\ 0.0000 & 1.0000 & 0.2716 & 0.0000 \end{bmatrix} \begin{bmatrix} \beta \\ p \\ r \\ \phi \end{bmatrix}
$$

$$
+ \begin{bmatrix} 0.0000 & 0.0139 \\ -1.9624 & 0.2521 \\ -0.0615 & -0.5288 \\ 0.0000 & 0.0000 \end{bmatrix} \begin{bmatrix} \delta_{df} \\ \delta_{sr} \end{bmatrix}
$$

$y = Cx + Du$

$$
\begin{bmatrix} a_y \\ \beta \\ p \\ r \\ \phi \end{bmatrix} = \begin{bmatrix} -28.4455 & 21.6543 & 1.1186 & -0.0173 \\ 1.0000 & 0.0000 & 0.0000 & 0.0000 \\ 0.0000 & 1.0000 & 0.0000 & 0.0000 \\ 0.0000 & 0.0000 & 1.0000 & 0.0000 \\ 0.0000 & 0.0000 & 0.0000 & 1.0000 \end{bmatrix} \begin{bmatrix} \beta \\ p \\ r \\ \phi \end{bmatrix}
$$

$$
+ \begin{bmatrix} 0.0000 & 2.5606 \\ 0.0000 & 0.0000 \\ 0.0000 & 0.0000 \\ 0.0000 & 0.0000 \\ 0.0000 & 0.0000 \end{bmatrix} \begin{bmatrix} \delta_{df} \\ \delta_{sr} \end{bmatrix}
$$

B.18

Table B.17 Cessna 402B Lateral-Directional Mathematical Model For Sea Level Climb

$$\dot{x} = Ax + Bu$$

$$
\begin{bmatrix} \dot{\beta} \\ \dot{p} \\ \dot{r} \\ \dot{\phi} \end{bmatrix}
=
\begin{bmatrix}
-0.1879 & 0.0874 & -0.9971 & 0.1505 \\
-3.7107 & -2.6275 & 0.3918 & -0.0070 \\
3.7138 & -0.2901 & -0.3503 & -0.0065 \\
0.0000 & 1.0000 & 0.1700 & 0.0000
\end{bmatrix}
\begin{bmatrix} \beta \\ p \\ r \\ \phi \end{bmatrix}
$$

$$
+
\begin{bmatrix}
0.0000 & 0.0162 \\
-2.6247 & 0.3362 \\
-0.0611 & -0.7013 \\
0.0000 & 0.0000
\end{bmatrix}
\begin{bmatrix} \delta_{df} \\ \delta_{sr} \end{bmatrix}
$$

$$y = Cx + Du$$

$$
\begin{bmatrix} a_y \\ \beta \\ p \\ r \\ \phi \end{bmatrix}
=
\begin{bmatrix}
-39.6290 & 18.4390 & 0.6125 & 0.0193 \\
1.0000 & 0.0000 & 0.0000 & 0.0000 \\
0.0000 & 1.0000 & 0.0000 & 0.0000 \\
0.0000 & 0.0000 & 1.0000 & 0.0000 \\
0.0000 & 0.0000 & 0.0000 & 1.0000
\end{bmatrix}
\begin{bmatrix} \beta \\ p \\ r \\ \phi \end{bmatrix}
$$

$$
+
\begin{bmatrix}
0.0000 & 3.4133 \\
0.0000 & 0.0000 \\
0.0000 & 0.0000 \\
0.0000 & 0.0000 \\
0.0000 & 0.0000
\end{bmatrix}
\begin{bmatrix} \delta_{df} \\ \delta_{sr} \end{bmatrix}
$$

Table B.18 Cessna 402B Lateral-Directional Mathematical Model For Climb at 5000 Feet

$$\dot{x} = Ax + Bu$$

$$
\begin{bmatrix} \dot{\beta} \\ \dot{p} \\ \dot{r} \\ \dot{\phi} \end{bmatrix}
=
\begin{bmatrix}
-0.1742 & 0.0876 & -0.9969 & 0.1397 \\
-3.7132 & -2.4327 & 0.3639 & -0.0060 \\
3.7107 & -0.2692 & -0.3246 & -0.0056 \\
0.0000 & 1.0000 & 0.1653 & 0.0000
\end{bmatrix}
\begin{bmatrix} \beta \\ p \\ r \\ \phi \end{bmatrix}
$$

$$
+
\begin{bmatrix}
0.0000 & 0.0150 \\
-2.6244 & 0.3363 \\
-0.0612 & -0.7012 \\
0.0000 & 0.0000
\end{bmatrix}
\begin{bmatrix} \delta_{df} \\ \delta_{sr} \end{bmatrix}
$$

$$y = Cx + Du$$

$$
\begin{bmatrix} a_y \\ \beta \\ p \\ r \\ \phi \end{bmatrix}
=
\begin{bmatrix}
-39.6047 & 19.9233 & 0.6936 & 0.0113 \\
1.0000 & 0.0000 & 0.0000 & 0.0000 \\
0.0000 & 1.0000 & 0.0000 & 0.0000 \\
0.0000 & 0.0000 & 1.0000 & 0.0000 \\
0.0000 & 0.0000 & 0.0000 & 1.0000
\end{bmatrix}
\begin{bmatrix} \beta \\ p \\ r \\ \phi \end{bmatrix}
$$

$$
+
\begin{bmatrix}
0.0000 & 3.4121 \\
0.0000 & 0.0000 \\
0.0000 & 0.0000 \\
0.0000 & 0.0000 \\
0.0000 & 0.0000
\end{bmatrix}
\begin{bmatrix} \delta_{df} \\ \delta_{sr} \end{bmatrix}
$$

B.20

Table B.19 Cessna 402B Lateral-Directional
Mathematical Model For Cruise at 20,000 Feet

$\dot{x} = Ax + Bu$

$$\begin{bmatrix} \dot{\beta} \\ \dot{p} \\ \dot{r} \\ \dot{\phi} \end{bmatrix} = \begin{bmatrix} -0.1843 & 0.0482 & -0.9993 & 0.0898 \\ -5.3309 & -2.3284 & 0.3048 & -0.0039 \\ 6.3295 & -0.1677 & -0.3141 & -0.0032 \\ 0.0000 & 1.0000 & 0.0482 & 0.0000 \end{bmatrix} \begin{bmatrix} \beta \\ p \\ r \\ \phi \end{bmatrix}$$

$$+ \begin{bmatrix} 0.0000 & 0.0151 \\ -4.1555 & 0.5331 \\ -0.0435 & -1.1090 \\ 0.0000 & 0.0000 \end{bmatrix} \begin{bmatrix} \delta_{df} \\ \delta_{sr} \end{bmatrix}$$

$y = Cx + Du$

$$\begin{bmatrix} a_y \\ \beta \\ p \\ r \\ \phi \end{bmatrix} = \begin{bmatrix} -65.9673 & 17.2417 & 0.2434 & 0.0107 \\ 1.0000 & 0.0000 & 0.0000 & 0.0000 \\ 0.0000 & 1.0000 & 0.0000 & 0.0000 \\ 0.0000 & 0.0000 & 1.0000 & 0.0000 \\ 0.0000 & 0.0000 & 0.0000 & 1.0000 \end{bmatrix} \begin{bmatrix} \beta \\ p \\ r \\ \phi \end{bmatrix}$$

$$+ \begin{bmatrix} 0.0000 & 5.4192 \\ 0.0000 & 0.0000 \\ 0.0000 & 0.0000 \\ 0.0000 & 0.0000 \\ 0.0000 & 0.0000 \end{bmatrix} \begin{bmatrix} \delta_{df} \\ \delta_{sr} \end{bmatrix}$$

B.21

Table B.20 Cessna 402B Lateral-Directional
Mathematical Model For Sea Level Approach

$$\dot{x} = Ax + Bu$$

$$
\begin{bmatrix} \dot{\beta} \\ \dot{p} \\ \dot{r} \\ \dot{\phi} \end{bmatrix}
=
\begin{bmatrix}
-0.1452 & 0.0871 & -0.9971 & 0.2008 \\
-2.1765 & -2.0130 & 0.3034 & -0.0072 \\
2.1817 & -0.2224 & -0.2692 & -0.0067 \\
0.0000 & 1.0000 & 0.0348 & 0.0000
\end{bmatrix}
\begin{bmatrix} \beta \\ p \\ r \\ \phi \end{bmatrix}
$$

$$
+
\begin{bmatrix}
0.0000 & 0.0125 \\
-1.5409 & 0.1974 \\
-0.0357 & -0.4117 \\
0.0000 & 0.0000
\end{bmatrix}
\begin{bmatrix} \delta_{df} \\ \delta_{sr} \end{bmatrix}
$$

$$y = Cx + Du$$

$$
\begin{bmatrix} a_y \\ \beta \\ p \\ r \\ \phi \end{bmatrix}
=
\begin{bmatrix}
-23.2752 & 13.9586 & 0.4583 & 0.0216 \\
1.0000 & 0.0000 & 0.0000 & 0.0000 \\
0.0000 & 1.0000 & 0.0000 & 0.0000 \\
0.0000 & 0.0000 & 1.0000 & 0.0000 \\
0.0000 & 0.0000 & 0.0000 & 1.0000
\end{bmatrix}
\begin{bmatrix} \beta \\ p \\ r \\ \phi \end{bmatrix}
$$

$$
+
\begin{bmatrix}
0.0000 & 2.0036 \\
0.0000 & 0.0000 \\
0.0000 & 0.0000 \\
0.0000 & 0.0000 \\
0.0000 & 0.0000
\end{bmatrix}
\begin{bmatrix} \delta_{df} \\ \delta_{sr} \end{bmatrix}
$$

Table B.21 Summary of Longitudinal RQAS Response
            for a Sea-Level Take-off -- Control-Rate-Weighting

Time Domain Response:

	Open Loop		Baseline RQAS		Percent Reduction	
	Max.	RMS	Max.	RMS	Max.	RMS
a_z (f/s2)	16.2	5.7	10.3	3.4	36%	40%
α (deg)	4.4	1.6	5.4	1.8	-23%	-12%
u (f/s)	2.1	1.2	3.4	1.9	-62%	-58%
q (deg/s)	2.4	1.0	3.7	1.6	-54%	-60%
θ (deg)	2.6	0.9	3.5	1.3	-35%	-44%
δ_{se} (deg)	-	-	4.4	1.6	-	-
δ_f (deg)	-	-	15.0	5.6	-	-
$\dot{\delta}_{se}$ (deg/s)	-	-	7.9	-	-	-
$\dot{\delta}_f$ (deg/s)	-	-	83.8	-	-	-

Table B.21 Summary of Longitudinal RQAS Response
         for a Sea-Level take-off--Control-Rate-Weighting
         (Continued)

<u>System Eigenvalues</u>:

	Open Loop		Baseline RQAS	
	Frequency	Damping	Frequency	Damping
Phugoid	0.15	0.02	0.09	0.87
Phugoid	0.15	0.02	0.09	0.87
Short Period	2.1	1.0	6.3	0.70
Short Period	6.6	1.0	6.3	0.70
Servo	10.0	1.0	2.4	1.0
Servo	10.0	1.0	11.6	1.0
Filter	–	–	14.6	1.0
Filter	–	–	36.6	1.0

Note 1: Baseline RQAS Frequency and Damping are based on
        roots of the W'-Plane.

Note 2: Control-Rate-Weighting introduces 2 filter states.

<u>Optimal Gain Matrix</u>:

$$K = \begin{bmatrix} 5.4211 & -0.0021 & -4.0595 & -9.0508 & 7.9180 & 1.9853 \\ 110.92 & 0.1610 & 12.198 & 22.167 & 1.5731 & 26.910 \end{bmatrix}$$

<u>Weighting Matrices</u> -- <u>Diagonal Elements</u>:

Q' = (0.05, 10.0, 0.0001, 15.0, 20.0)

R' = (0.77, 3.06)

S' = (0.07, 0.06)

B.24

Table B.22 Summary of Longitudinal RQAS Response
for a Sea-Level Climb -- Control-Rate-Weighting

Time Domain Response:

	Open Loop		Baseline RQAS		Percent Reduction	
	Max.	RMS	Max.	RMS	Max.	RMS
a_z (f/s2)	13.1	6.3	12.2	3.4	7%	46%
α (deg)	2.8	1.3	3.6	1.5	-29%	-15%
u (f/s)	1.9	1.1	4.1	2.4	-116%	-118%
q (deg/s)	1.8	0.9	2.7	1.4	-50%	-56%
θ (deg)	1.6	1.0	2.0	1.1	-25%	-10%
δ_{se} (deg)	-	-	4.3	2.3	-	-
δ_f (deg)	-	-	11.8	3.4	-	-
$\dot{\delta}_{se}$ (deg/s)	-	-	11.4	-	-	-
$\dot{\delta}_f$ (deg/s)	-	-	91.1	-	-	-

Table B.22 Summary of Longitudinal RQAS Response
        for a Sea-Level Climb -- Control-Rate-Weighting
        (Continued)

System Eigenvalues:

	Open Loop		Baseline RQAS	
	Frequency	Damping	Frequency	Damping
Phugoid	0.15	0.04	0.09	0.79
Phugoid	0.15	0.04	0.09	0.79
Short Period	2.4	1.0	6.0	0.68
Short Period	7.1	1.0	6.0	0.68
Servo	10.0	1.0	3.5	1.0
Servo	10.0	1.0	11.8	1.0
Filter	-	-	15.3	1.0
Filter	-	-	63.8	1.0

Note 1: Baseline RQAS Frequency and Damping are based on
         roots of the W'-Plane.

Note 2: Control-Rate-Weighting introduces 2 filter states.

Optimal Gain Matrix:

$$
K = \begin{bmatrix} 27.930 & 0.0123 & -2.5093 & -13.634 & 8.8770 & 6.1749 \\ 171.39 & 0.1719 & 14.655 & 24.772 & 3.0441 & 38.537 \end{bmatrix}
$$

Weighting Matrices -- Diagonal Elements:

Q' = (0.05, 10.0, 0.0001, 3.0, 20.0)

R' = (0.12, 0.33)

S' = (0.02, 0.03)

Table B.23 Summary of Longitudinal RQAS Response
for a Climb at 5000 feet-- Control-Rate-Weighting

Time Domain Response:

	Open Loop		Baseline RQAS		Percent Reduction	
	Max.	RMS	Max.	RMS	Max.	RMS
a_z (f/s2)	10.2	3.6	7.3	2.1	28%	42%
α (deg)	2.2	0.8	3.1	1.2	-41%	-50%
u (f/s)	2.4	1.4	4.2	2.4	-75%	-71%
q (deg/s)	1.5	0.7	2.1	0.9	-40%	-28%
θ (deg)	2.2	1.1	2.4	1.2	-9%	-9%
δ_{se} (deg)	-	-	4.2	2.2	-	-
δ_f (deg)	-	-	9.0	4.1	-	-
$\dot{\delta}_{se}$ (deg/s)	-	-	6.4	-	-	-
$\dot{\delta}_f$ (deg/s)	-	-	35.3	-	-	-

Table B.23 Summary of Longitudinal RQAS Response
           for a Climb at 5000 feet--Control-Rate-Weighting
           (Continued)

System Eigenvalues:

	Open Loop		Baseline RQAS	
	Frequency	Damping	Frequency	Damping
Phugoid	0.14	0.04	0.08	0.80
Phugoid	0.14	0.04	0.08	0.80
Short Period	2.5	1.0	6.1	0.63
Short Period	6.2	1.0	6.1	0.63
Servo	10.0	1.0	3.5	1.0
Servo	10.0	1.0	11.6	1.0
Filter	-	-	15.6	1.0
Filter	-	-	64.1	1.0

Note 1: Baseline RQAS Frequency and Damping are based on roots of the W'-Plane.

Note 2: Control-Rate-Weighting introduces 2 filter states.

Optimal Gain Matrix:

$$K = \begin{bmatrix} 25.662 & 0.0105 & -3.2351 & -12.532 & 9.2575 & 6.1700 \\ 171.79 & 0.1520 & 14.182 & 25.136 & 3.0844 & 38.631 \end{bmatrix}$$

Weighting Matrices -- Diagonal Elements:

Q' = (0.05, 15.0, 0.0001, 3.0, 20.0)

R' = (0.12, 0.33)

S' = (0.02, 0.03)

Table B.24 Summary of Longitudinal RQAS Response for a Cruise at 20000 feet-- Control-Rate-Weighting

Time Domain Response:

	Open Loop		Baseline RQAS		Percent Reduction	
	Max.	RMS	Max.	RMS	Max.	RMS
a_z (f/s2)	7.0	2.9	4.0	1.5	43%	48%
α (deg)	0.9	0.4	1.4	0.6	-56%	-50%
u (f/s)	1.5	0.9	2.4	1.5	-60%	-67%
q (deg/s)	1.2	0.6	1.3	0.6	-8%	0%
θ (deg)	1.3	0.7	1.4	0.8	-8%	-14%
δ_{se} (deg)	-	-	2.0	0.9	-	-
δ_f (deg)	-	-	4.9	2.3	-	-
$\dot{\delta}_{se}$ (deg/s)	-	-	7.0	-	-	-
$\dot{\delta}_f$ (deg/s)	-	-	25.3	-	-	-

Table B.24 Summary of Longitudinal RQAS Response
for a Cruise at 20000 ft -- Control-Rate-Weighting
(Continued)

System Eigenvalues:

	Open Loop		Baseline RQAS	
	Frequency	Damping	Frequency	Damping
Phugoid	0.10	0.08	0.08	0.78
Phugoid	0.10	0.08	0.08	0.78
Short Period	4.5	0.9	10.2	0.48
Short Period	4.5	0.9	10.2	0.48
Servo	10.0	1.0	1.3	1.0
Servo	10.0	1.0	11.5	1.0
Filter	–	–	27.9	1.0
Filter	–	–	125	1.0

Note 1: Baseline RQAS Frequency and Damping are based on
roots of the W'-Plane.

Note 2: Control-Rate-Weighting introduces 2 filter states.

Optimal Gain Matrix:

$$K = \begin{bmatrix} 29.784 & -0.0443 & -15.303 & -5.6702 & 18.406 & 4.8751 \\ 254.71 & 0.0959 & 15.162 & 21.686 & 3.9323 & 55.227 \end{bmatrix}$$

Weighting Matrices -- Diagonal Elements:

Q' = (0.05, 10.0, 0.0001, 15.0, 20.0)

R' = (0.06, 0.11)

S' = (0.01, 0.01)

**Table B.25 Summary of Longitudinal RQAS Response
for an Approach at Sea-Level
Control-Rate-Weighting**

<u>Time Domain Response</u>:

	Open Loop		Baseline RQAS		Percent Reduction	
	Max.	RMS	Max.	RMS	Max.	RMS
a_z (f/s2)	12.9	4.9	10.7	3.9	17%	20%
α (deg)	4.8	1.8	4.7	1.7	2%	6%
u (f/s)	2.9	1.6	3.5	2.1	-21%	-31%
q (deg/s)	2.2	1.0	3.5	1.7	-59%	-70%
θ (deg)	2.7	1.3	3.5	1.5	-30%	-15%
δ_{se} (deg)	-	-	4.4	1.6	-	-
δ_f (deg)	-	-	15.5	6.4	-	-
$\dot{\delta}_{se}$ (deg/s)	-	-	16.8	-	-	-
$\dot{\delta}_f$ (deg/s)	-	-	101.4	-	-	-

Table B.25 Summary of Longitudinal RQAS Response
for an Approach at Sea-Level
Control-Rate-Weighting (Continued)

System Eigenvalues:

	Open Loop		Baseline RQAS	
	Frequency	Damping	Frequency	Damping
Phugoid	0.21	0.15	0.19	0.93
Phugoid	0.21	0.15	0.19	0.93
Short Period	1.8	1.0	7.4	0.67
Short Period	5.4	1.0	7.4	0.67
Servo	10.0	1.0	3.2	1.0
Servo	10.0	1.0	10.6	1.0
Filter	-	-	21.4	1.0
Filter	-	-	32.4	1.0

Note 1: Baseline RQAS Frequency and Damping are based on
roots of the W'-Plane.

Note 2: Control-Rate-Weighting introduces 2 filter states.

Optimal Gain Matrix:

$$
K = \begin{bmatrix} -12.514 & -0.7461 & -14.385 & -23.176 & 16.034 & -0.1902 \\ 138.74 & 0.3300 & 31.573 & 74.169 & -1.3032 & 23.9256 \end{bmatrix}
$$

Weighting Matrices -- Diagonal Elements:

Q' = (0.01, 10.0, 0.0001, 15.0, 20.0)

R' = (2.01, 1.002)

S' = (0.01, 0.002)

Table B.26 Summary of Lateral-Directional RQAS Response for a Take-off at Sea-Level--Control-Rate-Weighting

Time Domain Response:

	Open Loop		Baseline RQAS		Percent Reduction	
	Max.	RMS	Max.	RMS	Max.	RMS
a_y (f/s2)	5.2	2.2	3.4	1.1	35%	50%
β (deg)	7.6	2.9	5.5	2.2	28%	24%
p (deg/s)	5.6	2.5	1.7	0.5	70%	8%
r (deg/s)	11.3	4.5	6.0	2.7	47%	40%
ϕ (deg)	3.7	1.6	1.8	0.8	51%	50%
δ_{df} (deg)	-	-	8.5	2.7	-	-
δ_{sr} (deg)	-	-	13.4	6.0	-	-
$\dot{\delta}_{df}$ (deg/s)	-	-	43.4	-	-	-
$\dot{\delta}_{sr}$ (deg/s)	-	-	32.8	-	-	-

Table B.26 Summary of Lateral-Directional RQAS Response
for a Take-off at Sea-Level--Control-Rate-Weighting
(Continued)

System Eigenvalues:

	Open Loop		Baseline RQAS	
	Frequency	Damping	Frequency	Damping
Spiral Mode	0.04	-1.0	0.36	1.0
Roll Mode	2.5	1.0	2.8	1.0
Dutch Roll	1.8	0.13	2.0	0.55
Dutch Roll	1.8	0.13	2.0	0.55
Servo	10.0	1.0	5.9	0.85
Servo	10.0	1.0	5.9	0.85
Filter	-	-	12.6	1.0
Filter	-	-	21.3	1.0

Note 1: Baseline RQAS Frequency and Damping are based on
roots of the W'-Plane.

Note 2: Control-Rate-Weighting introduces 2 filter states.

Optimal Gain Matrix:

$$K = \begin{bmatrix} 29.886 & -17.330 & -7.8019 & -13.481 & 19.073 & -1.5378 \\ -4.5862 & 3.1201 & -9.9103 & 2.4044 & -0.2559 & 5.3043 \end{bmatrix}$$

Weighting Matrices -- Diagonal Elements:

$Q' = (0.025, 7.00, 0.07, 5.0, 1.5)$

$R' = (3.007, 1.07)$

$S' = (0.007, 0.07)$

Table B.27 Summary of Lateral-Directional RQAS Response
for a Sea-Level Climb -- Control-Rate-Weighting

Time Domain Response:

	Open Loop		Baseline RQAS		Percent Reduction	
	Max.	RMS	Max.	RMS	Max.	RMS
a_y (f/s2)	6.1	2.7	3.5	1.3	43%	52%
β (deg)	6.2	2.8	5.8	1.9	6%	32%
p (deg/s)	6.4	2.7	1.5	0.5	77%	81%
r (deg/s)	10.6	4.8	7.1	2.8	33%	42%
ϕ (deg)	3.2	1.3	1.0	0.4	69%	69%
δ_{df} (deg)	-	-	4.8	2.1	-	-
δ_{sr} (deg)	-	-	14.7	5.8	-	-
$\dot{\delta}_{df}$ (deg/s)	-	-	30.0	-	-	-
$\dot{\delta}_{sr}$ (deg/s)	-	-	30.8	-	-	-

Table B.27 Summary of Lateral-Directional RQAS Response for a Sea-Level Climb -- Control-Rate-Weighting (Continued)

System Eigenvalues:

	Open Loop		Baseline RQAS	
	Frequency	Damping	Frequency	Damping
Spiral Mode	0.02	-1.0	0.59	1.0
Roll Mode	2.7	1.0	3.3	1.0
Dutch Roll	2.1	0.12	2.8	0.51
Dutch Roll	2.1	0.12	2.8	0.51
Servo	10.0	1.0	5.5	0.88
Servo	10.0	1.0	5.5	0.88
Filter	–	–	12.6	1.0
Filter	–	–	21.3	1.0

Note 1: Baseline RQAS Frequency and Damping are based on roots of the W'-Plane.

Note 2: Control-Rate-Weighting introduces 2 filter states.

Optimal Gain Matrix:

$$K = \begin{bmatrix} 22.429 & -9.4558 & -6.6832 & -12.139 & 16.148 & -0.6806 \\ -1.9138 & 3.7262 & -14.873 & 3.5634 & -0.4145 & 7.2291 \end{bmatrix}$$

Weighting Matrices -- Diagonal Elements:

$Q' = (0.01, 15.0, 0.07, 0.5, 1.5)$

$R' = (2.007, 0.52)$

$S' = (0.007, 0.02)$

Table B.28 Summary of Lateral-Directional RQAS Response for a Climb at 5000 ft-- Control-Rate-Weighting

Time Domain Response:

	Open Loop		Baseline RQAS		Percent Reduction	
	Max.	RMS	Max.	RMS	Max.	RMS
a_y (f/s2)	2.9	1.2	2.1	0.9	28%	25%
β (deg)	3.3	1.3	3.2	1.2	3%	8%
p (deg/s)	2.6	1.1	0.9	0.4	65%	64%
r (deg/s)	3.9	1.9	4.0	1.6	-3%	16%
ϕ (deg)	1.1	0.5	0.5	0.2	55%	60%
δ_{df} (deg)	-	-	3.3	1.6	-	-
δ_{sr} (deg)	-	-	7.5	3.2	-	-
$\dot{\delta}_{df}$ (deg/s)	-	-	23.1	-	-	-
$\dot{\delta}_{sr}$ (deg/s)	-	-	20.0	-	-	-

Table B.28 Summary of Lateral-Directional RQAS Response for a Climb at 5000 ft-- Control-Rate-Weighting (Continued)

System Eigenvalues:

	Open Loop		Baseline RQAS	
	Frequency	Damping	Frequency	Damping
Spiral Mode	0.02	-1.0	0.58	1.0
Roll Mode	2.5	1.0	3.2	1.0
Dutch Roll	2.1	0.11	2.7	0.50
Dutch Roll	2.1	0.11	2.7	0.50
Servo	10.0	1.0	5.6	0.85
Servo	10.0	1.0	5.6	0.85
Filter	-	-	12.6	1.0
Filter	-	-	21.8	1.0

Note 1: Baseline RQAS Frequency and Damping are based on roots of the W'-Plane.

Note 2: Control-Rate-Weighting introduces 2 filter states.

Optimal Gain Matrix:

$$K = \begin{bmatrix} 25.050 & -10.715 & -7.7077 & -11.876 & 16.368 & -0.6975 \\ -2.1522 & 3.9191 & -15.067 & 3.7219 & -0.4313 & 7.2545 \end{bmatrix}$$

Weighting Matrices -- Diagonal Elements:

$Q' = (0.01, 15.0, 0.07, 0.5, 1.5)$

$R' = (2.007, 0.52)$

$S' = (0.007, 0.02)$

Table B.29 Summary of Lateral-Directional RQAS Response for a Cruise at 20000 ft--Control-Rate-Weighting

Time Domain Response:

	Open Loop		Baseline RQAS		Percent Reduction	
	Max.	RMS	Max.	RMS	Max.	RMS
a_y (f/s2)	2.4	1.1	1.7	0.5	29%	55%
β (deg)	1.9	0.8	1.5	0.5	21%	38%
p (deg/s)	2.3	1.0	0.8	0.3	65%	70%
r (deg/s)	4.1	1.8	2.3	0.9	44%	50%
ϕ (deg)	1.0	0.4	0.4	0.1	60%	25%
δ_{df} (deg)	-	-	2.0	0.8	-	-
δ_{sr} (deg)	-	-	4.5	1.8	-	-
$\dot{\delta}_{df}$ (deg/s)	-	-	13.8	-	-	-
$\dot{\delta}_{sr}$ (deg/s)	-	-	13.4	-	-	-

Table B.29 Summary of Lateral-Directional RQAS Response
for a Cruise at 20000 ft--Control-Rate-Weighting
(Continued)

Underline System Eigenvalues:

	Open Loop		Baseline RQAS	
	Frequency	Damping	Frequency	Damping
Spiral Mode	0.003	-1.0	0.80	1.0
Roll Mode	2.4	1.0	2.6	1.0
Dutch Roll	2.6	0.08	3.5	0.45
Dutch Roll	2.6	0.08	3.5	0.45
Servo	10.0	1.0	6.3	0.72
Servo	10.0	1.0	6.3	0.72
Filter	-	-	14.1	1.0
Filter	-	-	23.6	1.0

Note 1: Baseline RQAS Frequency and Damping are based on roots of the W'-Plane.

Note 2: Control-Rate-Weighting introduces 2 filter states.

Optimal Gain Matrix:

$$K = \begin{bmatrix} 41.555 & -10.172 & -11.371 & -10.074 & 17.282 & -0.7426 \\ -11.781 & 3.6869 & -14.791 & 4.9004 & -0.5793 & 8.5732 \end{bmatrix}$$

Weighting Matrices -- Diagonal Elements:

$Q' = (0.01 ,15.00, 0.07, 0.5, 1.5)$

$R' = (2.007, 0.52)$

$S' = (0.007, 0.02)$

Table B.30 Summary of Lateral-Directional RQAS Response
for an Approach at Sea-Level—Control-Rate-Weighting

Time Domain Response:

	Open Loop		Baseline RQAS		Percent Reduction	
	Max.	RMS	Max.	RMS	Max.	RMS
a_y (f/s2)	5.8	2.4	2.6	1.2	55%	50%
β (deg)	10.2	4.2	5.6	2.5	45%	40%
p (deg/s)	7.5	3.1	2.0	0.9	73%	71%
r (deg/s)	10.5	5.8	6.4	3.4	39%	41%
ϕ (deg)	3.8	2.0	1.1	0.6	71%	70%
δ_{df} (deg)	–	–	4.6	2.1	–	–
δ_{sr} (deg)	–	–	11.7	6.2	–	–
$\dot{\delta}_{df}$ (deg/s)	–	–	14.3	–	–	–
$\dot{\delta}_{sr}$ (deg/s)	–	–	21.6	–	–	–

Table B.30 Summary of Lateral-Directional RQAS Response
for an Approach at Sea-Level--Control-Rate-Weighting
(Continued)

System Eigenvalues:

	Open Loop		Baseline RQAS	
	Frequency	Damping	Frequency	Damping
Spiral Mode	0.003	-1.0	0.55	1.0
Roll Mode	2.1	1.0	2.7	1.0
Dutch Roll	1.6	0.11	1.8	0.40
Dutch Roll	1.6	0.11	1.8	0.40
Servo	10.0	1.0	5.1	1.00
Servo	10.0	1.0	7.6	1.00
Filter	–	–	11.9	1.0
Filter	–	–	19.4	1.0

Note 1: Baseline RQAS Frequency and Damping are based on roots of the W'-Plane.

Note 2: Control-Rate-Weighting introduces 2 filter states.

Optimal Gain Matrix:

$$
K = \begin{bmatrix} 10.580 & -8.5909 & -1.1162 & -12.695 & 15.332 & -0.4045 \\ 1.9229 & 2.8267 & -14.721 & 2.9242 & -0.2052 & 7.7058 \end{bmatrix}
$$

Weighting Matrices -- Diagonal Elements:

$Q' = (0.01\ ,15.00,\ 0.07,\ 0.5,\ 1.5)$

$R' = (2.007,\ 1.02)$

$S' = (0.007,\ 0.02)$

**Table B.31 Summary of Longitudinal RQAS Response
for Take-Off at Sea Level--Output-Weighting**

Time Domain Response:

	Open Loop		Baseline RQAS		Percent Reduction	
	Max.	RMS	Max.	RMS	Max.	RMS
a_z (f/s2)	16.2	5.7	10.4	3.3	36%	42%
α (deg)	4.4	1.6	5.4	1.8	-23%	-13%
u (f/s)	2.1	1.2	3.1	1.8	-48%	-50%
q (deg/s)	2.4	1.0	3.4	1.5	-42%	-50%
θ (deg)	2.6	0.9	3.3	1.2	-27%	-33%
δ_{se} (deg)	-	-	4.9	1.8	-	-
δ_f (deg)	-	-	15.0	5.6	-	-
$\dot{\delta}_{se}$ (deg/s)	-	-	9.4	-	-	-
$\dot{\delta}_f$ (deg/s)	-	-	103.9	-	-	-

Table B.31 Summary of Longitudinal RQAS Response
for Take-Off at Sea-Level--Output-Weighting
(Continued)

System Eigenvalues:

	Open Loop		Baseline RQAS	
	Frequency	Damping	Frequency	Damping
Phugoid	0.15	0.02	0.09	1.00
Phugoid	0.15	0.02	0.11	1.00
Short Period	2.1	1.0	8.7	0.87
Short Period	6.6	1.0	8.7	0.87
Servo	10.0	1.0	2.1	1.0
Servo	10.0	1.0	11.1	1.0

Note 1: Baseline RQAS Frequency and Damping are based on roots of the W'-Plane.

Optimal Gain Matrix:

$$K = \begin{bmatrix} -0.1664 & -0.0011 & -0.6194 & -1.3505 \\ 4.1356 & 0.0060 & 0.4927 & 1.1368 \end{bmatrix}$$

Weighting Matrices -- Diagonal Elements:

$Q' = (0.04, 1.00, 0.0001, 18.0, 40.0)$

$R' = (8.0, 2.5)$

Table B.32 Summary of Longitudinal RQAS Response
for a Sea-Level Climb -- Output-Weighting

Time Domain Response:

	Open Loop		Baseline RQAS		Percent Reduction	
	Max.	RMS	Max.	RMS	Max.	RMS
a_z (f/s2)	13.1	6.3	11.8	3.3	10%	48%
α (deg)	2.8	1.3	3.7	1.6	-32%	-23%
u (f/s)	1.9	1.1	4.0	2.3	-111%	-110%
q (deg/s)	1.8	0.9	2.5	1.2	-39%	-33%
θ (deg)	1.6	1.0	1.8	1.1	-13%	-10%
δ_{se} (deg)	-	-	5.0	2.5	-	-
δ_f (deg)	-	-	11.7	5.4	-	-
$\dot{\delta}_{se}$ (deg/s)	-	-	22.3	-	-	-
$\dot{\delta}_f$ (deg/s)	-	-	98.8	-	-	-

B.45

Table B.32 Summary of Longitudinal RQAS Response
for a Sea-Level Climb -- Output-Weighting
(Continued)

System Eigenvalues:

	Open Loop		Baseline RQAS	
	Frequency	Damping	Frequency	Damping
Phugoid	0.15	0.04	0.09	0.89
Phugoid	0.15	0.04	0.09	0.89
Short Period	2.4	1.0	11.6	0.66
Short Period	7.1	1.0	11.6	0.66
Servo	10.0	1.0	1.9	1.0
Servo	10.0	1.0	11.3	1.0

Note 1: Baseline RQAS Frequency and Damping are based on roots of the W'-Plane.

Optimal Gain Matrix:

$$
K = \begin{bmatrix} -0.5014 & -0.0018 & -1.5609 & -2.5312 \\ 4.5062 & 0.0046 & 0.5469 & 0.9847 \end{bmatrix}
$$

Weighting Matrices -- Diagonal Elements:

Q' = (0.05, 10.0, 0.0001, 18.0, 40.0)

R' = (2.2, 1.0)

Table B.33 Summary of Longitudinal RQAS Response
for a Climb at 5000 ft -- Output-Weighting

Time Domain Response:

	Open Loop		Baseline RQAS		Percent Reduction	
	Max.	RMS	Max.	RMS	Max.	RMS
a_z (f/s2)	10.2	3.6	7.5	2.1	26%	42%
α (deg)	2.2	0.8	3.3	1.3	-50%	-63%
u (f/s)	2.4	1.4	4.1	2.3	-71%	-64%
q (deg/s)	1.5	0.7	1.8	0.8	-20%	-14%
θ (deg)	2.2	1.1	2.2	1.2	0%	9%
δ_{se} (deg)	-	-	5.0	2.5	-	-
δ_f (deg)	-	-	9.6	2.1	-	-
$\dot{\delta}_{se}$ (deg/s)	-	-	11.4	-	-	-
$\dot{\delta}_f$ (deg/s)	-	-	39.5	-	-	-

Table B.33 Summary of Longitudinal RQAS Response
            for a Climb at 5000 ft-- Output-Weighting
            (Continued)

System Eigenvalues:

	Open Loop		Baseline RQAS	
	Frequency	Damping	Frequency	Damping
Phugoid	0.14	0.04	0.09	0.89
Phugoid	0.14	0.04	0.09	0.89
Short Period	2.6	1.0	11.5	0.64
Short Period	6.2	1.0	11.5	0.64
Servo	10.0	1.0	2.0	1.0
Servo	10.0	1.0	11.2	1.0

Note 1: Baseline RQAS Frequency and Damping are based on
         roots of the W'-Plane.

Optimal Gain Matrix:

$$K = \begin{bmatrix} -0.6918 & -0.0016 & -1.6333 & -2.4691 \\ 4.5239 & 0.0041 & 0.5369 & 0.9860 \end{bmatrix}$$

Weighting Matrices -- Diagonal Elements:

Q' = (0.05, 15.0, 0.0001, 18.0, 40.0)

R' = (2.2, 1.0)

C-2

Table B.34 Summary of Longitudinal RQAS Response
for Cruise at 20000 ft--Output-Weighting

Time Domain Response:

	Open Loop		Baseline RQAS		Percent Reduction	
	Max.	RMS	Max.	RMS	Max.	RMS
a_z (f/s2)	7.0	2.9	4.3	1.5	39%	48%
α (deg)	0.9	0.4	1.4	0.5	-56%	-25%
u (f/s)	1.5	0.9	2.4	1.5	-60%	-67%
q (deg/s)	1.2	0.6	1.3	0.6	- 8%	0%
θ (deg)	1.3	0.7	1.4	0.7	-8%	0%
δ_{se} (deg)	-	-	2.3	0.9	-	-
δ_f (deg)	-	-	4.8	2.0	-	-
$\dot{\delta}_{se}$ (deg/s)	-	-	9.0	-	-	-
$\dot{\delta}_f$ (deg/s)	-	-	23.8	-	-	-

Table B.34 Summary of Longitudinal RQAS Response
        for Cruise at 20000 ft--Output-Weighting
        (Continued)

<u>System Eigenvalues</u>:

	Open Loop		Baseline RQAS	
	Frequency	Damping	Frequency	Damping
Phugoid	0.10	0.08	0.08	0.81
Phugoid	0.10	0.08	0.08	0.81
Short Period	4.5	0.94	13.5	0.51
Short Period	4.5	0.94	13.5	0.51
Servo	10.0	1.0	1.9	1.0
Servo	10.0	1.0	11.3	1.0

Note 1: Baseline RQAS Frequency and Damping are based on
         roots of the W'-Plane.

<u>Optimal Gain Matrix</u>:

$$K = \begin{bmatrix} -1.2008 & -0.0031 & -1.7778 & -1.5653 \\ 4.7486 & 0.0020 & 0.4348 & 0.6318 \end{bmatrix}$$

<u>Weighting Matrices</u> -- <u>Diagonal Elements</u>:

$Q' = (0.05, 10.0, 0.0001, 18.0, 40.0)$

$R' = (2.2, 1.0)$

Table B.35 Summary of Longitudinal RQAS Response
for an Approach at Sea-Level--Output-Weighting

Time Domain Response:

	Open Loop		Baseline RQAS		Percent Reduction	
	Max.	RMS	Max.	RMS	Max.	RMS
a_z (f/s2)	12.9	4.8	10.6	3.8	18%	21%
α (deg)	4.8	1.8	4.5	1.7	- 6%	- 6%
u (f/s)	2.9	1.6	3.5	2.1	-21%	-31%
q (deg/s)	2.2	1.0	3.9	1.9	-77%	-90%
θ (deg)	2.7	1.3	3.8	1.6	-41%	-23%
δ_{se} (deg)	-	-	4.8	1.5	-	-
δ_f (deg)	-	-	14.6	5.8	-	-
$\dot{\delta}_{se}$ (deg/s)	-	-	23.4	-	-	-
$\dot{\delta}_f$ (deg/s)	-	-	104.5	-	-	-

Table B.35 Summary of Longitudinal RQAS Response
for an Approach at Sea-Level--Output-Weighting
(Continued)

System Eigenvalues:

	Open Loop		Baseline RQAS	
	Frequency	Damping	Frequency	Damping
Phugoid	0.21	0.15	0.18	0.94
Phugoid	0.21	0.15	0.18	0.94
Short Period	1.8	1.00	6.9	0.86
Short Period	5.4	1.00	6.9	0.86
Servo	10.0	1.0	4.5	1.0
Servo	10.0	1.0	10.3	1.0

Note 1: Baseline RQAS Frequency and Damping are based on roots of the W'-Plane.

Optimal Gain Matrix:

$$K = \begin{bmatrix} -1.1832 & -0.0050 & -0.7078 & -1.3297 \\ 5.3214 & 0.0135 & 1.0758 & 2.7676 \end{bmatrix}$$

Weighting Matrices -- Diagonal Elements:

Q' = (0.02, 10.0, 0.0001, 18.0, 40.0)

R' = (9.5, 3.2)

Table B.36 Summary of Lateral-Directional RQAS Response
for Take-Off at Sea-Level--Output-Weighting

Time Domain Response:

	Open Loop		Baseline RQAS		Percent Reduction	
	Max.	RMS	Max.	RMS	Max.	RMS
a_y (f/s2)	5.2	2.2	3.1	1.0	40%	55%
β (deg)	7.6	2.9	5.4	2.2	29%	24%
p (deg/s)	5.6	2.4	1.6	0.5	71%	79%
r (deg/s)	11.3	4.5	5.9	2.7	48%	40%
ϕ (deg)	3.7	1.6	1.6	0.8	57%	50%
δ_{df} (deg)	-	-	9.7	2.9	-	-
δ_{sr} (deg)	-	-	14.4	6.4	-	-
$\dot{\delta}_{df}$ (deg/s)	-	-	55.1	-	-	-
$\dot{\delta}_{sr}$ (deg/s)	-	-	42.2	-	-	-

Table B.36 Summary of Lateral-Directional RQAS Response
for Take-Off at Sea-Level--Output-Weighting
(Continued)

System Eigenvalues:

	Open Loop		Baseline RQAS	
	Frequency	Damping	Frequency	Damping
Spiral Mode	0.04	-1.0	0.67	1.0
Roll Mode	2.5	1.0	7.5	1.0
Dutch Roll	1.8	0.13	2.0	0.60
Dutch Roll	1.8	0.13	2.0	0.60
Servo	10.0	1.0	6.9	0.86
Servo	10.0	1.0	6.9	0.86

Note 1: Baseline RQAS Frequency and Damping are based on
roots of the W'-Plane.

Optimal Gain Matrix:

$$K = \begin{bmatrix} 1.8623 & -1.2121 & -0.7767 & -1.3093 \\ 0.4506 & 1.8538 & -2.9208 & 1.4859 \end{bmatrix}$$

Weighting Matrices -- Diagonal Elements:

$Q' = (0.05, 10.0, 0.1, 0.75, 10.0)$

$R' = (5.0, 1.0)$

Table B.37 Summary of Lateral-Directional RQAS Response for a Sea-Level Climb -- Output-Weighting

Time Domain Response:

	Open Loop		Baseline RQAS		Percent Reduction	
	Max.	RMS	Max.	RMS	Max.	RMS
a_y (f/s2)	6.1	2.7	3.4	1.1	44%	59%
β (deg)	6.2	2.8	6.0	1.9	3%	32%
p (deg/s)	6.4	2.7	1.8	0.6	72%	78%
r (deg/s)	10.6	4.8	6.8	2.7	36%	44%
ϕ (deg)	3.2	1.3	1.7	0.7	47%	46%
δ_{df} (deg)	–	–	6.2	2.8	–	–
δ_{sr} (deg)	–	–	14.7	5.7	–	–
$\dot{\delta}_{df}$ (deg/s)	–	–	51.4	–	–	–
$\dot{\delta}_{sr}$ (deg/s)	–	–	27.1	–	–	–

Table B.37 Summary of Lateral-Directional RQAS Response for a Sea-Level Climb -- Output-Weighting (Continued)

System Eigenvalues:

	Open Loop		Baseline RQAS	
	Frequency	Damping	Frequency	Damping
Spiral Mode	0.02	-1.0	0.78	1.0
Roll Mode	2.7	1.0	7.4	1.0
Dutch Roll	2.1	0.12	2.2	0.58
Dutch Roll	2.1	0.12	2.2	0.58
Servo	10.0	1.0	6.8	0.87
Servo	10.0	1.0	6.8	0.87

Note 1: Baseline RQAS Frequency and Damping are based on roots of the W'-Plane.

Optimal Gain Matrix:

$$K = \begin{bmatrix} 2.0004 & -0.8556 & -0.6140 & -1.0563 \\ -0.0932 & 1.1370 & -2.4060 & 1.1638 \end{bmatrix}$$

Weighting Matrices -- Diagonal Elements:

$Q' = (0.05, 10.0, 0.1, 0.75, 10.0)$

$R' = (7.0, 1.8)$

Table B.38 Summary of Lateral-Directional RQAS Response
for a Climb at 5000 ft-- Output-Weighting

Time Domain Response:

	Open Loop		Baseline RQAS		Percent Reduction	
	Max.	RMS	Max.	RMS	Max.	RMS
a_y (f/s2)	2.9	1.2	1.9	0.7	34%	42%
β (deg)	3.3	1.3	3.2	1.2	3%	8%
p (deg/s)	2.6	1.1	0.7	0.3	73%	73%
r (deg/s)	3.9	1.9	3.3	1.4	15%	26%
ϕ (deg)	1.1	0.5	0.6	0.3	45%	40%
δ_{df} (deg)	-	-	3.1	1.5	-	-
δ_{sr} (deg)	-	-	9.3	3.9	-	-
$\dot{\delta}_{df}$ (deg/s)	-	-	28.8	-	-	-
$\dot{\delta}_{sr}$ (deg/s)	-	-	22.8	-	-	-

Table B.38 Summary of Lateral-Directional RQAS Response
for a Climb at 5000 ft-- Output-Weighting
(Continued)

System Eigenvalues:

	Open Loop		Baseline RQAS	
	Frequency	Damping	Frequency	Damping
Spiral Mode	0.02	-1.0	0.70	1.0
Roll Mode	2.5	1.0	6.1	1.0
Dutch Roll	2.1	0.11	2.4	0.73
Dutch Roll	2.1	0.11	2.4	0.73
Servo	10.0	1.0	6.8	0.89
Servo	10.0	1.0	6.8	0.89

Note 1: Baseline RQAS Frequency and Damping are based on
roots of the W'-Plane.

Optimal Gain Matrix:

$$K = \begin{bmatrix} 1.7209 & -0.7476 & -0.6779 & -0.8545 \\ 0.1127 & 1.5494 & -3.1532 & 1.4838 \end{bmatrix}$$

Weighting Matrices -- Diagonal Elements:

Q' = (0.05, 10.0, 0.1, 0.75, 10.0)

R' = (10.0, 1.0)

Table B.39 Summary of Lateral-Directional RQAS Response for Cruise at 20000 ft--Output-Weighting

Time Domain Response:

	Open Loop		Baseline RQAS		Percent Reduction	
	Max.	RMS	Max.	RMS	Max.	RMS
a_y (f/s2)	2.4	1.1	1.5	0.4	38%	64%
β (deg)	1.9	0.8	1.6	0.5	16%	38%
p (deg/s)	2.3	1.0	1.0	0.4	57%	60%
r (deg/s)	4.1	1.8	1.8	0.8	56%	56%
ϕ (deg)	1.0	0.4	0.6	0.3	40%	25%
δ_{df} (deg)	-	-	2.2	0.9	-	-
δ_{sr} (deg)	-	-	5.2	2.1	-	-
$\dot{\delta}_{df}$ (deg/s)	-	-	18.2	-	-	-
$\dot{\delta}_{sr}$ (deg/s)	-	-	22.8	-	-	-

Table B.39 Summary of Lateral-Directional RQAS Response
for Cruise at 20000 ft--Output-Weighting
(Continued)

System Eigenvalues:

	Open Loop		Baseline RQAS	
	Frequency	Damping	Frequency	Damping
Spiral Mode	0.003	-1.0	1.1	1.0
Roll Mode	2.4	1.0	2.7	1.0
Dutch Roll	2.6	0.08	3.9	0.70
Dutch Roll	2.6	0.08	3.9	0.70
Servo	10.0	1.0	8.0	0.81
Servo	10.0	1.0	8.0	0.81

Note 1: Baseline RQAS Frequency and Damping are based on
roots of the W'-Plane.

Optimal Gain Matrix:

$$
K = \begin{bmatrix} 2.6890 & -0.6745 & -0.8628 & -0.6222 \\ -1.4528 & 1.2040 & -2.7719 & 1.6245 \end{bmatrix}
$$

Weighting Matrices -- Diagonal Elements:

$Q' = (0.05, 10.0, 0.1, 0.75, 10.0)$

$R' = (10.0, 1.0)$

Table B.40 Summary of Lateral-Directional RQAS Response
for an Approach at Sea-Level--Output-Weighting

Time Domain Response:

	Open Loop		Baseline RQAS		Percent Reduction	
	Max.	RMS	Max.	RMS	Max.	RMS
a_y (f/s2)	5.8	2.4	2.6	1.1	50%	54%
β (deg)	10.2	4.2	5.9	2.6	42%	38%
p (deg/s)	7.4	3.1	1.6	0.7	78%	77%
r (deg/s)	10.5	5.8	6.6	3.4	37%	41%
ϕ (deg)	3.8	2.0	0.9	0.4	76%	56%
δ_{df} (deg)	-	-	4.7	2.1	-	-
δ_{sr} (deg)	-	-	12.1	6.2	-	-
$\dot{\delta}_{df}$ (deg/s)	-	-	17.8	-	-	-
$\dot{\delta}_{sr}$ (deg/s)	-	-	24.5	-	-	-

Table B.40 Summary of Lateral-Directional RQAS Response
for an Approach at Sea-Level--Output-Weighting
(Continued)

<u>System Eigenvalues:</u>

	Open Loop		Baseline RQAS	
	Frequency	Damping	Frequency	Damping
Spiral Mode	0.003	-1.0	0.65	1.0
Roll Mode	2.1	1.0	2.6	1.0
Dutch Roll	1.6	0.11	1.7	0.40
Dutch Roll	1.6	0.11	1.7	0.40
Servo	10.0	1.0	8.5	1.00
Servo	10.0	1.0	9.0	1.00

Note 1: Baseline RQAS Frequency and Damping are based on
roots of the W'-Plane.

<u>Optimal Gain Matrix:</u>

$$\mathbf{K} = \begin{bmatrix} 0.8230 & -0.6195 & -0.2863 & -0.9670 \\ 0.2765 & 0.4704 & -1.8866 & 0.4482 \end{bmatrix}$$

<u>Weighting Matrices</u> -- <u>Diagonal Elements:</u>

$\mathbf{Q'} = (0.05, \ 10.0, \ 0.1, \ 0.75, \ 10.0)$

$\mathbf{R'} = (10.0, \ 3.0)$

Table B.41 Longitudinal Control-Rate-Weighting
         Fixed Gain Stability for Sea-Level Take-Off

Baseline Eigenvalues:

Mode	Frequency	Damping
Phugoid	0.0940	0.868
Phugoid	0.0940	0.868
Short Period	6.28	0.700
Short Period	6.28	0.700
Servo	2.38	1.0
Servo	11.6	1.0
Filter	14.6	1.0
Filter	36.6	1.0

Fixed Gain Eigenvalues:

Foward c.g.		Mid c.g.		Aft c.g.	
Freq.	Damp.	Freq.	Damp.	Freq.	Damp.
0.222	0.309	0.224	0.311	0.221	0.318
0.222	0.309	0.224	0.311	0.221	0.318
6.51	0.743	6.13	0.723	5.81	0.702
6.51	0.743	6.13	0.723	5.81	0.702
2.40	1.0	2.71	1.0	3.03	1.0
11.5	1.0	11.5	1.0	11.5	1.0
15.2	1.0	15.0	1.0	14.9	1.0
63.6	1.0	63.8	1.0	63.9	1.0

Table B.42 Longitudinal Control-Rate-Weighting
Fixed Gain Stability for Sea-Level Climb

Baseline Eigenvalues:

Mode	Frequency	Damping
Phugoid	0.0874	0.791
Phugoid	0.0874	0.791
Short Period	6.02	0.682
Short Period	6.02	0.682
Servo	3.47	1.0
Servo	11.8	1.0
Filter	15.3	1.0
Filter	63.8	1.0

Fixed Gain Eigenvalues:

Foward c.g.		Mid c.g.		Aft c.g.	
Freq.	Damp.	Freq.	Damp.	Freq.	Damp.
0.213	0.368	0.214	0.370	0.214	0.372
0.213	0.368	0.214	0.370	0.214	0.372
6.80	0.699	6.44	0.671	6.14	0.643
6.80	0.699	6.44	0.671	6.14	0.643
2.56	1.0	2.88	1.0	3.17	1.0
11.7	1.0	11.7	1.0	11.7	1.0
15.9	1.0	15.7	1.0	15.8	1.0
63.5	1.0	63.7	1.0	63.9	1.0

Table B.43 Longitudinal Control-Rate-Weighting
Fixed Gain Stability for Climb at 5000 ft

Baseline Eigenvalues:

Mode	Frequency	Damping
Phugoid	0.0837	0.798
Phugoid	0.0837	0.798
Short Period	6.13	0.633
Short Period	6.13	0.633
Servo	3.48	1.0
Servo	11.7	1.0
Filter	15.6	1.0
Filter	64.1	1.0

Fixed Gain Eigenvalues:

Foward c.g.		Mid c.g.		Aft c.g.	
Freq.	Damp.	Freq.	Damp.	Freq.	Damp.
0.197	0.372	0.195	0.378	0.198	0.376
0.197	0.372	0.195	0.378	0.198	0.376
6.59	0.675	6.23	0.642	5.95	0.610
6.59	0.675	6.23	0.642	5.95	0.610
2.80	1.0	3.14	1.0	3.46	1.0
11.6	1.0	11.6	1.0	11.6	1.0
15.6	1.0	15.5	1.0	15.4	1.0
63.5	1.0	63.7	1.0	63.9	1.0

Table B.44 Longitudinal Control-Rate-Weighting
Fixed Gain Stability for Cruise at 20,000 ft

Baseline Eigenvalues:

Mode	Frequency	Damping
Phugoid	0.0806	0.778
Phugoid	0.0806	0.778
Short Period	10.2	0.481
Short Period	10.2	0.481
Servo	1.27	1.0
Servo	11.5	1.0
Filter	27.9	1.0
Filter	126	1.0

Fixed Gain Eigenvalues:

Foward c.g.		Mid c.g.		Aft c.g.	
Freq.	Damp.	Freq.	Damp.	Freq.	Damp.
0.143	0.513	0.143	0.517	0.146	0.508
0.143	0.513	0.143	0.517	0.146	0.508
6.97	0.510	6.69	0.461	6.48	0.417
6.97	0.510	6.69	0.461	6.48	0.417
3.48	1.0	3.79	1.0	4.03	1.0
11.6	1.0	11.6	1.0	11.6	1.0
16.5	1.0	16.4	1.0	16.3	1.0
63.4	1.0	63.7	1.0	63.9	1.0

Table B.45 Longitudinal Control-Rate-Weighting
Fixed Gain Stability for Sea-Level Approach

Baseline Eigenvalues:

Mode	Frequency	Damping
Phugoid	0.187	0.934
Phugoid	0.187	0.934
Short Period	7.36	0.667
Short Period	7.36	0.667
Servo	3.22	1.0
Servo	10.6	1.0
Filter	21.4	1.0
Filter	32.4	1.0

Fixed Gain Eigenvalues:

Foward c.g.		Mid c.g.		Aft c.g.	
Freq.	Damp.	Freq.	Damp.	Freq.	Damp.
0.286	0.518	0.289	0.582	0.294	0.648
0.286	0.518	0.289	0.582	0.294	0.648
5.56	0.727	5.24	0.745	4.97	0.767
5.56	0.727	5.24	0.745	4.97	0.767
3.97	1.0	3.86	1.0	3.71	1.0
10.4	1.0	10.4	1.0	10.4	1.0
14.2	1.0	14.1	1.0	14.0	1.0
64.1	1.0	64.1	1.0	64.2	1.0

Table B.46 Lateral Directional Control-Rate-Weighting
Fixed Gain Stability for Sea-Level Take-Off

	Baseline		Fixed Gain	
	Frequency	Damping	Frequency	Damping
Spiral	0.361	1.0	0.485	1.0
Roll	2.76	1.0	4.14	1.0
Dutch Roll	2.04	0.550	2.07	0.558
Dutch Roll	2.04	0.550	2.07	0.558
Servo	5.87	0.855	5.01	0.972
Servo	5.87	0.855	5.01	0.972
Filter	11.2	1.0	12.1	1.0
Filter	25.5	1.0	21.4	1.0

Table B.47 Lateral Directional Control-Rate-Weighting
Fixed Gain Stability for Sea-Level Climb

	Baseline		Fixed Gain	
	Frequency	Damping	Frequency	Damping
Spiral	0.594	1.0	0.570	1.0
Roll	3.25	1.0	3.06	1.0
Dutch Roll	2.75	0.514	2.77	0.507
Dutch Roll	2.75	0.514	2.77	0.507
Servo	5.47	0.882	5.59	0.871
Servo	5.47	0.882	5.59	0.871
Filter	12.6	1.0	12.4	1.0
Filter	21.3	1.0	21.8	1.0

Table B.48 Lateral Directional Control-Rate-Weighting
Fixed Gain Stability for Climb at 5000 ft

	Baseline		Fixed Gain	
	Frequency	Damping	Frequency	Damping
Spiral	0.581	1.0	0.613	1.0
Roll	3.19	1.0	3.11	1.0
Dutch Roll	2.72	0.503	2.74	0.498
Dutch Roll	2.72	0.503	2.74	0.498
Servo	5.57	0.847	5.41	0.880
Servo	5.57	0.847	5.41	0.880
Filter	12.6	1.0	12.4	1.0
Filter	21.8	1.0	21.8	1.0

Table B.49 Lateral Directional Control-Rate-Weighting
Fixed Gain Stability for Cruise at 20,000 ft

	Baseline		Fixed Gain	
	Frequency	Damping	Frequency	Damping
Spiral	0.799	1.0	0.814	1.0
Roll	2.55	1.0	2.39	1.0
Dutch Roll	3.48	0.449	3.92	0.333
Dutch Roll	3.48	0.449	3.92	0.333
Servo	6.27	0.716	5.93	0.717
Servo	6.27	0.716	5.93	0.717
Filter	14.1	1.0	13.2	1.0
Filter	23.6	1.0	22.6	1.0

Table B.50 Lateral Directional Control-Rate-Weighting
Fixed Gain Stability for Sea-Level Approach

	Baseline		Fixed Gain	
	Frequency	Damping	Frequency	Damping
Spiral	0.546	1.0	0.511	1.0
Roll	2.74	1.0	3.31	1.0
Dutch Roll	1.85	0.404	1.75	0.468
Dutch Roll	1.85	0.404	1.75	0.468
Servo	5.12	1.0	4.40	1.0
Servo	7.61	1.0	7.03	1.0
Filter	11.9	1.0	11.7	1.0
Filter	19.4	1.0	21.1	1.0

Table B.51 Longitudinal Output-Weighting Fixed
Gain Stability for Sea-Level Take-Off

Baseline Eigenvalues:

Mode	Frequency	Damping
Phugoid	0.0895	1.0
Phugoid	0.111	1.0
Short Period	8.72	0.866
Short Period	8.72	0.866
Servo	2.09	1.0
Servo	11.1	1.0

Fixed Gain Eigenvalues:

Foward c.g.		Mid c.g.		Aft c.g.	
Freq.	Damp.	Freq.	Damp.	Freq.	Damp.
0.224	0.350	0.226	0.350	0.224	0.355
0.224	0.350	0.226	0.350	0.224	0.355
11.2	0.704	10.8	0.695	10.5	0.689
11.2	0.704	10.8	0.695	10.5	0.689
1.70	1.0	1.82	1.0	1.92	1.0
11.1	1.0	11.1	1.0	11.2	1.0

Table B.52 Longitudinal Output-Weighting Fixed Gain Stability for Sea-Level Climb

Baseline Eigenvalues:

Mode	Frequency	Damping
Phugoid	0.0887	0.886
Phugoid	0.0887	0.886
Short Period	11.6	0.661
Short Period	11.6	0.661
Servo	1.94	1.0
Servo	11.3	1.0

Fixed Gain Eigenvalues:

Foward c.g.		Mid c.g.		Aft c.g.	
Freq.	Damp.	Freq.	Damp.	Freq.	Damp.
0.216	0.420	0.216	0.419	0.217	0.418
0.216	0.420	0.216	0.419	0.217	0.418
12.1	0.668	11.7	0.658	11.4	0.649
12.1	0.668	11.7	0.658	11.4	0.649
1.77	1.0	1.89	1.0	1.99	1.0
11.3	1.0	11.3	1.0	11.3	1.0

Table B.53 Longitudinal Output-Weighting Fixed
Gain Stability for Climb at 5000 ft

Baseline Eigenvalues:

Mode	Frequency	Damping
Phugoid	0.0849	0.885
Phugoid	0.0849	0.885
Short Period	11.5	0.636
Short Period	11.5	0.636
Servo	2.02	1.0
Servo	11.2	1.0

Fixed Gain Eigenvalues:

Foward c.g.		Mid c.g.		Aft c.g.	
Freq.	Damp.	Freq.	Damp.	Freq.	Damp.
0.199	0.424	0.198	0.428	0.201	0.422
0.199	0.424	0.198	0.428	0.201	0.422
11.8	0.653	11.5	0.643	11.2	0.634
11.8	0.653	11.5	0.643	11.2	0.634
1.86	1.0	1.98	1.0	2.09	1.0
11.2	1.0	11.2	1.0	11.3	1.0

Table B.54 Longitudinal Output-Weighting Fixed
Gain Stability for Cruise at 20,000 ft

Baseline Eigenvalues:

Mode	Frequency	Damping
Phugoid	0.0772	0.809
Phugoid	0.0772	0.809
Short Period	13.6	0.514
Short Period	13.6	0.514
Servo	1.93	1.0
Servo	11.3	1.0

Fixed Gain Eigenvalues:

Foward c.g.		Mid c.g.		Aft c.g.	
Freq.	Damp.	Freq.	Damp.	Freq.	Damp.
0.145	0.585	0.145	0.585	0.148	0.571
0.145	0.585	0.145	0.585	0.148	0.571
13.3	0.542	12.9	0.529	12.6	0.518
13.3	0.542	12.9	0.529	12.6	0.518
2.17	1.0	2.30	1.0	2.41	1.0
11.2	1.0	11.2	1.0	11.2	1.0

Table B.55 Longitudinal Output-Weighting Fixed
         Gain Stability for Sea-Level Approach

Baseline Eigenvalues:

Mode	Frequency	Damping
Phugoid	0.178	0.939
Phugoid	0.178	0.939
Short Period	6.89	0.861
Short Period	6.89	0.861
Servo	4.50	1.0
Servo	10.3	1.0

Fixed Gain Eigenvalues:

Foward c.g.		Mid c.g.		Aft c.g.	
Freq.	Damp.	Freq.	Damp.	Freq.	Damp.
0.281	0.543	0.283	0.598	0.287	0.651
0.281	0.543	0.283	0.598	0.287	0.651
9.57	0.731	9.27	0.739	9.03	0.746
9.57	0.731	9.27	0.739	9.03	0.746
2.61	1.0	2.45	1.0	2.30	1.0
10.3	1.0	10.3	1.0	10.3	1.0

Table B.56 Lateral Directional Output-Weighting
         Fixed Gain Stability for Sea-Level Take-Off

	Baseline		Fixed Gain	
	Frequency	Damping	Frequency	Damping
Spiral	0.669	1.0	0.643	1.0
Roll	7.47	1.0	7.89	1.0
Dutch Roll	1.95	0.606	1.77	0.561
Dutch Roll	1.95	0.606	1.77	0.561
Servo	6.90	0.862	6.58	0.908
Servo	6.90	0.862	6.58	0.908

Table B.57 Lateral Directional Output-Weighting
         Fixed Gain Stability for Sea-Level Climb

	Baseline		Fixed Gain	
	Frequency	Damping	Frequency	Damping
Spiral	0.776	1.0	0.683	1.0
Roll	7.39	1.0	7.06	1.0
Dutch Roll	2.22	0.578	2.30	0.586
Dutch Roll	2.22	0.578	2.30	0.586
Servo	6.84	0.874	7.31	0.833
Servo	6.84	0.874	7.31	0.833

Table B.58 Lateral Directional Output-Weighting
          Fixed Gain Stability for Climb at 5000 ft

	Baseline		Fixed Gain	
	Frequency	Damping	Frequency	Damping
Spiral	0.699	1.0	0.715	1.0
Roll	6.08	1.0	7.06	1.0
Dutch Roll	2.44	0.728	2.30	0.572
Dutch Roll	2.44	0.728	2.30	0.572
Servo	6.78	0.890	7.17	0.837
Servo	6.78	0.890	7.17	0.837

Table B.59 Lateral Directional Output-Weighting
          Fixed Gain Stability for Cruise at 20,000 ft

	Baseline		Fixed Gain	
	Frequency	Damping	Frequency	Damping
Spiral	1.09	1.0	0.822	1.0
Roll	2.67	1.0	4.61	1.0
Dutch Roll	3.92	0.702	3.82	0.606
Dutch Roll	3.92	0.702	3.82	0.606
Servo	7.97	0.808	8.28	0.722
Servo	7.97	0.808	8.28	0.722

Table B.60 Lateral Directional Output-Weighting
Fixed Gain Stability for Sea-Level Approach

	Baseline		Fixed Gain	
	Frequency	Damping	Frequency	Damping
Spiral	0.652	1.0	0.643	1.0
Roll	2.63	1.0	5.58	1.0
Dutch Roll	1.68	0.403	1.62	0.467
Dutch Roll	1.68	0.403	1.62	0.467
Servo	8.49	1.0	6.01	1.0
Servo	9.06	1.0	8.34	1.0

APPENDIX C.

MODIFICATION DRAWINGS

This appendix contains a full set of preliminary structural drawings for the proposed Cessna 402B modifications discussed in Chapter 4. Note that all of these drawings have been reduced from the originals and therefore, the indicated scales no longer apply. The original drawings are on file at the University of Kansas Flight Research Laboratory.

SEPARATE SURFACE ELEVATOR
AREA: 3.84 FT²
DEFLECTION: 65°
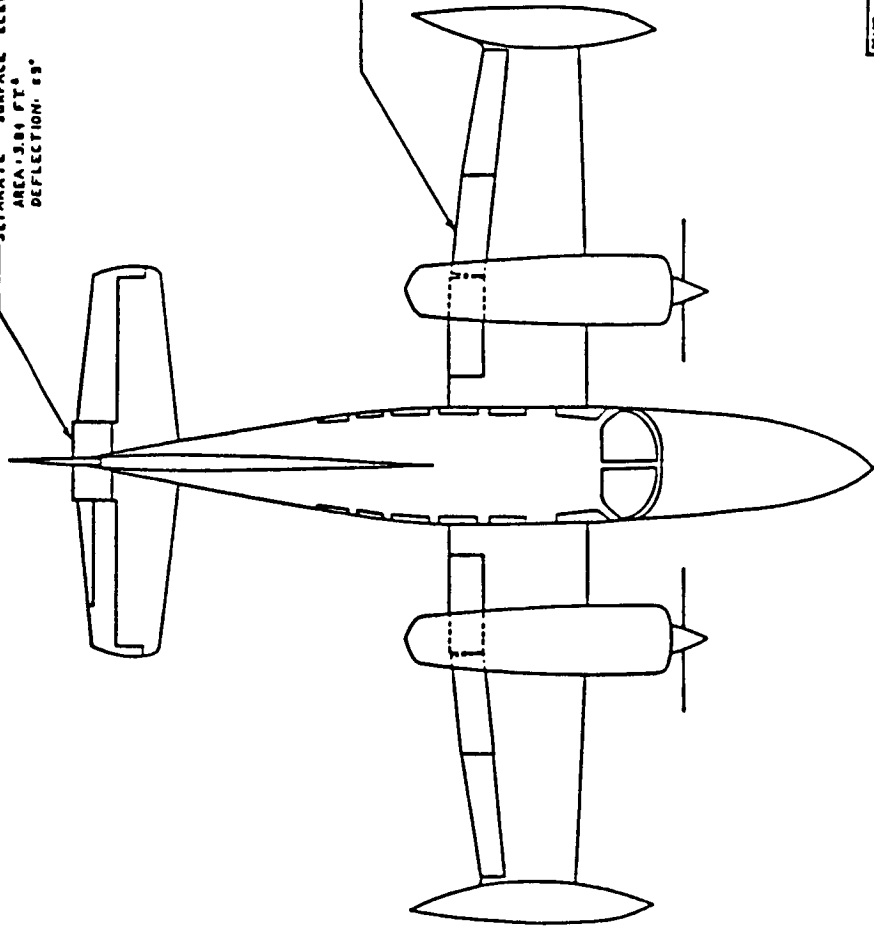
MODIFIED FLAP (PLAIN FLAP)
DEFLECTION: 15° UP
45° DOWN

FLIGHT RESEARCH LABORATORY
THE UNIVERSITY OF KANSAS CENTER FOR RESEARCH, INC.

RIDE QUALITY MODIFICATIONS
TO CESSNA 402B

DETAIL 17
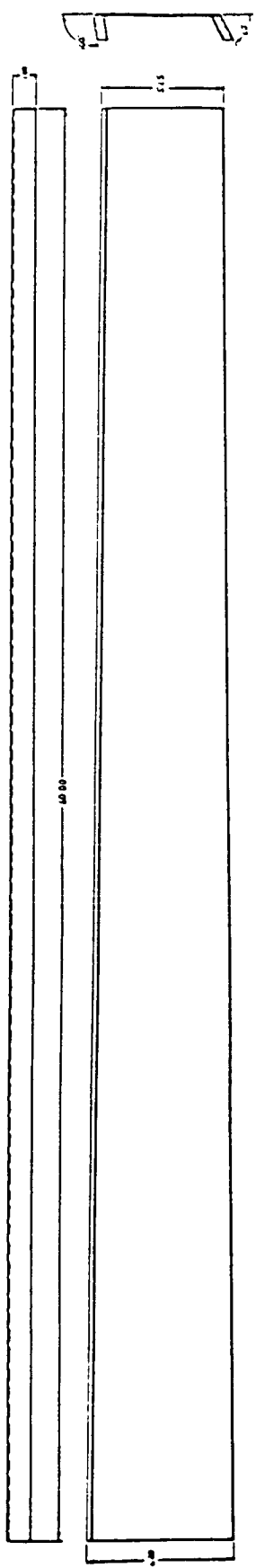
DETAIL 18

DETAIL 19

ORIGINAL PAGE IS
OF POOR QUALITY

DETAIL -7

DETAILS -23 THRU -35

DETAILS -9 THRU -21

FULL SCALE
DETAIL -87

NOTES
1. ALL BEND .12R

FLIGHT RESEARCH LABORATORY
RIDE QUALITY FLAP
DETAILS

D 615203

SECTION A-A

ORIGINAL PAGE IS
OF POOR QUALITY

ORIGINAL PAGE IS
OF POOR QUALITY

C.12

Standard Bibliographic Page

1. Report No. NASA CR-4014	2. Government Accession No.	3. Recipient's Catalog No.
4. Title and Subtitle Preliminary Control Law and Hardware Designs for a Ride Quality Augmentation System for Commuter Aircraft		5. Report Date September 1986
		6. Performing Organization Code
7. Author(s) Donald J. Davis, Dennis J. Linse, Reiner Suikat, and David P. Entz		8. Performing Organization Report No. KU-FRL-6132-2
9. Performing Organization Name and Address University of Kansas Center for Research, Inc. Lawrence, Kansas 66045		10. Work Unit No.
		11. Contract or Grant No. NAG1-345
12. Sponsoring Agency Name and Address National Aeronautics and Space Administration Washington, DC 20546		13. Type of Report and Period Covered Contractor Report
		14. Sponsoring Agency Code 505-61-41-02

15. Supplementary Notes

Langley Technical Monitor: Earl C. Hastings, Jr.
Phase 2 report

16. Abstract

This report documents the continued investigation of the design of Ride Quality Augmentation Systems (RQAS) for commuter aircraft. The purpose of these RQAS is the reduction of the vertical and lateral acceleration response of the aircraft due to atmospheric turbulence by the application of active control. The current investigations include the refinement of the sample data feedback control laws based on the control-rate-weighting and ouput-weighting optimal control design techniques. These control designs were evaluated using aircraft time simulations driven by Dryden spectra turbulence. Fixed gain controllers were tested throughout the aircraft operating envelope. The preliminary design of the hardware modifications necessary to implement and test the RQAS on a commuter aircraft is included. These include a separate surface elevator and the flap modifications to provide both direct lift and roll control. A preliminary failure mode investigation was made for the proposed configuration.

The results indicate that vertical acceleration reductions of 45% and lateral reductions of more than 50% are possible. A fixed gain controller appears to be feasible with only minor response degradation.

17. Key Words (Suggested by Authors(s)) Ride quality Gust alleviation Active controls Active Ride Augmentation	18. Distribution Statement Unclassified - Unlimited Subject Category 08

19. Security Classif.(of this report) Unclassified	20. Security Classif.(of this page) Unclassified	21. No. of Pages 241	22. Price A11